Th-Pos238

A PHYSIOLOGICAL ROLE FOR ACTIN-TITIN INTERACTION IN CARDIAC MYOFIBRILS

((**W.A. Linke**[1], M. Ivemeyer[1], J.C. Rüegg[1] and M. Gautel[2])) [1]Physiology II, Univ. of Heidelberg, INF 326, D-69120 Heidelberg and [2]EMBL, Meyerhofstrasse 1, D-69012 Heidelberg, Germany

The high resting stiffness of cardiac muscle, relative to skeletal muscle, is explainable mainly by the expression of different length variants of titin (connectin), the giant elastic protein of the vertebrate myofibrillar cytoskeleton, in the two muscle types. However, additional molecular features may account for the high stiffness of cardiac myofibrils, such as interaction between titin and actin, which has previously been demonstrated *in vitro*. Therefore, we have investigated the issue of actin-titin interaction in isolated myofibrils from rat heart, to probe a possible physiological significance. Relaxed myofibrils were subjected to selective removal of actin filaments by a calcium-independent gelsolin fragment, and the "passive" stiffness of the specimens was recorded with a sensitive force transducer. We found that upon actin extraction, stiffness decreased by ~50%, and to a similar degree following high-salt extraction of thick filaments. Thus, actin-titin association may indeed be responsible for part of the high resting tension of cardiac myofibrils.

To identify possible sites of association, we employed a combination of different techniques. Immunofluorescence microscopy revealed that actin extraction increased the extensibility of the previously stiff Z-disc-flanking titin region. Actin-titin interaction within this region was confirmed in *in vitro* co-sedimentation assays, in which recombinant titin fragments were tested for their ability to interact with F-actin. By contrast, such assays showed no actin-titin-binding propensity for sarcomeric regions outside the Z-disc segment. The latter finding was supported by the results of mechanical measurements, which demonstrated that competition of native titin by recombinant titin fragments from both I-band and A-band did not interfere with relaxed myofibril stiffness. Finally, we also failed to detect a change in "active" stiffness upon application of recombinant A-band titin fragments to calcium-activated myofibrils. Thus, it remains unresolved, whether actin-titin interaction can perhaps be a factor in the regulation of active muscle contraction. In conclusion, these results indicate that it is actin-titin association near the Z-disc, but not along the remainder of the sarcomere, which helps to maintain a high stiffness of the relaxed cardiac myofibril *in vivo*.

Th-Pos239

***In Situ* Interactions of Dystrophin with Actin Revealed by Immuno-Resonance Energy Transfer.**

(Douglas D. Root) Department of Biological Sciences, University of North Texas, Denton, Texas 76203.

Biochemical evidence shows that purified actin binds to dystrophin *in vitro*; however, some proteins such as DNAse I, which also bind actin with high affinity *in vitro*, do not interact with actin *in situ*. Consequently, it is imperative to determine if interactions between actin and dystrophin occur within the cell. A novel method was developed to detect molecular level co-localization of dystrophin with actin in rat skeletal muscle cryostat sections by combining resonance energy transfer technology with immuno-labeling techniques. Highly luminescent terbium chelates were conjugated to anti-dystrophin mouse monoclonal antibodies and used as resonance energy transfer donors. Tetramethyl-rhodamine phalloidin can accept energy from these terbium chelates if the distance between the probes is within about 10 nm (about the size of an IgG_{2b} antibody molecule). Muscle tissue sections of 20 μm thickness were dual labeled with the conjugated anti-dystrophin antibody and tetramethyl-rhodamine phalloidin on actin. Verification that these two probes were within 10 nm of each other in the muscle section was established by measuring the sensitized emission of tetramethyl-rhodamine by the terbium chelate after a 200 μs delay following a flashlamp pulse. Sensitized emission was detectable only when both anti-dystrophin antibody and tetramethyl-rhodamine phalloidin were present. These results indicate that actin and dystrophin are closely associated within the cell. This method is generally applicable to the investigation of many types of intracellular associations.

TUBULIN AND MICROTUBULES

Th-Pos240

SEDIMENTATION VELOCITY STUDIES ON THE INTERACTION OF DOLASTATIN 10 WITH PC-TUBULIN

((**John J. Correia**§ and Sharon Lobert¶)) §Dept. of Biochemistry and ¶School of Nursing, Univ. of Mississippi Medical Center, Jackson, MS 39216.

Dolastatin 10, a drug isolated from the Pacific mollusk *Dolabella auricularia*, is reported to induce spiral polymers of tubulin similar to those induced by vinca alkaloids. We have conducted a sedimentation velocity study with phosphocellulose purified tubulin and dolastatin 10 at 25°C in 10 mM Pipes, pH 6.9, 1 mM $MgSO_4$, 2 mM EGTA, and 0.06% DMSO in the presence of 50 μM GTP or GDP. While the initial reaction (< 3 μM drug) suggested an indefinite, isodesmic polymerization, sedimentation distribution analysis [g(s)] revealed a stable intermediate of 20S in both GDP and GTP conditions. At higher drug concentrations (> 3-15 μM drug) a shoulder or an additional intermediate evolves, 30-40S, suggesting growth off this intermediate state. Above 15 μM drug, the entire zone gradually condenses into very large sheet-like aggregates that are visible by EM. In the ultracentrifuge at 30 μM drug these aggregates sediment as broad zones centered near 80S and 235S. GDP enhances the second phase of growth over GTP, but the size of the first intermediate is identical in the presence of either nucleotide. Thus, unlike vinca alkaloids, dolastatin 10-induced assembly of tubulin favors a stable intermediate. We estimate the size of this intermediate to correspond to 8-10 subunits, although we currently do not know its quaternary structure. Supported by NR00056 (S.L.).

Th-Pos241

SEDIMENTATION VELOCITY STUDIES OF VINCA ALKALOID INTERACTIONS WITH TUBULIN ISOTYPES

((**Sharon Lobert**¶, Anthony Frankfurter† and John J. Correia§)) ¶School of Nursing and §Dept. of Biochemistry, Univ. of MS Medical Center, Jackson, MS 39216 and †Dept. of Biology, Univ. of Virginia, Charlottesville, VA 22901.

We used sedimentation velocity to obtain thermodynamic parameters for vinca alkaloid interactions with purified tubulin isotypes, αβII and αβIII, as well as combined αβII and III, αβII and I&IV, and αβIII and I&IV. Data were collected at 25°C in 10 mM Pipes pH 6.9, 1 mM $MgSO_4$, and 2 mM EGTA in the presence of 50 μM GTP or GDP and were fit with an isodesmic ligand-mediated or ligand-mediated plus -facilitated model to obtain binding affinities. In the presence of vincristine and GTP, K_1, drug binding to tubulin heterodimers, is larger for purified αβII or αβIII tubulin compared to unfractionated tubulin (mean values $4.7 \times 10^5 \pm 0.8$ vs. $1.1 \times 10^5 \pm 0.1$ M^{-1}). Additionally purified αβII or αβIII tubulin form smaller spirals than unfractionated tubulin as evidenced in K_2 binding of drug to polymers. For example K_2 (M^{-1}) from data fit with the ligand-mediated model for αβIII is $4.5 \times 10^6 \pm 0.8$ vs. $1.8 \times 10^7 \pm 0.5$ for unfractionated tubulin. When αβII and III are combined or mixed with other isotypes, association constants approach the unfractionated tubulin values. These differences are not observed in the presence of vinblastine or vinorelbine or GDP. Thus we conclude that vincristine interacts differentially with individual tubulin isotypes, suggesting that tubulin isotype composition may impact drug efficacy and toxicity. Supported by NR00056 (S.L.) and NS21142 (A.F.).

Th-Pos242

ROLE OF GUANINE NUCLEOTIDES IN THE VINBLASTINE-INDUCED SELF-ASSOCIATION OF TUBULIN: EFFECTS OF GMPCPP AND GMPCP.

((**B. Vulevic**¶, S. Lobert§ and J.J.Correia¶)) ¶Department of Biochemistry and §School of Nursing, University of Mississippi Medical Center, Jackson, MS 39216.

Guanosine 5'-diphosphate (GDP) enhances tubulin self-association in the presence of vinblastine 2-4 fold over GTP [Lobert et al. (1995) *Biochemistry* 35, 6806-6814]. Here we analyze vinblastine-induced tubulin self-association in the presence of non-hydrolyzable guanine analogs, GMPCPP and GMPCP. Sedimentation velocity experiments were done in 10 and 100 mM Pipes, 1 mM $MgSO_4$, 2 mM EGTA, pH 6.9. In 100 mM Pipes, temperature is limited to < 20°C due to competing microtubule assembly induced by GMPCPP. We found that GMPCPP nearly perfectly mimics GTP in its effect on spiral assembly under all ionic strength conditions. In 10 mM Pipes, GMPCP enhances overall spiral formation by 0.59 ± 0.12 kcal/mol over GMPCPP. This is 0.37 kcal/mol less than the GDP vs GTP enhancement. In 100 mM Pipes overall enhancement for GDP/GTP and GMPCP/GMPCPP corresponds to 0.43 ± 0.13 kcal/mol on average and under these conditions it appears that both analogs mimic parental compounds. This reduction in GDP enhancement can also be achieved by adding 150 mM NaCl to 10 mM Pipes buffer, consistent with an electrostatic component to this nucleotide effect. These data suggest that, by the criteria of vinblastine-induced tubulin self-association, GMPCP is not a perfect GDP analog at low ionic conditions, while GMPCPP acts as a GTP analog under all studied conditions. Supported by NR00056 (S.L.).

Th-Pos243

TAXANE RING IS ENGULFED IN MICROTUBULE STRUCTURE DURING THE TUBULIN POLYMERIZATION.

((**R.Nicholov**, W.Y. Lo) IBME, University of Toronto, Toronto, ON, Canada, M5S 1A4

Spin probes TEMPO and TEPYRO were covalently attached either to C2 or C7 position of the taxane ring to produce spin labelled taxol analogues. The analogues compete with taxol for the same or overlapping binding site.

Tubulin-GTP complex in Mes was polymerized into microtubules in presence of spin labelled taxols. The polymerization of tubulin, confirmed by turbidity measurements and sedimentation assay, was monitored in real time by EPR spectroscopy. Molecular mobility of the analogues was studied before, during, and after microtubule assembly. Spin labelled taxol analogues with a TEMPO radical attached at C2 or at C7 position were not restrained in their molecular motion before the mictotubules assembly. With the increase of the sample temperature, which induces the formation of microtubule, the immobilization of the spin labelled molecule increased displayed by the splitting of the outer resonance lines, and broadening of the central line. Our experimental results show that the taxane ring is engulfed into microtubule structure and is not located at the protein/liquid interface. As a result of this study the orientation and mobility of taxol at its binding site will be determined.

Th-Pos244

TUBULIN SECONDARY STRUCTURE VISUALIZED IN A 4-Å MAP BY ELECTRON CRYSTALLOGRAPHY. ((**K.H. Downing**, E. Nogales and S.G. Wolf)) Life Sciences Div., Lawrence Berkeley National Laboratory, University of California, Berkeley CA 94720

We are in the process of determining the structure of tubulin using electron crystallography of zinc-induced, crystalline sheets. In our previous medium resolution reconstruction (6.5 Å) we tentatively identified a few secondary structure motifs within the tubulin molecule. We have now extended the resolution to 4 Å, and there are many features in the map that appear to show details of the secondary structure. X-ray crystallographers are well aware of the problems of interpreting maps with such limited resolution, and the additional problem of the missing cone of data inherent in electron crystallography may make interpretation even more difficult. Image simulations with a known structure, actin, under conditions similar to those of the tubulin map, support the limited interpretations we made previously in the 6.5 Å maps and the more extensive interpretations we make here in the 4 Å map. Most of the secondary structure of the tubulin dimer can now be identified. Regions that appeared as cylinders in the 6.5 Å map and were interpreted as alpha helices now show a clear, right-handed coil, confirming the handedness previously assigned to the map. Beta sheet regions are well resolved, also with the expected right-handed twist. Although only a few of the loop regions are resolved at present, we can now begin to search for structural homologies between tubulin and other proteins, and to interpret results of structure-motif predictions based on threading algorithms. In addition, there are sufficient details in some of thee apparent side-chain densities, for example along regions that are clearly alpha-helical, that we may be able to correlate parts of the density map with sequence segments predicted to be helical, in the first phase of building an atomic model of the structure. Sequence differences between the α and β monomers provide a strong constraint in this stage of interpreting the density map.

Th-Pos245

SELF ASSEMBLY OF TAXOL ((**S.V.Balasubramanian** and R.M.Straubinger)) Department of Pharmaceutics, State University of New York at Buffalo, Amherst NY 14260.

Taxol (paclitaxel) and several analogs are under intensive investigation for use as anti cancer agents. However, little is understood about their molecular mechanism of action. Based on Circular Dichroism (CD), Fluorescence, Nuclear Magnetic Resonance (NMR) and Resonance light scattering (RLS) studies, we found that taxol exists in a supra molecular assembly in aqueous environments. Further analysis of the CD spectrum in the presence of micro tubules suggests that taxol might have two distinct roles at the site of action: (i) binding of taxane monomer or smaller aggregates to the tubulin dimer; (ii) stabilization of the micro tubule assembly by larger self assembled taxane aggregates. We extended these conformational studies to several less-potent taxanes to investigate the relationship between the self assembling property and biological activity. Active analogs such as cephalomannine undergo self assembly, whereas the inactive Baccatin III does not. The data further implicate a role for taxane self assembly properties in pharmacological activity.

Th-Pos246

CONCENTRATION-DEPENDENCE OF VARIABILITY IN GROWTH RATES OF MICROTUBULES. ((**Susan Pedigo** and Robley C. Williams, Jr.)) Department of Molecular Biology, Vanderbilt University, Nashville, TN 37235

Growth and shortening of microtubules has previously been observed to occur at variable rates. Here we address the issue of whether variability in growth rates changes as a function of the concentration of tubulin, as might be expected if imperfections were incorporated into the tubulin lattice. Video-enhanced DIC light microscopy was used to monitor dynamic properties of microtubules nucleated by *Chlamydomonas* flagellar axonemal pieces in real time. Results from only plus-ended microtubules at tubulin concentrations between 1.7 and 3.5 mg/mL are reported. Contrary to our expectations, the coefficient of variation (standard deviation in the growth rate divided by the growth rate) decreased over the concentration range explored. This trend indicates that at higher growth rates either microtubules are more homogeneously nucleated or there is a decrease in the number of "microcatastrophes". In addition, we found that there was a linear relationship between the average growth rate of microtubule populations and tubulin concentration.

(supported by grant GM 25638 from the NIH)

Th-Pos247

KATANIN, A MICROTUBULE SEVERING ATPASE, BREAKS *CHLAMYDOMONAS* FLAGELLAR AXONEMES ((**T.A. Lohret**[1], F.J. McNally[2], and L.M. Quarmby[1])) [1]Dept. of Anatomy & Cell Biology, Emory University School of Medicine, Atlanta, GA 30322 and [2]Section of Molecular and Cellular Biology, U-C Davis, Davis, CA 95616.

The study of microtubule severing has been primarily limited to *in vitro* studies using taxol-stabilized microtubules (Vale, 1993, *Cell*, 64:827, McNally and Vale, 1993, *Cell* 75: 419). We are currently developing a new *in situ* assay to study the regulation and mechanism of microtubule severing using the axonemal microtubules of *Chlamydomonas reinhardtii*. The outer doublet microtubules of *Chlamydomonas* are broken in the transition zone of the axoneme in response to certain signals. This suggested to us that the double-walled microtubules of the axoneme might be severed by the same mechanism as severing of taxol-stabilized microtubules *in vitro*. Flagellar breakage can be effectively assayed in detergent permeabilized cells which provides experimental access to both the axonemal microtubules and to the machinery of excision. We find that katanin, a microtubule severing ATPase purified from sea urchin oocytes, induces breakage of flagellar microtubules in wild-type *Chlamydomonas* cells as well as in two *fa* (*f*lagellar *a*utonomy) mutants with defects in flagellar excision. These effects are ATP-dependent and inhibited by ADP and ATPγS. These results indicate that katanin can induce breakage of double-walled axonemal microtubules and suggests that microtubule breakage in deflagellation may proceed by the same mechanism as the severing of taxol-stabilized microtubules. [Supported in part by the University Research Council of Emory University].

Th-Pos248

EXPERIMENTAL EVIDENCE FOR A T-FORCE SWITCHING THRESHOLD IN BULL SPERM. ((D.L. Holcomb and **C.B. Lindemann**)) Department of Biological Sciences, Oakland University, Rochester, MI 48309.

The Geometric Clutch hypothesis of flagellar beating (*J. Theor. Biol. 1994, 168: 175-189*) contends that the engagement and disengagement of the dynein motors in the flagellar axoneme is regulated by force developed transverse to the outer doublets (the t-force). The t-force is in turn a product of the curvature of the flagellum and the cumulative longitudinal tension on an individual doublet. If this basic tenet of the hypothesis is correct, experimental conditions which limit either the curvature or the cumulative longitudinal tension should result in an arrest of the beat cycle by limiting the development of the critical t-force needed for dynein bridge switching. In this study we have used Triton X-100 extracted bull sperm, reactivated with 1mM MgATP, to evaluate the effects of curvature and total force on the beat cycle. A glass microneedle fashioned into a hook was used to block the movement of a beating bull sperm flagellum and thereby limit the development of curvature in the basal portion of the flagellum. This manipulation results in an arrest of the beat with the flagellum continuing to push actively against the probe. In a second procedure the flagellum was shortened by removing distal pieces by microdissection. This reduces the length of axoneme and hence the number of dynein arms which can contribute longitudinal force to the doublets. As the flagella of reactivated bull sperm are serially dissected, the beat frequency decreases with shortening until arrest occurs at an average length of 14 μm. Both of the observed results support the idea that a critical t-force is necessary for completion of the beat cycle. Analysis of the flagellar curvature at the arrest points may provide a means of quantitating the critical t-force needed for switching. Supported by NSF grant MCB-922910.

Th-Pos249

MUTATIONAL ANALYSIS OF THE DEFLAGELLATION PATHWAY OF *CHLAMYDOMONAS REINHARDTII*. ((**R.J. Finst**, T.A. Lohret, P.J. Kim & L.M. Quarmby)) Dept. Anatomy & Cell Biology, Emory University, Atlanta, GA 30322-3030.

Signal-induced deflagellation in *Chlamydomonas* involves breakage of the 9 outer-doublet axonemal microtubules at a specific site within the flagellar transition zone. We have recently isolated 13 new mutant strains with defects in acid-induced deflagellation. Five of these are defective in acid-activated Ca^{2+} influx (the *adf* mutants) and 8 are specifically defective in the Ca^{2+}-triggered breakage of the axonemal microtubules (the *fa*, flagellar autotomy, mutants). Genetic analysis of the *fa* strains revealed that, in addition to alleles of the known *fa* gene (mutant in *fa*-1 cells), we have discovered 2 new genes important for flagellar excision (we have designated the genes *fa1*, *fa2* and *fa3*). Heterokaryon analysis suggests that the *fa1*, *fa2* and *fa3* gene products may function as a complex. We are currently cloning these 3 genes and have identified a phage clone which rescues the deflagellation defect in *fa1* mutant cells. Molecularly tagged alleles of the *fa2* and *fa3* genes have also been isolated. Deflagellation appears to occur by a mechanism analogous to katanin-mediated microtubule-severing (see poster by Lohret *et al.*). Identification of the *fa1*, *fa2* and *fa3* genes may, therefore, provide a direct approach to the discovery of interacting or regulatory proteins for a katanin-like activity. [Supported by NSF award MCB-9317359 to LMQ].

Th-Pos250

INVESTIGATION OF THE SECONDARY STRUCTURES OF SIMIAN AND HUMAN INTERLEUKIN-15 (IL-15) USING CIRCULAR DICHROISM SPECTROSCOPY. ((**Leizl F. Sapico**, Jayson Gesme, Herbert Iijima, Rama Balakrishnan, Raymond Paxton‡ & Thamarapu Srikrishnan)) Center for Crystallographic Research and Department of Biophysics, Roswell Park Cancer Institute, Buffalo, NY 14263 and ‡ Department of Protein Chemistry, Immunex Corporation, Seattle, WA 98101.

Interleukin 15 (IL-15) is a novel cytokine that has been recently cloned from the simian kidney epithelial cell line. Although Il-15 has no sequence homology with IL-2, it uses the components of the IL-2R for binding and signal transduction. IL-15 is a ligand that activates human NK cells through components of the IL-2R receptor in a pattern that is similar to but not identical to that of IL-2. We present here a detailed report on the secondary structure of the human and simian IL-15 using circular dichroism spectroscopy (CD). CD spectra were recorded on a JASCO 500A Spectropolarimeter. We investigated the effects of temperature, pH, salt and solvent compositions on the secondary structure of IL-15. At room temperature in PBF buffer (pH 7.0) human IL-15 has 18% α-helix, 38% β and 42% random coil. The simian IL-15 has 33% α-helix, 32% β and 35% random coil. The simian IL-15 is very stable at higher temperatures, retaining as much as 19% helical structure at 80°C with 43% β and 38% random coil. At lower and at higher pHs, both human and the simian IL-15 have much less helical content that at physiological pH. At pH 9.0, the human has 5.8% helical content as against 12.0% for the simian. At pH of 2.8 the human is almost *non-helical* (2.8% α-helix) and the simian has 16.1% helical content. These studies indicate significant differences in the secondary structures of the human and the simian in the solution state, with a higher helical content for the simian than the human IL-15.

Th-Pos251

ANALYSIS OF THE SECONDARY STRUCTURE OF A SCHISTOSOMA MANSONI PROTEIN (Smp50) USING CIRCULAR DICHROISM SPECTROSCOPY. ((**Thamarapu Srikrishnan**, Herbert Iijima, Jonathan Penoyar and Philip T Lo Verde†)) Center for Crystallographic Research and Department of Biophysics, Roswell Park Cancer Institute, Buffalo, NY 14263 and Department of Microbiology†, School of Medicine & Biomedical Sciences, State University of New York Buffalo, Buffalo, NY 14214.

Cyclosporin A and FK506 are the drugs of choice for transplant patients. The protein receptor for the ligands FK506, Cyclosporin and Rapamycin are called Immunophilins. The Cyclosporin A binding receptors are called Cyclophilins and the FK506 and Rapamycin binding ligands are called FKBP (FK binding Proteins). Recently a 50 kilodalton FKBP protein(Smp50) from the trematode *Schistosoma mansoni* was produced in bacteria and shown to have biological activity. We present here a detailed analysis of the secondary structure of this protein using circular dichroism spectroscopy (CD). CD spectra were recorded on a JASCO 500A spectropolarimeter. We investigated the effects of temperature, pH, salt and solvent compositions on the secondary structure of Smp50. At room temperature and in a phosphate buffer (pH 7.1) Smp50 has 26% α-helix, 42% β-structure and 31% random coil structure. When the protein is cooled to 10°, the amount of α-helix increases to 32% with a 36% β-structure and a 33% random coil. When the pH is lowered to 4.0 with an acetate buffer, the α-helix decreases to 21%, whereas at high pH (borate buffer), the α-helix increases to 29%. The temperature of the protein was increased from room temperature, in steps of 10° to 80°C, using a temperature bath. Our results indicate that the protein structure is not destroyed at high temperatures, retaining as much as 20% α- helix at 80°C.

Th-Pos252

INTERACTIONS BETWEEN IgG MOLECULE AND HYDROPHOBIC DRUG TETHERED TO THE ANTIBODY SURFACE VIA POLYMER CHAIN.
((V. Omelyanenko, P. Kopečková and J. Kopeček))
Department of Pharmaceutics and Pharmaceutical Chemistry/CCCD, and of Bioengineering, University of Utah, USA

A major factor limiting the successful clinical application of anticancer agents is their systemic toxicity. Techniques designed to improve their therapeutic index have focused on decreasing nonspecific interactions with normal cells and increasing both accumulation of the drugs within solid tumors and specific interactions with cancer cells. One technique, the binding of drugs to a water soluble polymer chain targeted by antibody (Ab) against a cancer associated antigen has shown great promise. Coupling drugs to the Ab molecule via a polymer chain is beneficial as a high degree of drug loading can be obtained with low chemical modification of Ab. However, when tethered to the protein's surface, a hydrophobic compound may interact with hydrophobic protein domains and induce a change in conformation of the antigen combining site.
Here the results of a study of the influence of adriamycin (ADR) and meso chlorin e_6 (Mce_6) bound via N-(2-hydroxypropyl)methacrylamide (HPMA) copolymer to OV-TL16, an Ab directed against an ovarian cancer associated antigen, on the conformation and affinity of the Ab are presented. The excitation energy transfer between Tyr and Trp and the drugs (ADR and Mce_6), the spectral properties of the drugs and CD-spectroscopy were used to monitor the interactions between the Ab and the drugs. The quenching of the intrinsic fluorescence of the Ab was also employed to study its conformational changes. An attempt has been made to correlate the biorecognition of the HPMA-drug-Ab conjugates at the cellular surface with the changes in Ab conformation resulting from the interactions of the drugs with the Ab molecule.

Th-Pos253

HIGH PRESSURE INDUCES A STABLE MOLTON GLOBULE STATE IN TUBULIN. ((**Lesley Davenport**[1], Jay R. Knutson[2], and Dan L. Sackett[3])) 1.Brooklyn College of CUNY, Brooklyn NY 11210; 2. NHLBI, NIH; 3. NCI, NIH, Bethesda, MD 20892.

Applied hydrostatic pressure provides a valuable probe of structural transitions in proteins that does not require altering solution conditions. Solutions of tubulin exposed to pressures of 0.2 - 2 kbar show a smooth transition ($P_{1/2}$≈ 0.9 kbar) characterized by a decrease in tryptophan fluorescence intensity and an accompanying long wavelength shift in the center of spectral mass (cms) of Trp emission. Decay associated spectra (DAS), measured as a function of increasing pressure, reveal three fluorescence lifetimes (τ_{short}≈1.1ns; τ_{medium}≈3.6ns; τ_{long}≈6.5ns) with $\%I_{330}$ of 8, 47, and 45, respectively (from 0-0.8 kbar). τ_{short} reveals marginal sensitivity to the transition ($\%I_{330}$ ≈15 at 2.0 kbar). In contrast, cms analyses of DAS suggest that spectral shifts arise exclusively from τ_{short} and τ_{medium} contributions (DAS for τ_{long} remains persistently red-shifted). The fluorescence of tubulin-bound colchicine analogs increases at lower pressures and is rapidly lost above 1 kbar. If the hydrophobic probe TNS is present, its fluorescence increases dramatically coincident with the decrease in tubulin tryptophan fluorescence. None of these changes are reversed by return to atmospheric pressure. Following pressure release, the protein structure appears more open, as evidenced by increased acrylamide quenching of tryptophan, increased rates of cleavage by proteases as well as appearance of new cleavage sites, and increased reactivity of cysteines with DTNB, accompanied by the appearance of disulfide bonds not present in the native protein. Addition of DTT does not prevent the observed changes with increased pressure or enhance their reversal on pressure release. We conclude that these pressures induce a transition in tubulin from the native form to an alternate stable molton globule-like state.

Th-Pos254

STRUCTURAL BIOLOGY OF THE CALCIUM-MODULATED PHOSPHOPROTEIN CALTRACTIN. ((**P.A. Fagan**, C. Jenkins[1], V.D. Lee[1], C. Weber, B. Huang[1], W.J. Chazin)) Departments of Molecular Biology and Cell Biology[1], The Scripps Research Institute, La Jolla, CA 92037.

Caltractin (also known as centrin), a 19.5 kDa phosphoprotein, is of considerable interest due to its implicated role in the cell cycle and its ubiquitous distribution in eukaryotes. Caltractin belongs to the EF-hand superfamily of calcium-binding proteins, and shares approximately 50% sequence similarity with calmodulin. Caltractin displays distinct functional, physical and spectroscopic properties not shared by other members of the EF-hand superfamily. Of particular interest, caltractin is phosphorylated *in vivo*, distinguishing caltractin among related proteins. During the cell cycle, the binding of calcium by proteins and protein phosphorylation are known to function as signaling pathways in regulation of the cell cycle. We are interested in examining the interplay of the calcium- and phosphorylation-dependent properties of caltractin. Multidimensional NMR spectroscopy will be used to perform structural studies on caltractin. Fragments of caltractin have been expressed and purified, and preliminary NMR data have been acquired.

Th-Pos255

CAGED PEPTIDES TARGETED AGAINST CALMODULIN AND MYOSIN LIGHT CHAIN KINASE. ((R. Sreekumar, M. Ikebe*, R.E. Carraway*, F.S. Fay* and J.W. Walker)) Department of Physiology, University of Wisconsin, Madison, WI 53706, and *Department of Physiology, University of Massachusetts, Worcester, MA 01655

Synthetic peptides show great promise as selective activators or inhibitors of protein-protein interactions involved in signaling, motility or secretion. Application of peptides to experiments in living cells is hampered by their low membrane permeability leading to the need for reversible permeabilization, microinjection, or intracellular perfusion. Caged photoactivatable peptides would be a useful way to dissociate the incorporation process from the onset of biological actions, allowing normal cell function to be verified before active peptide is released. In many organized biological systems, diffusional delays associated with peptide application could be overcome by use of caged peptides. We describe general strategies for preparing caged peptides by derivatizing lysine, tyrosine or glycine side chains with photolabile moieties, then incorporating these modified residues into peptides during Merrifield solid phase synthesis. The approach requires a reliable in vitro assay of peptide function to establish structure-activity relationships and to confirm the efficacy of peptide caging. Initial efforts are focused on two biochemically well-characterized peptides: RS-20, a 20 amino acid high affinity peptide inhibitor of calmodulin, and SM-1, a 13 amino acid autoinhibitory domain peptide from myosin light chain kinase. Caged forms of RS-20 and SM-1 are described whose potency is increased by nearly 100-fold by near-UV photolysis, and a photolabile form of RS-20 whose potent activity is destroyed by near-UV photolysis. [Supported by NIH and NSF]

Th-Pos256

RESONANCE ASSIGNMENTS AND SECONDARY STRUCTURAL FEATURES OF BOVINE α_{S1}-CASEIN PEPTIDES BY 1D- AND 2D-NMR SPECTROSCOPY ((M.H. Alaimo[1], M.W. Germann[2], E.L. Malin[1] and H.M. Farrell[1], Jr.)) [1]US Department of Agriculture, Wyndmoor, PA 19038 and [2]Thomas Jefferson University, Philadelphia, PA 19107

The major protein component of the bovine casein micelle is α_{S1}-casein. This protein is believed to form the framework for the colloidal casein micelle because it does not exhibit highly temperature-dependent interactions. A major chymosin cleavage site for α_{S1}-casein is located at the Phe-Phe bond of residues 23 and 24. The peptide α_{S1}-casein(1-23), which represents the hydrophilic N-terminus of the protein, has been postulated to be an integral part of the micellar framework. Hydrophobic portions of α_{S1}-casein can be involved in sheet-sheet interactions to form α_{S1}- dimers (136-159) or act as κ-α_{S1} sites of interaction (162-175) within the interior of submicelles. Both of these sites are contained in the cyanogen bromide cleavage peptide α_{S1}-casein(136-196). Structural and dynamic aspects of the two peptides will be discussed. Assignment of proton spin systems was accomplished by two-dimensional homonuclear (DQF-COSY, TOCSY, NOESY) and heteronuclear (HSQC, HMQC) measurements. Conformational information on α_{S1}-casein fragments was obtained from molecular mechanics/molecular dynamics, with dynamic constraints derived from measurement of NOE buildup rates and J coupling constants. The temperature dependence of the NH proton chemical shift and NH exchange rates were used to determine structural constraints arising from hydrogen bonding. Experimental evidence to solution state peptide conformation and behavior from analytical ultracentrifugation, circular dichroism (CD) and infrared (FTIR) spectroscopic measurements will also be presented.

Th-Pos257

NMR AND TIME-RESOLVED FLUORESCENCE STUDIES OF A CYCLIC PEPTIDE ANALOG OF SOMATOSTATIN. ((**P.D. Adams**, W.D. Treleaven, and M.D. Barkley)) Depts. of Biochemistry and Chemistry, LSU, Baton Rouge, La. 70703.

We have done NMR and fluorescence studies on a cyclic somatostatin analog, c[FWFdPY(OP)T], in aqueous solution. This molecule is similar to a six amino acid rigid cyclic analog of somatostatin previously studied. We are interested in determining whether a water-soluble analog will also have a rigid backbone. In examining the ground-state structure of the molecule by ^{1}H-NMR, we observed only one resonance for the indole NH of Trp in the 1-D spectrum at all temperatures studied. This finding could indicate that there is only one side chain conformer for Trp, or that there is a fast equilibrium between side chain rotamers of trp that cannot be resolved on the NMR time scale. Excited state properties of the peptide were examined by steady-state and time-resolved fluorescence spectroscopy. The quantum yield and fluorescence lifetime of the peptide were measured and the lifetimes of the rotamer populations were correlated with the NMR results.

Th-Pos258

THE pH-DEPENDENT CONFORMATIONAL CHANGE OF A LECTIN FROM *Lens cullinaris*. A THERMAL/INFRARED STUDY. ((**J.L.R. Arrondo**, I. Iloro, R. Chehín, M.J. Marcos and E. Villar)) Dept. Biochemistry, Univ. Basque Country, Bilbao and Dept. Biochemistry, Univ. Salamanca, Spain.

A lectin from *Lens cullinaris* has been isolated and its conformation and thermal behaviour measured at different pHs. At pH 7.4. the infrared spectrum is similar to that of concanavalin A, with a maximum around 1633 cm^{-1} and shoulders around 1690, 1674, 1659, 1646 and 1620 cm^{-1} in a D_2O solution. Quantization of the amide I band shows that the 1633 cm^{-1} band represents a 33% of the structure being the major conformation of the protein. The presence of bands at 1620 and 1690 cm^{-1} is similar to those found in concanavalin and attributed in principle to ß-edge, and more recently, to a ß-hairpin. Change in the pH of the medium does not change the percentage of ß-sheet present, but there are changes in the percentage of the other bands. The process of thermal denaturation has been followed by looking at the changes in bandwidth produced by the aggregation of the protein induced by temperature, and by looking at changes in the different bands that constitute the amide I band envelope. The differences in denaturation temperature are consistent with DSC data, where the protein has a maximum denaturation temperature in a pH range between 5 and 7.5, decreasing the denaturation temperature above and below such range.

Th-Pos259

Structural Dependence of Leptin on pH and Ionic Strength As Investigated by FT-Raman Spectroscopy ((T. Li*, B. Chang# and T. Arakawa*)) *Protein Chemistry and #Pharmaceutics Department, Amgen Inc., 1840 Dehavilland Dr., Thousand Oaks, CA 91320. (Spon. by J. Philo)

Leptin is a 16 kDa protein expressed primarily in adipose tissues. It has recently been demonstrated that injection of purified recombinant leptin reduces significantly body weight of *ob/ob* and wild-type mice (Pelleymounter *et al.*, Science **269**, 540; Halaas *et al.*, Science **269**, 543, 1995). The structure of leptin remains tc be determined. In this study, we have investigated the structure of recombinant human leptin and examined its structural dependence on pH and ionic strength in solution by employing FT-Raman spectroscopy. Raman spectra of leptin in solution at pHs 3.0 and 5.0 reveal only slight difference in protein secondary structures between the two pHs. Leptin at both pHs contain dominant amount of α-helix and lesser extent of β-structures. However, major changes in protein side chain conformations have been observed between pHs 3.0 and 5.0. Interactions of leptin with docusate sodium (DSS) and glycerol have also been investigated by using FT-Raman spectroscopy. Raman spectra indicate that both DSS and glycerol induce the formation of significant amount of β-structures at the expense of α-helix in leptin. The current data provide some insight about leptin structure and its conformational flexibility under various experimental conditions.

Th-Pos260

Structure Determination of Amylin - a Molecular Level Approach to the Understanding of Diabetes

((U. Ilangovan', M. T. Dehring', S. Sankarapandi[1], R. Manoharan[2], J. L. Zweier[1], M. S. Feld[2], and A. Ramamoorthy')) 'Biophysics Research Division and Department of Chemistry, The University of Michigan, Ann Arbor, MI 48109; [1]Division of Cardiology, School of Medicine, Johns Hopkins University, Baltimore, MD 21224; George R. Harrison Spectroscopy Lab., Massachusetts Institute of Technology, Cambridge, MA 02139

Amylin, a 37-residue polypeptide hormone, is the principal constituent of the islet amyloid deposits that form in the islets of Langerhans in the pancreases of patients with type-II diabetes mellitus. It forms voltage-dependent, non-selective, ion-permeable channels in planar phospholipid bilayer membranes. The toxicity of human amylin is related to its membrane insertion and channel formation, and it is believed that its β-sheet structure plays a pivotal role in the ion-channel formation. Since amyloid fibrils show low solubility under physiological conditions and are non-crystalline, solid-state NMR and EPR, which do not require crystalline samples, are used to determine the structure and describe the dynamics of a synthetic amylin peptide in various membrane environments, namely, oriented and unoriented phospholipid bilayers and detergent micelles. From the order parameters calculated from EPR experimental results, 0.62 for amylin and 0.59 for magainin compared to 0.52 in the absence of the proteins in mebrane bilayers, we predict that the local phase near the membrane surface becomes rigid due to interaction with the proteins.

Th-Pos261

DESIGN, SYNTHESIS, EXPRESSION, AND CHARACTERIZATION OF MOUSE FcγII RECEPTOR b1 AND b2 CYTOPLASMIC REGIONS. ((**Lixin Chen**, Nancy L. Thompson and Gary J. Pielak)) Department of Chemistry, University of North Carolina, Chapel Hill, NC 27599-3290

The cytoplasmic regions of mouse low affinity FcγII receptor isoforms play a key role in signal transduction by mediating different cellular functions. mFcγRIIb1 has a 94 residue cytoplasmic region whereas mFcγRIIb2 has a 47 residue cytoplasmic region. The primary structure of the isoforms is identical except for an in-frame 47 amino acid insertion in the cytoplasmic domain of mFcγRIIb1, generated by cell-type specific alternative mRNA splicing. A gene encoding the cytoplasmic domain of mouse FcγRIIb1 (mFcγRIIb1-94) was designed, synthesized, and expressed as a cleavable fusion protein in *Escherichia coli*. A sequence-specific protease, thrombin, was used to cleave the fusion protein and release the mFcγRIIb1-94 peptide, which was purified using HPLC. The cytoplasmic domain of mFcγRIIb2, mFcγRIIb2-47 peptide, was chemically synthesized. To compare the structures of mFcγRIIb1-94 and mFcγRIIb2-47, circular dichroism spectropolarimetry was employed. Both peptides were largely unstructured in aqueous solution at ≤ 300 mM, but became structured in membrane mimetic solvents such as trifluoroethanol or methanol. These results demonstrate that the cytoplasmic domains of mouse FcγRII are structured under certain conditions. These conditions may mimic mechanisms that trigger signaling *in vivo*. Supported by NIH grant GM-37145.

Th-Pos262

STRUCTURAL BASIS OF NEUROFILAMENT PHOSPHORYLATION BY CYCLIN DEPENDENT KINASE-5 ((**Pushkar Sharma**[1], Xiaolin Huang[2], Joseph J. Barchi Jr.[2], Harish C. Pant[1])) 1 Lab of Neurochemistry, National Institute of Neurological Disease and Stroke, National Institute of Health, Bethesda, MD, 2 Lab of Medicinal Chemistry, Division of Basic Sciences, National Cancer Institute, National Institute of Health, Bethesda, MD 20814. (Sponsored by Harish C. Pant)

The neurofilament (NF) proteins are a class of intermediate filaments that are exclusively found in neurons and are a major component of the axonal cytoskeleton. The high molecular weight NF-subunits (NF-M and NF-H) are highly phosphorylated in vivo primarily in the axon. The phosphorylation sites are located mainly on serine residues in KSP motifs within the C-terminal tail domain of NF-M and NF-H. These motifs mainly exist as KSPXXXK and KSPXK. We as well as others identified CDK5 as the kinase responsible for the phosphorylation of KSPXK sites but not KSPXXXK. We analysed the conformation of four peptides derived from the rat and human NF-H with either KSPXK or KSPXXXK motifs. The conformation of these sets of peptides was found to be significantly different. The KSPXXXK peptide exhibited a CD spectra indicative of a helical conformation, however under the same conditions the KSPXK peptide did not show any folded secondary structure . These results suggest : 1) different conformation for the KSPXXXK and KSPXK motifs in the neurofilament subunits, 2) the substrate specificity for CDK5-depends upon accommodation of very linear structures substrate motifs in its catalytic site but not folded structures as observed for KSPXXXK peptides. The preliminary NMR studies suggest there is no folded structure for KSPXK peptides in water. However extensive studies to analyse the conformation of these peptides in various conditions by NMR are carried out.

Th-Pos263

MAGNETIC RESONANCE MICROIMAGING (MRM) OF ATHEROSCLEROTIC LESIONS. ((**Joel Morrisett**, Gerald Lawrie, Michael DeBakey, Ed Ezell, and David Gorenstein)) Departments of Medicine and Biochemistry, Baylor College of Medicine, Houston, TX & Sealy Center for Structural Biology, UTMB-Galveston, TX

The objective of this study was to determine the spacial localization of atherosclerotic lesions and their components in bypass vein grafts, carotid plaques, and coronary plaques ex vivo. The 9.4 Tesla T2- weighted image of a resected vein graft showed the intimal boundary of the vessel in high contrast to the darker components that fully occlude the lumen. Cholesterol clefts displayed high pixel intensity, fibrotic material was dark, and thrombus showed varying levels of gray. The outside boundary of the thickened intima is sometimes highlighed by the internal elastic lamina which is dark. The media and intima both appear dark and are not clearly distinguishable from each other. The morphology of the vessel indicated by the microimages closely matched that of corresponding histologic thin sections treated with Movat or trichrome stain. Although the MRM slice (~600 microns) and thin sections (~6 microns) differ in thickness, good registration between them could be obtained. Areas of intra-lumenal structures well defined in the MRM images were compared to the corresponding areas in the thin sections and had excellent correlation (r=0.952; p=.003; n=6). Areas of the entire lumen, of the intima, and of the media/adventitia were not as well correlated (r=0.707, 0.702, and 0.748) more because of the ill-defined boundaries in the thin sections than in the microimages. In contrast to the lipid- and thrombus-rich lesions of failed bypass grafts, carotid plaques contain extensive calcification. This component does not contain much water and therefore appears rather dark on a T1-weighted image. Coronary artery plaques (~1-3 mm diam) removed intact at atherectomy and imaged (Te=26msec;Tc=4sec;4.65G/cm slice select gradient) were of sufficient resolution (~0.1mm) to calculate accurately the % stenosis. These results demonstrate the capability of MRM to discriminate between the different components of atherosclerotic lesions in different vessel plaques, and its potential for in vivo application (Supported in part by a grant from the DeBakey Foundation and by grant HL27341).

Th-Pos264

MICROINTERFEROMETRIC MEASUREMENT OF SINGLE-MOLECULE PROTEIN/DNA INTERACTIONS: BINDING AND BENDING OF DNA BY TATA BINDING PROTEIN ON A 0.5-1.0KB EUCARYOTIC PROMOTER.
((**J.D.B. SUTIN**, D. Scott, J. M. Beechem)) Dept. of Molecular Physiology & Biophysics, Vanderbilt University, Nashville, TN, 37232.

In these studies we are examining the properties of single DNA molecules by measuring the displacements of a 200nm polystyrene bead attached to one end of the DNA, with the other DNA end attached to a microscope cover slip. Data is obtained on these tethered DNA's using a home-built microinterferometer which operates in two modes: wide-field DIC with white-light excitation/CCD detection; and micro-interferometric mode with He-Ne laser excitation/photodiode detection. Since our interests in protein/DNA interactions are in understanding real-time kinetics, the micro-interferometer of the microscope has been built with high bandwidth capability. In this manner, we are attempting to utilize changes in the high frequency Brownian motion regime to detect very quickly the instantaneous state of the DNA (i.e., bound or free). Experiments are currently being performed on 0.5Kb and 1.0Kb DNA fragments of the intact eucaryotic promoter from the PEPCK gene ± TATA Binding Protein (TBP). The Brownian motion of the tethered bead generates a fluctuating time series of nanometer-scale bead displacements, which are monitored in the microinterferometer. From the time series data, the frequency of fluctuation of the TBP bound promoter was found to be greater than for the free promoter. The autocorrelation function can discriminate between the bound and free cases. The $t_{1/2}$ of the autocorrelation function for TBP bound promoter and free DNA promoter were 2.3 msec ± 0.4 and 9.7 msec ± 1.8 respectively. Current experiments are attempting to determine the physical mechanism for the higher frequency of bead motions in the TBP bound promoter. Experiments conducted in collaboration with the D.K. Granner and P.A.Weil laboratories.

Th-Pos265

CONFORMATION AND ORIENTATION OF KL_4 AND SYNTHETIC SP-C SURFACTANT PEPTIDES IN STRUCTURE-PROMOTING SOLVENT AND PALMITIC ACID MULTILAYERS. ((**A.J. Waring**, K.Y.C. Lee, M.M. Lipp, J.A. Zasadzinski, K. Faull and L.M. Gordon)) Perinatal Laboratories, Harbor-UCLA, CA 90502-2064; Department of Chemical Engineering, UCSB, CA 94306-5080; Center for Molecular and Medical Mass Spectrometry, UCLA, CA 90024. (Spon. by A.J. Waring)

The conformation and orientation of KL_4, a 21 residue peptide with a repeat sequence of KLLLL units and synthetic SP-C protein based on the 35 residue human sequence (FGIPCCPVHLKRLLAVAVAVALAVAVAVGALLMGL), were studied by circular dichroism (CD) and Fourier transform infrared (FTIR) spectroscopy. Circular dichroic measurements of peptide suspensions in the structure promoting solvent system consisting of hexafluoroisopropanol:water (8:2, v:v) with 0.1 % formic acid suggested that both peptides have a dominant α-helical conformation with minor contributions from disordered structures. When the peptides were incorporated into palmitic acid multilayers spread on a germanium attenuated total reflectance crystal (ATR), FTIR spectra of KL_4 and SP-C peptides showed similar amounts of helical conformations and disordered structures observed by CD. Polarized FTIR measurements of KL_4 and SP-C in palmitic acid films indicate that the helical axis is oriented approximately parallel to the fatty acid acyl chains of the multilayer lipid film. These measurements suggest that KL_4 and SP-C assume transmultilayer helical structures in palmitic acid films.

Supported by NIH HL 55534 (AJW, LMG) and NIH 51177 (KYCL, MML, JAZ).

Th-Pos266

^1H-^{13}C HMQC Detection of Pro76 Isomers in *E. Coli* Thioredoxin. ((**M. Baschky**, J. Fuchs and C. Woodward)) Department of Biochemistry, University of Minnesota, St. Paul, MN 55108.

Due to its unique imide ring structure, proline-containing peptide bonds may be either *cis* or *trans*. Our group is interested in cis-trans isomerization of the isoleucine 75 — proline 76 bond in the oxoreductase protein *E. coli* thioredoxin. Earlier gel electrophoresis work indicates that Ile75—Pro76 isomerization occurs, and that the cis isomer is more stable than the trans in both oxidized and reduced thioredoxin (Langsetmo et al. *Biochemistry* 1989 28:3211). However, NMR results from Dyson et al. (Chandrasekhar et al. *J. Biomol NMR* 1994 4:411) appear to negate this possibility. To probe this question more fully, auxotrophic bacteria were utilized to incorporate ^{13}C α-labeled proline and isoleucine into thioredoxin. HMQC, HMQC-NOESY, and HMQC-TOCSY 2D-NMR experiments show the existence of *two* crosspeaks for Pro76 in thioredoxin, one in the oxidized form and a different one in reduced. The identity of these peaks is confirmed in NOESY and TOCSY experiments. The most probable explanation for two isomeric forms of Pro76 is cis-trans proline isomerization of the Ile75—Pro76 amide bond. NMR spectra supporting this hypothesis will be presented.

Th-Pos267

THE EFFECT OF PEPTIDE BACKBONE MODIFICATION ON HELIX STRUCTURE.
((**Chi-Fon Chang** and Micheal H. Zehfus)) The Ohio-State University, Ohio 43210

The hydrogen bond between amides and carbonyls along the peptide backbone is an important feature of the α-helix. A helical peptide acetyl-WGG(RAAAA)$_4$ R-amide has been chosen as the model peptide to study the backbone hydrogen bond interactions. The backbone hydrogen bonds of this helix have been disrupted in two ways. In the first, the hydrogen bond donor ability of specific peptide bonds has been removed by replacing the NH group with a NCH_3 group. In the second modification, the hydrogen bond accepting ability of a residue is eliminated by replacing the CO functional group with a CH_2 group. These modifications have been placed into the model peptide so that the same hydrogen bond is removed. Circular dichroism has been used to follow the helix-coil transition of the model peptide and derivative peptides. Both the N-methylation and the reduction of carbonyl decrease the helicity of peptides; however, the amount of destabilization is more than expected. The thermodynamic properties of the disruption have been analyzed using a simple two state model and the more complicated Lifson-Roig statistics. Different backbone-backbone interactions may be addressed by comparing the two different backbone modifications.

Th-Pos268

CORRECTING CIRCULAR DICHROISM SPECTRA OF PEPTIDES FOR AROMATIC SIDE-CHAINS.

((C. **Krittanai** and W.C. Johnson)) Department of Biochemistry and Biophysics, Oregon State University, Corvallis, OR 97331 USA.

A method is introduced for correcting the CD spectra of polypeptides for the contribution from aromatic side-chains. The method makes use of the common component vectors derived from Singular Value Decomposition analysis, to fit a portion of CD spectra which is not affected by aromatic side-chains. The corrected spectra are then regenerated using coefficients from the fitting and the common component vectors. The CD difference spectra indicate the contribution from aromatic side-chains to the CD spectra of as much as 20% in the 210-230 nm range.

Th-Pos269

EVIDENCE THAT COLD DENATURATION OF PROTEINS NEAR 0°C IS A GENERAL PHENOMENON.

(L. I. Tsonev, A.G. Hirsh, **P.M. Mehl** and S.V. Litvinovich) Transfusion and Cryopreservation Research Program, Naval Medical Research Institute, 8901 Wisconsin Avenue, Bldg. 29, Bethesda, MD 20889, USA.

Three new techniques for the analysis of fluorescence and circular dichroic (CD) data have been developed that, for the first time, enable the experimental demonstration of protein denaturation in dilute aqueous solutions at temperatures down to -18°C. A series of typical monomeric proteins have been studied, with detailed data collected for β-lactoglobulin (βLG) and myoglobin. All proteins appear significantly destabilized at 0°C and most show partial restabilization upon supercooling. Additional data from high sensitivity microcalorimetry (DSC) indicate that the some of the changes induced by cold denaturation at temperatures near 0°C persist after rewarming to high temperature. With prolonged exposure at 0°C deviation from the native state increases over periods of days, months and perhaps years. This implies that the structure and function of proteins that have been exposed to cold may no longer be representative of the native state and that the native state may not be the global free energy minimum. Supported by Naval Medical Research and Development Command, Work Unit # 1465. The opinions and assertions contained herein are the privates ones of the writers and are not to be construed as official at large.

Th-Pos270

DESIGN AND TESTS OF CONFORMATIONAL CHANGE FOR A TRANSCRIPTIONAL REPRESSOR PROTEIN.

((**Liskin Swint-Kruse**, B. Montgomery Pettitt, and Kathleen Shive Matthews.)) W. M. Keck Center for Computational Biology; Department of Biochemistry and Cell Biology, Rice University, Houston, TX 77251; Institute of Molecular Design,The University of Houston, Houston, TX 77204.

A prototypical system for negative transcription control is the *lac* repressor protein of *E. coli*. The DNA binding sites of this homotetramer are each comprised of the two N-termini of a dimer. Each half binding site is connected to the protein core by a hinge region historically thought to be disordered. However, the X-ray structure of DNA-bound repressor shows that the first seven amino acids of the hinge actually form an alpha helix [Lewis, M., et al. (1996) *Science 217*, 1247 - 1254]. This supports the hypothesis that the hinge region is disordered in the apo state and folds upon binding DNA [Ha, J. H., et al. (1989) *J. Mol. Biol. 209*, 801 - 816]. To explore this possibility, we have designed a construct consisting of the N-terminal fragment plus the hinge helix terminated by the sequence glycine-cysteine-glycine. These monomers may be "dimerized" via a disulfide bond and thus form a complete binding site. Our proposed studies utilize a two-pronged approach: (1) Spectroscopic techniques will be employed to monitor structural changes that occur upon dimerization or DNA binding, and (2) molecular dynamics will be used to simulate changes in the bound structure upon "removal" of the DNA. Protein purification of this construct is in progress. Furthermore, more than 900 ps of molecular dynamics simulations have been collected for a hydrated, oxidized dimer. To this point, no major structural changes have been observed. Simulations of a monomeric species and other controls are also in progress.

Th-Pos271

THE DESIGN OF TWO-STRANDED TROPOMYOSIN-LIKE COILED-COIL PEPTIDES.

((**N.J. Greenfield** and S.E. Hitchcock-DeGregori)) Dept. Neurosci. and Cell Biol., Robert Wood Johnson Medical School, Piscataway, NJ 08854

It is difficult to design well-packed coiled coils with a predicted number of polypeptide chains. Several researchers have suggested that using Leu residues in the *d* positions, and β-branched amino acids in the *a* positions of the *abcdefg* heptad repeat of designed coiled-coil α-helical peptides, along with one Asn in an *a* position, helps insure formation of dimers rather than higher ordered species. We designed a 35mer based on the sequence of striated α-tropomyosin (αTM) called TM35. The first two heptads were identical to αTM, but the last three heptads had the residues I, N, I in the *a* positions and L in the *d* positions. This peptide aggregated to form a three or four-chained species at high peptide concentration, and appeared to be in a molten globule-like state above 25 °C. A 32 residue chimera consisting of the first two heptads of αTM and the last 18 residues of the GCN4 P1 peptide[1] (TMZip) with the sequence AcMDAIKKKMQMLKLDNYHLENEVARLKKLVGER, however, folded in a two-state cooperative transition with no evidence of molten globule intermediates or multiple assembly states. Model building showed that the N15 residues from each chain could form an interchain hydrogen bond in the TMZip peptide which would allow tight packing at the interface of the first two heptads in a two-chained species, but such a bond could not be formed by the N22 residues of the TM35 peptide unless the N-terminus was much more loosely packed. The results show the importance of position and context of the interface residues in determining the packing and number of chains in coiled-coils. [1]Oas et al. Biochemistry 29: 2891-4 (1990) Funded by NIH GM36326.

Th-Pos272

EXPLORING PEPTIDE CONFORMATIONAL FREE ENERGY SURFACES

((**Krzysztof Kuczera** and Yan Wang)) Department of Chemistry and Biochemistry, The University of Kansas, Lawrence, KS 66045. kuczera@tedybr.chem.ukans.edu (Spon. By Thomas Squier)

A new multidimensional thermodynamic integration method is presented, allowing the calculation of the free energy gradient with respect to an arbitrary set of conformational coordinates from a single constrained molecular dynamics simulation. The approach opens new possibilities for exploration of molecular conformational free energy surfaces, including generation of free energy maps, identification and characterization of stable states, transition states, and evaluation of higher free energy derivatives. The method is applied to two systems. For model peptides $(Ala)_n$ and $(Aib)_n$ where n=6,8,10 and Aib is α -methylalanine in vacuum, free energy maps in ϕ-ψ spaces are used to identify, locate and characterize the local free energy minima in the region of regular helical conformers. For the linear form of the opioid peptide DPDPE in aqueous solution, the effective local sampling of constrained simulations is used to calculate the free energy difference between the open and cyclic-like structures providing an estimate of the free energy of pre-organizing the peptide for disulfide bond formation.

Th-Pos273

NON TWO-STATE DENATURING TRANSITION FROM NATIVE TO "MOLTEN GLOBULE" STATES OF APO-α-LACTALBUMIN.

((**D.B.Veprintsev**[1], E.A.Permyakov[1,2] and L.J.Berliner[3])) [1]Institute of Biological Instrumentation, Russian Academy of Science, Pushchino, Moscow reg., 142292, RUSSIA. [2]Institute of Theoretical and Experimental Biophysics, Russian Academy of Science, Pushchino, Moscow reg., 142292, RUSSIA. [3]Department of Chemistry, The Ohio State University, 120 West 18th Avenue, Columbus, Ohio, 43210. (Spon. by Dr. E.I. Shakhnovich)

Thermal denaturation of apo-α-lactalbumin, a classical example of a protein which exhibits "molten globule" state, was studied by circular dichroism (CD) spectroscopy, differential scanning calorimetry (DSC) and intrinsic protein fluorescence at neutral pH and low ionic strength (10mM borate buffer, pH 8.0, 1mM EGTA). Each method reports cooperative transition, with a mid-points of a transition about 30 °C for DSC and fluorescence and 20 °C for CD. The noncoincidence of the transition monitored by different methods suggests an existence of a populated intermediate state in the course of denaturation. Since apo-α-lactalbumin is in the classical "molten globule" state at temperatures above 40 °C under this conditions, this state is not the "molten globule" but a "compact molten globule", with physical properties intermediate between native and "molten globule" states.

Th-Pos274

LORENTZIAN FORMAMIDINIUM CURRENT NOISE IN GRAMICIDIN A CHANNELS.
((T. Fairbanks and D. D. Busath)) Brigham Young University, Provo, UT 84602.

Seoh and Busath (Biophys. J. 68:2271, 1995) showed that with formamidinium, single gramidicin A channels were lengthened and noisy at low voltages and had superlinear I-V's, all three properties being absent in gramicidin M channels in which the interfacial Trp's are each replaced by Phe. The single channel noise power spectra were measured to help identify the mechanism of these disparate but connected properties. Monoolein bilayers were formed on a 20 μm aperture in freshly prepared formamidinium chloride solution (0.1, 0.3 or 1.0 M). Single gramicidin A channel currents were measured at 50, 100, 150 and 200 mV using a 20 kHz low pass filter sampling at 48,000/s. 5-7 single channels and a similar number of baseline episodes were identified from digitally filtered data and their raw data spectra analyzed using 256, 1024, and 8192 point FFT's. The channel and baseline spectra were averaged and subtracted to eliminate bilayer capacitance noise. The hardware and software, including the power spectra normalization, were verified by measurement of the Johnson noise of a 10 MΩ resistor. For the series 50, 100, 150 mV (where noise power was sufficient), the spectra were Lorentzian with characteristic frequencies of 130, 270, and 900 Hz (0.1 M) and 1000, 2900, 5100 Hz (1 M), and with S_0's of 110, 180, and 64 fA^2/Hz (0.1 M) and 140, 210, 100 fA^2/Hz (1.0 M). The very low f_c suggests coupling of the blocking "gates" (equal or related to the Trp's) to long-range vibrations. The increase in f_c with V_m invalidates the "decreased coupling" mechanism (Seoh and Busath), indicating that the "gate" vibration frequency is proportional to the ion passage rate or velocity. F_c also increases with bulk ion concentration, so the rate of ion collisions with the channel entry governs the vibrations. The biphasic relationship between S_o and V_m is consistent with a monotonic increase in p_o because a maximum S_o is expected at p_o=0.5. It thus argues for a mechanism where increasing force on permeating ions maintains the channel open for longer periods and argues against "external" mechanisms such as induced external conductance or bilayer capacitance fluctuations. Thus formamidinium induces low frequency vibrations (such as bilayer surface waves) which in turn modulate the channel conductance, perhaps via Trp dipole motions.

Th-Pos275

GRAMICIDIN A CHANNEL AS A SENSOR OF MEMBRANE LIPID TITRATION.
((**V.Aguilella**, T.K.Rostovtseva, I.Vodyanoy, S.M.Bezrukov. and V.A.Parsegian)) Univ. Jaume I, Castellon, Spain & LSB/DCRT, NIH, Bethesda, MD 20982

We manipulate the lipid bilayer surface charge, and its influence on Gramicidin A channel conductance, by two strategies:

- dilution of a charged lipid by a neutral one, and
- titration of the lipid charge by varying bulk solution pH.

Comparison of the two data sets permits us to separate contributions of different ion species to the channel conductance and to introduce a new method for the 'bilayer pKa' determination. Using DPhPS/DPhPC bilayers with low-concentration CsCl water solutions, we show that the channel conductance titration is masked by increasing proton conductance when bulk solution pH goes below pH 4. Our model also accounts for the partial blockage of proton conductance by Cs^+ that we have seen in experiments with neutral lipids. To relate the bilayer surface charge density with the intrinsic pKa and bulk pH, we assume that the equilibrium constant K of lipid carboxyl group titration changes exponentially vs. the electric potential confronting protons at the surface. This approach is compared with the classical one formulated for poorly charged membrane surfaces where K is considered to be a constant independent of surface potential and, consequently, of bulk pH. Fitting gramicidin A channel conductance at different pH values to theoretical prediction we measure the intrinsic pKa of the lipid.

Th-Pos276

GRAMICIDIN STRUCTURE: INFLUENCE OF A LIPID-LIKE SOLVENT.
((**B. M. Burkhart**, R. M. Gassman, W. Pangborn, and W. L. Duax)) Hauptman-Woodward Medical Research Institute, Buffalo, NY 14203. (Spon. by J. Bruenn).

The biological relevance of crystal structures of commercially available gramicidin D (80% gramicidin A, 5% gramicidin B, and 15% gramicidin C) crystallized from methanol and ethanol has been questioned. It has recently been discovered that these structures incorporate tyrosine enriched heterodimers within the crystals and exhibit atypical behavior of tryptophan residues at the heterogeneous position 11. A newly determined structure of gramicidin D crystallized from the more lipid-like solvent, n-propanol ($P2_12_12_1$; a = 24.434Å, b = 32.461Å, c = 24.148Å; 1.13Å resolution, R = 7.75%), casts further light upon interesting trends noted in the structures obtained from the shorter-chain alcohols. Unlike the methanol or ethanol structures, there appears to be no tyrosine present at position 11, however isoleucine does appear to be present at position 1. Furthermore, solvent interactions noted in the methanol, and ethanol structures differ at many positions with n-propanols forming "pseudo micelles" with many tail-tail interactions. Hydrogen bonds holding the ends of the gramicidin dimers together which have been weakened on going from methanol to ethanol solvents, are now broken in the n-propanol solvent. These interactions may be a clue to the unwinding of gramicidin helices as they form the functional dimer in lipid environments.
Research supported in part by NIH grant GM32812.

Th-Pos277

OPTICALLY MODULATED IONIC CONDUCTION OF A GRAMICIDIN CHANNEL
(**F. Separovic**, A.S. Martin, D. Milojevic, P.D.J. Osman, C. Tansey) School of Chemistry University of Melbourne Parkville VIC 3052 Australia

Gramicidin A (gA) has been synthesized with a photo-isomerizable group linked to the C-terminus of the channel. An additional gA variant was synthesized with a lysine (lys-16) connected to trp-15. Using single channel BLM measurements, we have demonstrated the effect of irradiating a BLM containing an optically-gateable gramicidin on channel conduction and lifetime. In addition, single channel measurements were carried out using the lysinated gramicidin derivative. A parallel study of the conformation of the linker region of the ion channel was carried out by NMR spectroscopy of samples i) before exposure to UV, ii) after exposure to UV but without subsequent exposure to white light, and iii) after exposure to white light. It was found that the channel conduction was substantially altered by exposure to UV irradiation and that this subsequently reversed on exposure to white light.

Th-Pos278

DOUBLE-STRANDED CHANNELS ARE FORMED BY GRAMICIDIN ANALOG, V^9GLW
((W. Huang, **Shobana S.**, O.S. Andersen, D.V. Greathouse* and R.E. Koeppe II*)) Dept. of Physiology & Biophysics, Cornell Univ. Med. Coll., New York, NY 10021, * Dept. of Chem. & Biochem., Univ. of Arkansas, Fayetville, Arkansas 72701 (Spon. by Henry J. Sackin)

Gramicidin A (gA) forms channels that are right-handed, single-stranded (SS) $\beta^{6.3}$ helical dimers. This predominance of single-stranded β-helical dimers is not seen in the analog of gramicidin, gLW with the sequence: Formyl- L-Val- D-Gly- L-Ala- D-Leu- L-Ala- D-Val- L-Val- D-Val- L-Leu- D-Trp- L-Leu- D-Trp- L-Leu- D-Trp- L-Leu- ethanolamine. gLW has a strong preference for double-stranded (DS) channels. The experimental evidence for dominance of DS channels is that channels form with equal ease whether the peptide is added to both sides of the membrane or one side of the membrane. SS channels form much readily when gA is added to both sides of the membrane, as compared to one-sided addition. To understand the role of the amino acid sequence in changing the folding preference, experiments are carried out with V^9gLW. These experiments show the presence of at least two kinds of channels: (1) high-conductance, long-lived channels with an average duration of ~ 30s, (2) low-conductance, short-lived channels. The long-lived channels are DS as determined by single- and double-sided additions.

Th-Pos279

TRYPTOPHAN AS SWITCH FOR THE CONFORMATIONAL CONVERSION OF GRAMICIDIN IN LIPID BILAYERS.
((M. Cotten and T.A. Cross)) Department of Chemistry, National High Magnetic Field Laboratory, Florida State University, Tallahassee, FL 32306-4005.

Tryptophan is a very important and versatile amino acid in membrane bound peptides and proteins. We have used gramicidin A (gA), a pentadecapeptide cation channel with four indoles as a model system to study this amino acid. Samples of gramicidin in planar bilayers have been prepared by codissolving the peptide and lipids in an organic solvent prior to drying and hydration. In organic solvents, this peptide forms double helical structures and must go through a conformational interconversion to form the single stranded channel state in lipid bilayers. To study this structural rearrangement, homodimers and heterodimers of gramicidin A and gramicidin M (gM, all Trp replaced by Phe) have been structurally characterized by NMR before and after insertion into the bilayer. Both gM and gA/gM heterodimers form stable double helical structures in lipid bilayers.

Hybrids offer a molecular system where relatively subtle influences on structure can be assessed. Numerous tryptophans are apparently required to convert an otherwise stable double helical structure to the channel state. For the gA/gM hybrids, indoles are buried in the middle of the membrane. Their specific position and orientation is presumed to be important for the stability of this structure. Studies of additional gramicidin analogs will also be useful for addressing this problem. Knowledge from these experiments will lead to better models of the double helical gA homodimers prior to structural conversion to a single stranded helix. Furthermore, these experiments will provide insights into the energetics of the kinetically trapped (Aramugam et al. 1996. *Proc. Natl. Acad. Sci. U.S.A.* 93:5872-5876) parallel double helical conformation of gA.

Th-Pos280

STERIC INTERACTIONS OF VALINES IN [VALINE-5, D-ALANINE-8] GRAMICIDIN A CHANNELS.

((**Jude, A.R.,**)) Dept. Chem. Biochem., Univ. Arkansas, Fayetteville, AR 72701

When the central valine residues 6, 7, and 8 of gramicidin A (gA) are shifted by one position, the resulting [Val^5,D-Ala^8]gA forms right-handed channels with a single-channel conductance and average duration somewhat less than gA channels (J. Biol. Chem. 269:12567). The reduction in channel duration has been attributed to steric conflict between the side chain of Val^1 and Val^5 in opposing monomers. To investigate the orientations and motions of valines in [Val^5,D-Ala^8]gA, we have incorporated ^2H labels at Val 1, 5, or 7 and recorded ^2H NMR spectra of oriented and unoriented samples in hydrated DMPC. Spectra of unoriented samples at 4 °C reveal powder patterns that indicate rapid side chain "hopping" for valines 5 and 7, and an intermediate rate of "hopping" for Val^1 that is somewhat slower than that of Val^1 in gA. Oriented samples of deuturated Val^1 and Val^7 show large changes in the methyl and C_β-^2H quadrupolar splittings ($\Delta\nu_q$) from native gA. For Val^7, the $\Delta\nu_q$ values can be fit by a rapid "hopping" model in which the side chain is 80% at χ_1 of 180° and 20% at 300°. Three $\Delta\nu_q$ values of 0.0, 7.8, and 10.9 kHz for the Val^1 methyls, together with an intermediate unoriented-sample spectrum at 4 °C, suggest unusual side chain dynamics. The reduction in "hopping" rate for Val^1 in [Val^5,D-Ala^8]gA is consistent with a steric conflict that has been introduced between the two opposing monomers.

Th-Pos281

NEIGHBORING ALIPHATIC/AROMATIC SIDE CHAIN INTERACTIONS BETWEEN RESIDUES 9 AND 10 IN GRAMICIDIN CHANNELS

((**Greathouse, D.V.**, Hatchett, J., Jude, A.R., Koeppe, R.E. II, Providence, L.L., Andersen, O.S.)) Dept. Chem. Biochem., Univ. Arkansas, Fayetteville, AR 72701, Dept. Physiol. Biophys., Cornell Univ. Medical College, N.Y., NY 10021

Two conformations have been proposed for Trp^9 in gramicidin A (gA) channels: one in which the indole ring stacks against Trp^{15} and one in which the ring abuts and shields Leu^{10}. In addition, the peaks in the solid-state ^2H-NMR spectrum of hydrated, oriented, ring-labeled-Trp^9-gA in DMPC can be assigned to the ring in four different ways (Hu et al., *Biochemistry* 34:14138). We have investigated gramicidins in which Trp^9 is ring-labeled and Leu^{10} is replaced by Val, Ala or Phe. The single-channel conductance for all 3 analogues is lower than that of gA. For [Ala^{10}]gA, the average channel duration is reduced 3-fold. ^2H-NMR spectra of oriented samples in DMPC show large changes for the Trp^9 ring when residue 10 is modified, suggesting a 9/10 interaction, in agreement with previous acylation studies (Koeppe et al., *Biochemistry* 34:9299). The outer quadrupolar splitting is unchanged with Phe^{10}, but increases 20 kHz with Val^{10} and decreases 10 kHz with Ala^{10}. With Ala^{10} or Val^{10}, the outer resonance splits into two in a temperature-dependent manner. This result is consistent with the assignment scheme in *Biophys. J.* 66:14; it could also indicate that Trp^9 exhibits multiple conformations in these analogues (or both). We conclude that Leu^{10} helps to determine the orientation of Trp^9 for gA channels in lipid bilayers.

Th-Pos282

A STUDY OF CHANNEL KINETICS OF GRAMICIDIN ANALOGUES IN PLANAR BILAYER MEMBRANES BY SENSITIZED PHOTOINACTIVATION

((**Antonenko, Yu. N.**[1], Rokitskaya, T.I.[1], Kotova, E.A.[1], Koeppe, R.E. II[2], Andersen, O.S.[3])) [1]A.N. Belozersky Phys. Chem. Biol. Inst., Moscow Univ., Moscow 119899 Russia, [2]Dept. Chem. Biochem., Univ. Arkansas, Fayetteville, AR 72701, [3]Dept. Physiol. Biophys., Cornell Univ. Medical College, N.Y., NY 10021

Modification of gramicidin A (gA) by changes in its amino acid sequence and by covalent acylation with fatty acids alters the channel assembly process and the monomer-dimer equilibrium dramatically (Koeppe & Andersen **1996** *Annu. Rev. Biophys.* 25:231). In particular, single-channel measurements with gA analogues have revealed large deviations from gA in channel duration and channel-forming potency. True channel formation rate constants have not been accessible. Recently a novel flash-initiated sensitized photoinactivation method has been developed which allow one to determine the rate constants for channel formation and dissociation (Rokitskaya et al. **1996** *Biochim. Biophys. Acta* 1275:221). This approach is based on measurements of the gramicidin-induced current transients following a short light flash in the presence of a photosensitizer. Here the data on the variations of the time constant of the current transient as a function of the membrane conductance induced by different gA analogues will be presented. We will report values of the channel association/dissociation rate constants estimated for acyl gramicidins and [$Ala^{1,5}$]gA. The dissociation rate constants agree with those determined by single-channel methods.

Th-Pos283

IONIC SELECTIVITY IN GRAMICIDIN CONFORMERS. ((M.B. Partenskii, V.L. Dorman and **P.C. Jordan**)) Dept. of Chemistry, Brandeis University, Waltham, MA 02254-9110. (Spon. by E. Marder)

Using a semi-microscopic Monte Carlo approach, we previously analyzed ionic selectivity in the head-to-head (HH) $\beta^{6.3}$-helical form of gramicidin (Dorman, Partenskii and Jordan, *Biophys. J.*, **70**, 121 [1996]), the conformer mainly responsible for gramicidin's ability to form transmembrane ion channels. Earlier work explicitly described only the ion, channel water and the backbone carbonyl groups. We extend our approach to include the electrical influence of all backbone moieties (carbonyls, amides and α-carbons). We re-investigate factors governing conductivity in the HH form and also model the anti-parallel double stranded helical (APDS) form of the peptide. As before, the model calculations (now including the ion, water dipoles and all backbone charges) are exactly soluble, incorporating all long range interactions; the rest of the system (amino acid side chains, bulk solvent and lipid membrane) is modeled as dielectric continua. We find that, incorporated in low dielectric surroundings, ion channels formed by both HH and APDS conformers should be preferentially cation selective. Our analysis suggests that, relative to water, cation entry into the APDS conformer is less favorable than entry into the HH conformer. It further indicates that, in crystalline phases, both channels could preferentially incorporate monatomic anions instead of monatomic cations; such behavior has been observed for the APDS conformer when crystallized from a methanolic CsCl solution (Wallace and Ravikumar, *Science*, **241**, 182 [1988]).

Th-Pos284

THE BINDING SITE OF SODIUM IN THE GRAMICIDIN CHANNEL. COMPARISON OF MOLECULAR DYNAMICS AND SOLID-STATE NMR DATA

((**B. Roux**[1] and T.B. Woolf[2])) [1]GRTM, Départements de Physique et de Chimie, Université de Montréal, Montréal, Québec, Canada H3C 3J7; [2]Johns Hopkins University, School of Medicine, Baltimore, MD 21205, USA.

The location of the main binding site for sodium in the gramicidin A (GA) channel was investigated with molecular dynamics simulations using an atomic model of the channel embedded in a fully hydrated dimyristoyl phosphatidycholine (DMPC) bilayer. Twenty-four separate umbrella sampling simulations in which a sodium was restrained at different locations along the channel axis were generated. The results are compared with previous carbonyl 13C chemical shift anisotropy solid-state NMR experimental data. The combined information from experiment and simulation strongly suggests that the main binding sites for sodium are near the channel's mouth, approximately 9.2 angstroms from the center of the dimer channel. The 13C chemical shift anisotropy of Leu10 is the most affected by the presence of a sodium ion in the binding site. In the binding site, the sodium ion is lying off axis, making contact with two carbonyl oxygens and two single-file water molecules. The main channel ligand is provided by the carbonyl group of the Leu10-Trp11 peptide linkage which exhibits the largest deviation from the ion-free channel structure. Transient contacts with the carbonyl group of Val8 and Trp15 are also present. The influence of the tryptophan side chains on the channel conductance is examined based on the current information about the binding site.

Th-Pos285

A MODEL FOR COUPLED BULK AND SURFACE DIFFUSION TO AN ION CHANNEL ENTRANCE. ((**M.F. Schumaker** and C.J. Kentler)) Department of Pure and Applied Mathematics, Washington State University, Pullman WA 99164.

Apell, Bamberg and Laüger (1979) found that Cs^{++} conductance through Gramicidin is greatly enhanced when the channels are embedded in negatively charged lipid bilayers. This enhancement may be due to attraction of the cations to the charged membrane, followed by quasi-2-dimensional diffusion near the interface to the channel entrance. We have developed a mathematical model for coupled bulk and surface diffusion in the ion entrance process. Construction begins with a random walk on a 3-dimensional lattice (modeling diffusion in the bulk) coupled with a walk on a 2-dimensional lattice (modeling diffusion at the membrane surface). When transitions between sites are scaled appropriately, a coupled system of equations is obtained in a limit. Transport in the bulk is described by simple diffusion, coupled to the membrane via a boundary condition. The ion current flowing from the bulk to the plane contributes a source term for the planar diffusion. A far field analysis applies the boundary conditions at infinity to the coupled system. Far from the channel entrance, the vector field describing the currents has the form of superimposed monopole and dipole fields, with the dipole component describing ion flow into the interface. A corresponding 2-dimensional concentration profile of ions on the membrane surface is also found. To the order of the dipole terms, only a single parameter depends on the description of the channel entrance. These results provide boundary conditions for numerical solution of the equations.

Th-Pos286

EFFECT OF H-BONDING COMPOUNDS ON THE INCORPORATION OF GRAMICIDIN CHANNELS IN LIPOSOMES. ((A. Vallejo, E. Romero, S. Porro, L. Gassa, J. Vilche and **S. Alonso - Romanowski**)). Depto de Ciencia y Tecnología. Universidad Nacional de Quilmes. R Sáenz Peña 180. (1876) Bernal. ARGENTINA.

The kinetics of the channel former gramicidin (GA) in the presence of H-bonding compounds was studied using liposomes as model system. The studies were performed by determination of spectroscopical features of merocyanine 540 (MC540), infrared(ir), electrochemical impedance and conttrast phase microscopy. The study is based on Easton's procedure (Biophys.J., 1990) for GA thermal incorporation. When GA is added to the bathing solution containing DPPC or EggPC liposomes a peak at 485 nm is obtained with the fluorescent probe MC540. We followed the thermal incubation analyzing aliquots as a function of time (every 15 minutes). When trehalose and Gramicidin are at the phospholipid/water interface competing, according to the first sample withdrawn, the MC540 spectrum is similar to that of trehalose, showing a characteristic peak increase at 570 nm The second sample shows a spectrum that is not indicative of trehalose /DPPC nor of Gramicidin/DPPC. The sequence then is followed by a spectrum that shows both: an increment at 570nm due to trehalose and the peak due to Gramicidin/DPPC at 485nm. This means that the trehalose exposure of the hydrophobic regions would facilitate the monomers entrance but at the same time GA dimer feels an steric effect of the trehalose at the Ga H-bond between the phospholipid C=O and the NH from he Trp15 indol. This effect is also compared with that produced by galactose and sialic acid on the kinetics of Ga channels. The phenomenology was also confirmed with ir spectroscopy, electrochemical impedance and the morphological changes with phase contrast microscopy.

Th-Pos287

THERMODYNAMIC REVERSIBILITY AND STATISTICAL CONVERGENCE OF ALCHEMICAL FREE ENERGY SIMULATIONS ((**Shobana** S., B. Roux[#], R.E. Koeppe II[*] and O.S. Andersen)) Dept. of Physiology & Biophysics, Cornell Univ. Med. Coll., NY, NY-10021, [#] Dept. of Chem., Univ. de Montreal, Montreal, Canada H3C 3J7, [*] Dept. of Chem. & Biochem., Univ. of Arkansas, Fayetville, ARK-72701. (Spon. by Lawrence G. Palmer)

It is becoming realistic to undertake quantitative comparisons between experimental and computational estimates of the free energy consequences of single amino acid substitutions. However, a clear assessment of the statistical convergence and accuracy of the calculated estimates is essential for a meaningful comparison with experiments. Our previous free energy simulations on gramicidin analogs showed that statistical convergence and thermodynamic reversibility could be achieved with a non-linear increment in the coupling parameter, λ, which describes the continuous transformation of one amino acid into another. The question of reversibility was probed further in terms of the shape of the transformation path, the number of sampling points and the simulation time using three different systems in which we evaluate the mutation of alanine to valine using CHARMm. First, formyl-alanine-ethanolamine simulations greater than 2ns, with a sigmoidal λ profile, give identical free energy differences for thermodynamic perturbation and integration methods and were reversible. Second, calculations were done on poly-(Ala) right- and left-handed helical peptides to test the behavioral consistency of this sigmoidal path. All mutation cycles were performed three times to obtain statistically significant results. The forward and backward free energy differences differed by less than kT/2. Third, investigations were made on left- and right-handed forms of gramicidin A analog, gLW whose sequence is l-Val - d-Gly - l-Ala - d-Leu - l-Ala - d-Val - l-Val - d-Val - l-Leu - d-Trp - l-Leu - d-Trp - l-Leu - d-Trp - l-Leu. Statistically convergent free energy differences and thermodynamical reversibility were achieved.

Th-Pos288

TETHERED LIPID BILAYER: FORMATION, IONOPHORE INCORPORATION AND PHYSICAL CHARACTERISATION (**V.L.B. Braach-Maksvytis**, B.A. Cornell, L.G. King, P.D.J. Osman, R.J. Pace, B. Raguse, L. Wieczorek) Cooperative Research Centre for Molecular Engineering, PO Box S295 Homebush NSW 2140 Australia

Bilayer membranes have been used as model systems both as black lipid bilayers (BLM) and as vesicles to study lipid and ionophore function. The utility of these systems is restricted due to the fragility of BLM's and the lack of direct electrical monitoring of the vesicle system.

We wish to present a new tethered membrane system that allows the formation of a highly stable, fluid bilayer membrane with a functional ionic reservoir adjacent to a gold electrode. The bilayer membrane is easy to produce through a two step self-assembly process, wherein the first step utilises gold/sulfur interaction and the second step utilises the spontaneous planar bilayer assembly of a lipid in the presence of buffer. The membrane structure is build up out of synthetic lipids that mimic the archaebacterial lipid membranes. The design, structure, and function of the lipids that make up the reservoir, the lipid membrane and the stabilising effect of membrane spanning lipids will be discussed.

The membrane has electrical impedance characteristics (such as capacitance and sealing characteristics) similar to those found in BLM's. A variety of ion carriers and ion channels can be readily incorporated. The conduction properties and ion selectivities can be measured and will be presented.

Th-Pos289

A SYNTHETIC GATED ION CHANNEL WITHIN A SYNTHETIC TETHERED MEMBRANE. (**B.A. Cornell**, V.L.B. Braach-Maksvytis, L.G. King, P.D.J. Osman, R.J. Pace, B. Raguse and L. Wieczorek) Cooperative research Centre for Molecular Engineering, PO Box S295 Homebush NSW 2140 Australia.

A synthetic receptor/channel complex has been assembled by attaching antibodies to the ethanolamine moiety of Gramicidin A. A gating mechanism is demonstrated that depends upon altering the gramicidin dimer population through cross-linking the channel-attached antibodies to an incoming analyte. A stable membrane incorporating the mechanism has been assembled on a smooth gold surface using a combination of sulfur-gold chemistry and physisorption. The membrane comprises amphiphiles and channel species, some tethered to the gold surface and some diffusing laterally within the plane of the membrane. By using sulfur containing lipids with extended domains of differing polarity a structure can be formed which is reminiscent of a biological membrane enclosing a hydrated compartment which may be electrically accessed by the gold electrode. This compartment provides a reservoir into which ions may flow when the membrane channels are conductive. The tethered membrane is stabilized using membrane spanning archaebacterial lipids. The arrival of analyte cross-links the mobile outer layer channels to membrane spanning lipid tethers. Because of the low density of channels within the membrane, cross-linking anchors the mobile outer layer channels distant from their immobilized inner layer partners. This reduces the number of dimers which is reported by a change in the membrane admittance measured by impedance spectroscopy. The gating mechanism is generic and may be adapted to many applications and analytes with no change in basic design. For the detection of analytes too small to allow the simultaneous binding events required for cross linking, a competitive version of the switch has been engineered.

Th-Pos290

A COMPUTER MODEL OF 2- AND 3-DIMENSIONAL KINETIC PROCESSES FOR A SYNTHETIC GATED ION CHANNEL IN A TETHERED BILAYER (**L. Wieczorek**, V.L.B. Braach-Maksvytis, B.A. Cornell, L.G. King, P.D.J. Osman, R.J. Pace and B. Raguse) Cooperative Research Centre for Molecular Engineering, PO Box S295 Homebush NSW 2140 Australia

A computer model has been developed to simulate the gating response of a gramicidin-based synthetic ion channel in a supported bilayer. The process requires both 3-dimensional kinetics for the binding of antigen from solution to the bilayer, and 2-dimensional kinetics for subsequent in-membrane processes giving rise to a change in ion flux across the membrane. Both diffusion and reaction limited processes are taken into account. Using experimentally derived kinetic parameters (where they are independently measurable), the model is used to provide support for the proposed gating mechanism.

Th-Pos291

ELECTRICAL METHODS FOR CHARACTERISING A GATED ION CHANNEL BIOSENSOR (**P.D.J. Osman**, V.L.B. Braach-Maksvytis, B.A. Cornell, L.G. King, R.J. Pace, B. Raguse and L. Wieczorek) Cooperative Research Centre for Molecular Engineering, PO Box S295 Homebush NSW 2140 Australia.

It has been shown that synthetic ion channels incorporated into a lipid bilayer, in particular gramicidin, can be made to switch on and off in response to an analyte (Cornell 1992). Thus it is possible to link gramicidin to an antibody and switch the channel on and off by exposing it to the appropriate antigen. In order to understand the sensor structure, its switching mechanism and the kinetic response, it is necessary to use a number of measurement techniques. This presentation will describe the electrical characterisation of the sensor.

Single channel measurements have been used to characterise the channel conduction and one of the modes of switching. Impedance spectroscopy has been used to deconvolute the electrical properties of the tethered bilayer. In particular the ionic complexation between the bilayer and substrate, the lipid bilayer permittivity and the channel conductance were derived from these measurements. Amperometry was also used to characterise the ionic complexation and to estimate the sodium ion charge density, in the diffuse region between the bilayer and the substrate, while impedance spectroscopy and differential harmonic analysis have been used to characterise the voltage dependence of the sensor. Simple electrical models for these responses have been derived and will also be described. Finally examples and demonstrations will be given showing that either the frequency or the admittance at the phase minimum of a Bode plot, can be used to speedily measure the biosensor response to analyte.

Reference 1. Cornell, B.A., (1992) *United States-Australia workshop on membrane biophysics.* Biophys J. 61, 1454-1461.

Th-Pos292

CHARACTERIZATION AND PORE-FORMING ACTIVITY OF A FLUORESCEIN-LABELED ALAMETHICIN. ((H. Duclohier, J.Y. Dugast, O. Helluin and **G. Molle**)). URA 500 CNRS-Univ. Rouen (IFRMP 23), 768321 Mont-Saint-Aignan, France. (Spon. by E. Rojas)

In order to follow with the FRAP technique the lateral diffusion of alamethicin and its conducting aggregates of varying sizes within planar lipid bilayers (see Ladha et al., Biophys. J. 71:1364-1374), a fluorescein-isothiocyanate (FITC) analogue of alamethicin was synthesized. The final product was characterized by mass spectroscopy ($M+H^+$ = 2410) and an adequate fragmentation. The influence of FITC addition (a bulky group) on the pore-forming activity of alamethicin was tested in macroscopic and single-channel experiments. From the analysis of macroscopic current-voltage curve and although the apparent mean number of monomers per conducting aggregate was equivalent, the voltage-dependence of the new analogue was slightly reduced and hystereses (for raising and falling limbs of the voltage ramp) were much broader. The pattern of single-channel activity is also similar with that of alamethicin but there are fewer substates and conductances are reduced, arguing for more restricted pore diameters. Nevertheless, increments between each levels are still in geometrical progression according to barrel-stave model. Also in agreement with macroscopic conductance data, the substates 'open lifetimes' are much longer for the FITC-analogue. This could reflect favourable interaction of the conjugated cycles of the probe with the lipid headgroups.
Supported by GdR 1153 CNRS "Amphipathic peptides and proteins".

Th-Pos293

INFLUENCE OF PROLINE-POSITION UPON ION CHANNEL ACTIVITY OF ALAMETHICIN ((C. Kaduk[1], M. Dathe[1], H. Duclohier[2], M. Beyermann[1],G. Molle[2] and M. Bienert[1]))[1] Institute of Molecular Pharmacology, A.-Kowalke-Str. 4, D-10315 Berlin, Germany; [2] URA 500 CNRS, Universite de Rouen, Bd. M. de Broglie, 76821 Mont-Saint-Aignan, France

Alamethicin, a 20-residue peptaibol induces voltage-dependent ion channels in lipid bilayers. In order to study relationships between the proline-14-induced kink region and the channel-forming behaviour of the peptide systematically, the structural and functional properties of a set of alamethicin analogs with proline incorporated at positions 11, 12, 13, 14, 15, 16 and 17, respectively, as well as an Ala^{14}-analog were investigated. Macroscopic conductance experiments show that the voltage dependence of the peptides is conserved, but the apparent mean number of monomers forming the channels is significantly reduced when proline is not located at position 14. This is confirmed in single-channel experiments. The analogs with amino acid replacement next to position 14 (i.e. 13, 15, 16) show stable conductance levels but of reduced number which follows the order Pro^{14} >Pro^{15} >Pro^{16} >Pro^{13}-alamethicin. This reduction in the number of levels is connected with changes in the lifetime of the channels. Analogs with proline at position 11, 12 and 17 produce erratic, extremely short-living current events. The changes in functional properties are related to structural differences as probed by circular dichroism. The results indicate that proline at position 14 in the native sequence has reached the optimal position through the pressure of molecular evolution.

Th-Pos294

MECHANISM OF VOLTAGE-GATING IN ALAMETHICIN: NMR STUDIES OF STRUCTURAL VARIANTS ((**J. Jacob**, D.S. Cafiso)). Department of Chemistry and Biophysics Program, The University of Virginia, Charlottesville, VA 22901.

Alamethicin produces voltage dependent ion-conductance in lipid bilayer systems. It belongs to a family of peptides called Peptaibols because of the abundance of Aib residues in its sequence and a reduced C-terminus. The dynamics of alamethicin are being investigated by measuring paramagnetic enhancements of nuclear spin-lattice relaxation rates produced by a nitroxide label attached to the peptide C-terminus. Distances obtained from these enhancements are much shorter than those expected for a linear structure and are expected to reflect the r^{-6} weighted average of electron-nuclear distances. This data provides strong evidence that alamethicin is flexible in solution, which could be a result of the helix breaking residues like proline and glycine found in the central region of the peptide (Biophys. J. 67, 1861, 1994). In order to investigate the role of proline in the dynamics of this peptide, an analog of alamethicin where proline 14 is replaced by alanine has been synthesized. Distance measurements obtained for this analog revealed that the electron-nuclear distances are longer than for native alamethicin. This data will be presented. Distance measurements obtained for another analog where both proline and glycine are replaced will also be presented.

Th-Pos295

TRANSMEMBRANE MIGRATION OF HYDROPHOBIC CHANNELL FORMING PEPTIDES IN LIPID VESICLES DETERMINED USING ^1H AND ^2H NUCLEAR MAGNETIC RESONANCE SPECTROSCOPY.((**Sajith Jayasinghe**, Melissa Barranger-Mathys, Jeffrey Ellena, Craig Franklin and David Cafiso)). Department of Chemistry and Biophysics program, University of Virginia, Charlottesville, VA 22901.

Alamethicin is a 20 amino acid peptide that forms voltage dependent ion channels in lipid bilayers. ^1H and ^2H nuclear magnetic resonance spectroscopy techniques were used to determine the transmembrane migration rate of the C-terminus of native alamethicin and a more hydrophobic analog that incorporates leucine in place of α-methylalanine (MeA). In the absence of a membrane potential the migration rate of native alamethicin was found to be no greater than 1.4×10^{-4} min^{-1}. The analog of alamethicin incorporating leucine in place of MeA was found to migrate at least 1000 times faster than the native peptide. Continuous wave power saturation EPR spectroscopy has shown that the leucine analog sits 3-4 Å deeper in the membrane than does the native peptide. The loss of hydrogen bonding between water and the C-terminus of alamethicin possibly prevents the migration of this peptide. The leucine analog does not experience such a barrier to migration as the C-terminus of the peptide is already buried in the membrane.

Th-Pos296

ALTERATIONS IN ION TRANSPORT INDUCED BY HIV-1 LENTIVIRUS LYTIC PEPTIDE-1 (LLP-1) AND gp160. ((**A.M.Comardelle***, P.J.Gatti*, D.R.Plymale*, B.Choi*, A.M.Haislip*, C.H.Norris*, C.D.Fermin*, T.P.Beary#, S.B.Tencsa#, R.C.Montelaro#, R.F.Garry*)) * - Tulane University School of Medicine, New Orleans, LA 70112, # - University of Pittsburgh School of Medicine, Pittsburgh, PA 15261

HIV-1 envelope glycoproteins gp120 and gp41 mediate several CD4-dependent activities: fusion of the viral and host cell membranes followed by virus entry, syncytium formation and single-cell lysis. The C-terminus of gp41 contains the amphipathic LLP-1 that has been shown to be cytolytic. Preliminary experiments were performed using two-electrode voltage clamping (TEVC) on Xenopus oocytes incubated with different concentrations of LLP-1. It was found that LLP-1 at concentrations 100 nM and above causes a significant loss of plasma membrane integrity. On the other hand, LLP-1 concentrations of 20-50 nM induce changes in the total transmembrane current similar to those induced by so-called "channel-forming" concentrations of bee venom melittin. To further address the question of disregulation of ion transport by HIV-1 envelope glycoproteins, transmembrane currents were studied using TEVC in Xenopus oocytes microinjected with precursor gp160 mRNA from CSF and HXBII strains of HIV-1. Whole cell outward conductance was found to increase in cells expressing gp160 for both strains of the virus. Time course and current-voltage relationship of currents associated with gp160 are similar to those of an ion channel. Tail current analysis suggests that the channel in question has a preferential permeability for K+. One mechanism by which gp160 allows HIV-1 replication, may be by alterations in K+ transport.

Th-Pos297

SYNTHESIS AND NMR STUDIES OF A MODEL CHANNEL FROM THE NICOTINIC ACETYLCHOLINE RECEPTORS. ((***K.-J. Shon**, ^C.S. Walker, ^W.R. Gray, *J. Ma,, and ^B.M. Olivera)) *Dept. of Physiology and Biophysics, Case Western Reserve Univ., Cleveland, OH 44106; ^Dept. of Biology, Univ. of Utah, S.L.C., UT 84112. (Spon. by J. Whittembury).

A model channel, based on the nicotinic acetylcholine receptors whose pentameric channel is formed by the second transmembrane domains (M2), has been designed, chemically synthesized in multimilligram quantities, and shown to retain the ability to transport ions. In building the model channel, we used a modular strategy in which M2δ and a linear template peptides were built separately, and then linked via thiol-maleimido couplings. The homopentamer from the coupling reaction was purified using the reversed-phase HPLC, demonstrated on SDS-PAGE gel to have the appropriate mass, and confirmed by mass spectrometry analysis. The model channel has been tested to form a cation selective channel once reconstituted in lipid bilayers. Currents were recorded at varying voltages ranging from +100 mV to -100 mV in a concentration gradient of 200 mM KCl (cis) / 50 mM KCl (trans), 1 mM $CaCl_2$, 10 mM HEPES, pH=7.0. Two frequent conductances, O1 and O2 (n=6) were G=48.2±1.6 pS with a reversal potential of Vm=-29.2±3.7 mV and G=91.3±2.4 pS with Vm=-30.9±2.7 mV respectively. It has been shown that the model channel in detergent micelles has a five-fold rotational symmetry around the ion conduction pathway. Preliminary NMR data supporting the feasibility of the structural studies of the model channel will be presented.

Th-Pos298

STRUCTURAL CHARACTERIZATION OF THE M2 TRANSMEMBRANE PEPTIDE BACKBONE USING SOLID STATE NMR.

((**F. A. Kovacs**, M.T. Brenneman, J. Quine and T.A. Cross)) National High Magnetic Field Laboratory, Institute of Molecular Biophysics, Department of Chemistry and Department of Mathematics, Florida State University, Tallahassee, FL 32306-4005.

M2 protein, found in influenza A virus, is believed to form a tetramer which acts as a monovalent ion channel. M2-TMP (transmembrane peptide), corresponding to the single putative transmembrane segment of M2, possesses the basic properties of M2: it adopts a primarily α-helical structure in DMPC and DOPC vesicles, has ion channel activity, is pH-voltage gated, and reversibly blocked by amantadine.

M2-TMP was modeled as an α-helix. Orientational constraints were obtained from SS NMR interactions in oriented samples, which were prepared in both DOPC and DMPC. ^{15}N chemical shift and ^{15}N-^{1}H dipolar interactions were observed for a limited number of sites. The orientation of the helix in the bilayer was characterized by 2 Euler rotations: ρ, a rotation about the helix axis, and τ, the angle between helix axis and the bilayer normal. These two parameters provided the basic information required to pack a symmetrical array of these transmembrane peptides. They were determined by rotating a model α-helix over all possible values of ρ and τ, computing the value of the SS NMR interactions for the measured sites that are related to each other by standard helical parameters, and then finding the (ρ,τ) pair which best fit the experimental data. Such an analysis showed that the helix axis was tipped by 30-35° with respect to the DMPC bilayer normal. While the data fit reasonably well to an ideal helix, a χ^2 analysis showed that this assumption is not statistically acceptable. For this reason, we have devised a mathematical method which will allow us to model non-uniform secondary structures.

Th-Pos299

ALZHEIMER'S DISEASE AMYLOID β-PROTEIN EVOKES Na^+ ENTRY ACROSS THE MEMBRANE OF UNILAMELLAR PHOSPHATIDYLSERINE (PS) BUT NOT PHOSPHATIDYLCHOLINE (PC) LIPOSOMES (J.M. Alarcón, E. Rojas and M. de la Fuente). Dept. of Physiol. Biophys., Fac. of Med., U. of Chile, Stgo., and LCBG, NIDDK, NIH, Bethesda, MD.

Incorporation of Alzheimer's amyloid β-protein (AβP) molecules into bilayer membranes leads to the formation of cation-selective channels (Arispe *et al.* PNAS. 90: 10573, 1993). To determine whether amyloid β-protein is also able to form such channels across liposomal membranes, we incubated either PS or PC unilamellar vesicles loaded with the impermeant Na^+ indicator SBFI (acid form) in a saline containing Na^+. As illustrated in the figure, the SBFI fluorescence rapidly rose to a saturating level (upper trace) after the application of 6.9 μM AβP[1-40] (arrow on the left) to PS liposomes. Since the AβP[1-40]-channel in planar bilayer membranes is cation-selective, we attribute the signal to Na^+ entry. Also shown in the figure (middle record) is the fluorescence increase elicited by AβP[1-40] added in the presence of Zn^{2+} (100 μM), and the lack of response to the peptide with the reverse sequence, *i.e.* AβP[40-1] (bottom record; 3.5 μM). Further addition of AβP[1-40] evoked a smaller signal (right arrow). These experiments were repeated using PC unilamellar liposomes with negative results. We conclude that the AβP[1-40] molecules forming the channel exhibit a preferential affinity for negatively charged PS membranes and binding sites specific for Zn^{2+}. (Supported by Fondecyt 1950774 and la Cátedra Presidencial de Chile 1996).

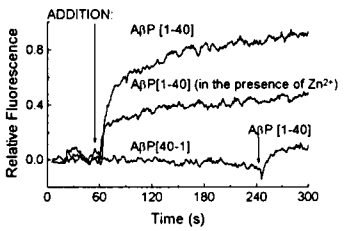

Th-Pos300

TRANSBILAYER PORE LINED WITH ACYL CHAINS: MOLECULAR MODELING OF PORE STRUCTURES USING SIMULATED ANNEALING AND RESTRAINED MOLECULAR DYNAMICS. ((**Z. Qi** and M. Sokabe)) Dept. Physiol. Nagoya Univ. Sch. Med., Nagoya 466, Japan (Spon. by A. Takai)

We have reported that cyclo((-Ala-Daba(C16)-)4, a synthetic tetrameric molecule of alanine-N'-acylated diamino benzoic acid, could form an ion channel in bilayer membranes, in which a structural model was proposed that the cyclic peptide forms an entrance and acyl chains line the wall of the channel, respectively. In the present study we made a molecular simulation on this hypothetical structure if it is energetically reasonable. An extensive conformational search was carried out using a combination of simulated annealing and restrained molecular dynamics with minimum assumption. Full conformations from the search were grouped into families using a clustering technique based on RMS fitting over the Cartesian coordinates of the atoms of the whole molecule. As a result, a conformation consistent with our electrophysiological experiments was obtained, within which pure hydrophobic acyl chains (derived from palmitic acid) line the wall of the pore across the channel to provide a cavity for the permeation of ions and the peptide ring cyclo(-Ala-Daba-)4, the only hydrophilic part of the molecule, forms an entrance of the channel at the membrane-water interface giving an ion binding site.

Th-Pos301

ESTIMATION OF LUMEN SIZE OF SYRINGOMYCIN E INDUCED ION CHANNELS BASED ON CONCENTRATION DEPENDENCE OF TRANSFERENCE NUMBERS. (Yu.A.Kaulin[1], V.V.Malev[1], L.V.Schagina[1], A.M. Feigin[2] M.P. Sidorova[3], J.Y. Takemoto[4]., J.H.Teeter[2], J.G.Brand[2]) [1]Inst. Cytol., St.Petersb., Russia;[2]Monell Chem. Senses Ctr, Philadelphia, USA; [3]St.Petersb., Univ.,Dept.Chem.,Russia;[4]Utah St. Univ., Logan, USA).

We demonstrated earlier that voltage gated ionic channels formed by syringomycin E (SRE) in planar lipid bilayers have a weak anion selectivity. The data showing that anion-cation selectivity of these channels depends on the electrolyte concentrations in bathing solutions are presented here. The selectivity was estimated by measuring zero current potentials at different concentrations of NaCl in the bathing solution on both sides of the bilayer formed from an equimolar mixture of DOPE and DOPS. The values of anion transference number were 0.83 ± 0.02, 0.77 ± 0.01, and 0.70 ± 0.01 at NaCl concentration gradients equal to 0.01/0.0025, 0.1/0.025, and 1/0.25 (mol/l), respectively. The observed dependence of channel selectivity on the concentration of NaCl allowed an estimate of internal diameter of the channel lumen. Experimentally found transference numbers are consistent with calculated values if: 1) the channel is a) not electroneutral; b) approximated by a cylinder with length equal to the thickness of lipid bilayer, and 2) the internal diameter of the channel lumen is ~3 nm. The same size of the internal diameter of the channel derives from molecular SRE dimensions taken from CPK model and the fact that at least six monomers are required for channel formation.

Th-Pos302

CHANNEL-LIKE ACTIVITIES OF AN ANTIMICROBIAL PEPTIDE, BUFORIN II, OBSERVED IN PLANAR LIPID BILAYER

((**J.H. Shin**, E.J. Park, and C.K. Suh)) Department of Physiology and Biophysics, Inha University College of Medicine, Inchon 402-751, KOREA

Buforin II is a peptide with 21 amino acid residues isolated from frog stomach. It has an antimicrobial activity with a relatively high potency (1). One of the explanations for the antimicrobial activity of the peptides is to form a pore in the plasmamembrane, thereby destroying the membrane potential and causing the cell to rupture. We used the planar lipid bilayer reconstitution technique to test whether channel-like activities are induced by buforin II. Two compartments, the cis and trans, separated by a lipid bilayer with a capacitance size of around 200pF, were filled with 150mM and 5mM NaCl, respectively. Upon adding buforin II in the cis, a steady current without any gating behavior was observed (n=5). This current was cation specific. When decreasing the driving force by increasing the concentration of the trans NaCl, the size of the current decreased accordingly. The size of the slope conductance of the stable steady current was over 300pS (n=2), and step-like changes in the steady current were observed in the direction of both increasing and decreasing the size of the current (n=4). The step-like change was often accompanied by channel-like gating between two levels. The appearance of the current was dependent upon the concentration of buforin II added, and observed at submicromolar level of buforin II, which is consistent with the data from the antimicrobial assay (1). These results suggest that the mechanism of the antimicrobial activity of buforin II is also due to forming a pore in the plasmamembrane of microorganisms.

1. Park et al. (1996) *BBRC* 218: 408

Th-Pos303

FLUORESCENCE MEASUREMENT OF PEPTIDE CHANNEL GATING IN PLANAR LIPID BILAYER.

((T. Yamada, **Y. Hanyu*** and G. Matsumoto)) *PRESTO (Japan Science and Technology Corporation) and Electrotechnical Laboratory, Tsukuba 305, Japan. (Spon. by M. Ichikawa)

We have developed a experimental system which can measure both optical and electrical signals from artificial planar lipid bilayers. Voltage-dependent conformational changes of the peptide channels was studied by fluorescence measurements with this system. Folded planar bilayers are made in the specially-designed Teflon chamber which has optical windows. Excitation laser light is focused on the restricted area in artificial planar lipid bilayers. Fluorescence emission from this area is collected to the photomultiplier and its intensity is measured with a photon counting system. Fluorescence-labeled melittin was incorporated into bilayers. Under controlling membrane potentials, ionic current and fluorescence emission were measured. Movement of N-terminals into bilayers with voltage gating was studied.

Th-Pos304

SQUALAMINE INTERACTS WITH ANIONIC PHOSPHOLIPIDS IN LARGE UNILAMELLAR VESICLES ((B.S. Selinsky, Z. Zhou, and S.R. Jones)) Department of Chemistry, Villanova University, Villanova, PA 19085.

Squalamine is a broad spectrum antimicrobial compound isolated from the dogfish shark *Squalus acanthias*. Squalamine releases trapped carboxyfluorescein from large unilamellar vesicles (LUVs) comprised of anionic phospholipids. The squalamine concentration required for dye release is dependent upon the anionic phospholipid, and increases in the order PG<PS<CL. Squalamine causes incomplete dye release from PC LUVs, for reasons which are not yet apparent. A series of studies were performed to attempt to explain incomplete dye release from PC LUVs. Negative stain electron microscopy shows no morphological changes in LUVs after addition of squalamine to effect 100% dye leakage in one minute. There is no indication of squalamine-induced fusion of PC vesicles, as measured by a contents-mixing assay. Using fluorescently-labeled lipid and fluorescence resonance energy transfer, there is no evidence of lipid mixing at squalamine concentrations which effect 100% dye leakage in one minute. We propose that dye leakage from LUVs caused by squalamine is the result of localized membrane disruption caused by squalamine aggregates. Aggregation of squalamine in membranes is promoted by anionic lipids, but inhibited by zwitterionic lipids. This work was supported by NIH R15 AI39757-01 and by Magainin Pharmaceuticals, Inc..

PHYSICAL PROPERTIES OF BILAYERS II

Th-Pos305

LATERAL LIPID ORGANIZATION IN POLYUNSATURATED MEMBRANES

((**D. Huster**[1,2], J.A. Barry[1], and K. Gawrisch[1])) [1]LMBB, NIAAA, NIH Rockville, MD 20852, USA, [2]University of Leipzig, Institute of Medical Physics and Biophysics, D-04103 Leipzig, GERMANY

The influence of lipid headgroups and cholesterol on chain order in polyunsaturated membranes has been investigated by ^{2}H NMR on 18:0_{d35}-22:6 PC/PE/PS/cholesterol (4/4/1/1, mol/mol/mol/mol) membranes. Addition of PE, PS, and cholesterol to membranes increased chain order of all lipids compared to pure polyunsaturated PC membranes. In PC/PE mixtures cholesterol interacts preferentially with PC. Addition of 5 mM Ca^{2+} results in an insignificant order increase of all lipids without indication of lateral phase segregation. More detailed information on nearest neighbor interaction in membranes was obtained with magic-angle spinning two-dimensional NOE spectroscopy. By diluting protonated lipids in a deuterated matrix, we determined that the major contribution to crosspeak intensity between lipid resonances is of intermolecular origin. Intensity differences between cholesterol-to-saturated vs. -polyunsaturated chain crosspeaks suggest that cholesterol interacts preferentially with saturated chains.

Th-Pos306

FORMATION OF GIANT LIPOSOMES HELPED BY DIVALENT ALKALI CATION. ((K. **Akashi**[1], H. Miyata[1], H. Itoh[2], K. Kinosita, Jr.[1])) [1]Dept. Phys., Fac. Sci. Tech., Keio Univ., Hiyoshi 3-14-1, Yokohama 223, Japan; [2]Tsukuba Res. Lab., Hamamatsu Photonics K. K., Tokodai, Ibaragi 300-26, Japan.

In the formation of giant liposomes, electrical charges on the lipid membranes seem to play an important role by exerting mutual repulsion between the membranes. Without the charges, giant liposomes are rarely formed in ionic conditions over 1 mM KCl. However, if a charged lipid, such as phosphatidylglycerol (PG, negatively charged), is added into the lipid composition, a large number of unilamellar liposomes, sizing up to several tens of micrometers, can be produced even at high salt concentrations(~ 100 mM KCl). In this study, we found that divalent cations such as Ca^{2+} helped the formation of giant liposomes. In solutions of 1~30 mM $CaCl_2$ or $MgCl_2$, a lot of giant unilamellar liposomes could be formed even with electrically neutral phosphatidylcholine(PC) alone. This is presumably because, as known from X-ray diffraction, NMR, etc., Ca^{2+}(or Mg^{2+}) binds to neutral phospholipids and make them positively charged. When 10% PG was mixed with PC, giant liposomes were found not in 10mM $CaCl_2$ but in 30mM $CaCl_2$. Our interpretation is that an enough amount of Ca^{2+} is needed to overcome the negative charge of PG and reverse the polarity on the membrane. These results show that the electrical charges required for the repulsion can be of extrinsic origin.

Th-Pos307

MULTIVESICULAR LIPOSOME ((S. Keller, D. Strahler, M. Spector, S. Walker, M. Kennedy, **J. A. Zasadzinski**, M. B. Sankaram*)) Department of Chemical Engineering, U. California, Santa Barbara, CA 93106; *DepoTech Corporation, 10450 Science Center Drive, San Diego, California 92121.

Freeze-fracture electron microscopy was used to characterize the microstructure of a novel multivesicular liposome (MVL) under investigation as a depot-type drug delivery vehicle. The interior of the MVL includes bilayer enclosed, water-filled compartments surrounded by an encapsulating outer membrane. The contacts between compartments exhibit tetrahedral coordination analogous to a gas-liquid foam that persists to the bilayer level and the compartments take on a variety of polyhedral shapes and sizes. The distribution of polyhedra is nearly identical to theoretical predictions and computer simulations of polytetrahedral random close packing. The MVL structure is one of the first experimental visualizations of the polytetrahedral random close packed molecular structure predicted for liquids and metallic glasses. We have followed the evolution of the MVL with time, and the relationship between structure and release of MVL-encapsulated cytarabine following incubation at 37°C in both human serum and artificial cerebral spinal fluid. Over 9 days, the internal compartments in the MVL grew in size and the average number of compartments per MVL decreased as cytarabine was released, suggesting that internal coalescence plays a role in drug release. The overall MVL size decreased during aging, and some particles adopted irregular shapes. However, a significant fraction of MVL retained their original multivesicular structure even after near-complete release of cytarabine. These results suggest that, at least for cytarabine, permeation of drug through the vesicle membranes is an important determinant of in vitro drug release.

Th-Pos308

COMBINATION OF ANTITUMOR ETHER LIPID WITH LIPIDS OF COMPLEMENTARY MOLECULAR SHAPE REDUCES ITS TRANSFER TO RBCs. ((**Walter R. Perkins**, Richard B. Dause, Xingong Li, J. Craig Franklin, Donna J. Cabral-Lilly, Yan Zha, Eugene H. Dank, Eric Mayhew, & Andrew S. Janoff))

The Liposome Company, Inc., 1 Research Way, Princeton, New Jersey 08540

We explored the use of lipid packing parameters to reduce the toxicity (hemolysis) of the antitumor ether lipid 1-*O*-octadecyl-2-*O*-sn-methyl-glycero-3-phosphorylcholine (ET-18-OCH_3) by designing structurally optimized liposomes. We postulated that combination of ET-18-OCH_3, which alone forms micellar structures, with lipid molecules of complementary molecular shape (opposite headgroup/chain volume) would likely yield a stable lamellar phase from which ET-18-OCH_3 exchange to red blood cell (RBCs) membranes could be reduced. To quantitate the degree of shape complementarity, we used a Langmuir trough and measured the mean molecular area per molecule (MMAM) for monolayers comprised of ET-18-OCH_3 and binary mixtures of varying mole percentage ET-18-OCH_3. The greatest degree of shape complementarity was observed with cholesterol which was surprisingly better, based on theoretical packing parameters, than DOPE; the order of complementarity was cholesterol >> DOPE > POPC ≈ DOPC. ^{31}P-NMR and TLC analyses of aqueous suspensions of ET-18-OCH_3 (40 mole %) with the host lipids revealed them to all be lamellar phase. For ET-18-OCH_3 at 40 mole % in liposomes, the hemolytic activity followed the trend of the reduction in MMAM and was least for the ET-18-OCH_3/cholesterol system (H_{50} = 661μM ET-18-OCH_3) followed by ET-18-OCH_3/DOPE (H_{50} = 91μM) and mixtures with POPC and DOPC which were comparable at H_{50} = 26μM and 38μM, respectively; the H_{50} concentration for free ET-18-OCH_3 was 16μM. This work suggests that cholesterol will be important in the design of multi-component liposomes necessary for site specific delivery of ET-18-OCH_3 in cancer chemotherapy.

Th-Pos309

INFLUENCE OF SIZE AND STERIC CROWDING ON SURFACE BINDING OF LIPID-COUPLED POLYETHYLENEGLYCOLS

((**Sybille Rex**, John R. Silvius and Martin Zuckermann)) Departments of Biochemistry and Physics, McGill University, Montréal, Québec, Canada

The binding of macromolecules to membrane surfaces may be governed not only by attractive hydrophobic and electrostatic interactions but also by opposing factors such as steric interactions with other molecules at the surface and the potential loss of macromolecular translational, rotational and/or conformational entropy in the surface-bound state. To examine these effects in a simple and controllable system, we are measuring the binding of different fluorescent (N-acylpeptide-macromolecule) conjugates to 'bare' or polymer-grafted large unilamellar lipid vesicles. Within a series of conjugates incorporating polyethyleneglycols (PEGs), the affinity of binding to 'bare' vesicles decreases by over 40-fold as the length of the PEG moiety increases from 1 to 115 monomer units. Measurements of the affinity of binding of fluorescent PEG-5000 or -2000 conjugates to vesicles incorporating the analogous PEG-phosphatidylethanolamines (PEG-PEs) permit an assessment of the activity of the surface-grafted polymers as a function of their surface density. Using this approach we observe a substantial variation of the activity of surface-grafted PEG-5000 polymers in the range 0-8% grafted PEG, with a much more modest variation observed for grafted PEG-2000 residues in the range 0-10%. While our results agree qualitatively with polymer theory at low polymer densities, the data obtained to date do not clearly demonstrate a mushroom-to-brush transition of the grafted PEG residues. (Supported by les Fonds FCAR du Québec).

Th-Pos310

ATOMIC FORCE MICROSCOPY IMAGING OF POLYETHYLENE GLYCOL-DISTEAROYL-PHOSPHATIDYLETHANOLAMINE AT LIPID-WATER INTERFACE.

((**A. Sen**, P. Chandaroy and S.W. Hui)) Department of Biophysics, Roswell Park Cancer Institute, Buffalo, NY 14263.

Polyethylene glycol conjugated phosphatidylethanolamine (PEG-PE) is commonly mixed with other lipids and used for preparation of "stealth" liposomes for drug delivery. A mushroom model has been proposed for the conformation of the PEG at the lipid-water interface, but this has not been confirmed by imaging. We have imaged PEG-PE (0.25 to 0.75 mole% PEG-PE, 5000 MW PEG) mixed with dipalmitoyl-dimethylphosphatidylethanolamine (DMetPE) using atomic force microscopy (AFM). First a monolayer of dipalmitoyl-PE (20mN/m surface pressure) and next a monolayer of mixed PEG-PE/DMetPE (5-8mN/m) were transferred onto clean glass coverslip (or freshly cleaved mica). AFM was performed in non-contact mode under water, using a Topometrix Explorer microscope. Particles of 15-20 nm diameter (1-3 nm height) were seen at the lipid surface. The sample with 0.25 mole% PEG-PE had far fewer of the particles as compared to that with 0.75 mole% PEG-PE. The volumes of these particles (250 to 500 nm^3) were similar to the volume for PEG predicted according to the mushroom model (300 nm^3 for 5000 MW PEG). The similarity in volumes of the particles (approximated by a disk shape) and the increasing numbers with PEG-PE concentration, suggest that the particles are individual PEG molecules at the lipid-water interface. We are currently examining the structure and distribution of the particles at higher resolutions to determine any fine structure.

Th-Pos311

THERMOTROPIC BEHAVIOR OF GALACTOSYLCERAMIDES WITH MONOUNSATURATED FATTY ACYL CHAINS.

((**V. S. Kulkarni** and R. E. Brown)) The Hormel Institute, University of Minnesota, Austin, MN

Galactosylceramides (GalCer) having monounsaturated acyl chains with the general formula "X:$1^{\Delta(X-9)cis}$ GalCer" (X=carbon atoms; here X=24, 22, 20, or 18) were prepared by semi-synthesis and their thermotropic phase behaviors were investigated in excess water by differential scanning calorimetry. Initial heating scans of 24:1 GalCer (incubated at 4°C for 2h) showed a single endothermic peak centered at (T_m) 66.7°C with an enthalpy (ΔH) of ~14.2 kcal/mol. Subsequent heating scans (incubated at 4°C for 100 min) showed two endothermic transitions, T_{m1}=~59°C (ΔH_1=6-7 kcal/mol) and T_{m2}=~64°C (ΔH_2=~3 kcal/mol). However, heating scans obtained after incubating the same sample at ~23°C for a minimum of 5 days showed thermograms identical with the initial scans (single peak, T_m=66.7°C, ΔH=14.9 kcal/mol). A similar thermotropic pattern was observed for 22:1 GalCer in that the first scan showed a single endotherm (T_m=59.7°C, ΔH=5.4 kcal/mol), subsequent heating scans showed two endothermic peaks (T_{m1}=53.2°C, ΔH_1=1.5 kcal/mol; T_{m2}=59.3°C, ΔH_2=3.2 kcal/mol), and heating scans obtained after incubating at 23°C for 4 days were identical to the first scan. However, the behavior of 20:1 GalCer (T_m=61.2°C, ΔH=7.3 kcal/mol) or 18:1 GalCer (T_m=47.3°C, ΔH=14.05 kcal/mol) showed no variation with respect to incubation time and temperature. Chain inequivalence ratios ($\Delta C/CL$) were determined to be 0.46, 0.41, 0.33, and 0.24 for 24:1, 22:1, 20:1, and 18:1 GalCer, respectively, following Huang's formulism. Accordingly, we predict a mixed-interdigitated bilayer motif for 24:1 GalCer but partially-interdigitated motifs for 22:1, 20:1 and 18:1 GalCer. [Support: USPHS GM-45928 and the Hormel Fndn.]

Th-Pos312

ROLE OF DEXAMETHASONE: LIPID INTERACTION IN PULMONARY SURFACTANT

((**[1]Campbell, Robert B.** ,[2]Balasubramanian, Sathyamangalam and [1,2] Straubinger, Robert M.)) [1]Department of Biophysics @ Roswell Park Cancer Institute ;[2] Department of Pharmaceutics, State University of NY @ Buffalo).

Respiratory distress syndrome (RDS), is a problem faced by many preterm neonates, and has been the focus of intense biomedical research. Corticosteroid treatment regimens have been designed to alter lung surfactant properties such as lowering the surface tension at the alveoli air-water interface. Unfortunately, very little is understood about the mechansim of steroid action at the molecular level. Our primary aim is to investigate the molecular mechanisms of dexamethasone-lipid interaction, and to investigate the relevance of these interactions to the therapy of RDS. Circular dichroism, Differential scanning calorimetry, and Fluorescence spectroscopy (DPH and Laurdan dependent polarization) were used to study dexamethasone-lipid interaction. The studies demonstrated that dexamethasone is preferentially located near the membrane interface, perturbing the hydration of the bilayer. Based on the results, the alteration of hydration-repulsion forces by dexamethasone((lipid/drug (160/1)) will destabilize the bilayer, leading to the formation of non-bilayer intermediates and promoting the spreading of the lipid at the air-water interface. Such a mechanism could play an important role in the action of dexamethasone-lipid physical state. We predict a mechanism which is at least in part responsible for the spreading of DPPC at the air-water interface along with other pharmacological effects.

Key words: RDS, Dexamethasone, non-bilayer intermediates, drug-lipid interaction, drug delivery

Th-Pos313

INTERACTIONS OF CYTOCHROME C WITH RECONSTITUTED CYTOCHROME C OXIDASE MEMBRANES. EVIDENCE FOR INCREASED CYTOCHROME C OXIDASE BOUNDARY LIPID INDUCED BY CYTOCHROME C.

((**Jörg H. Kleinschmidt***, Gary L. Powell** and Derek Marsh***)) *Dept. of Mol. Physiol. and Biol. Phys., Univ. of Virginia, Charlottesville, VA 22906-0011, **Dept. of Biological Sciences, Clemson Univ., Clemson, SC 29634-1903, ***MPI f. biophys. Chemie Göttingen, Abt. Spektroskopie, D-37077 Göttingen, Germany

Cytochrome oxidase isolated from beef-heart mitochondria has been reconstituted into DMPG bilayers at various enzyme/DMPG ratios. In addition, fractions of these samples were incubated with excess cytochrome c in buffer. Membrane complexes were then centrifuged to study lipid-protein interactions at 36 °C by spin label electron spin resonance (ESR) spectroscopy using phosphatidylglycerol spin-labeled at position 14 of the sn-2 acylchain (14-PGSL). For comparison, ESR spectra of this spin-label were recorded for model membranes without cytochrome oxidase but with cytochrome c. All samples were finally analyzed for lipid, cytochrome oxidase and cytochrome c content. It was found that the motionally restricted spin-label component in reconstituted cytchrome oxidase/DMPG bilayers corresponds to 55-60 immobilized lipids per cytochrome oxidase molecule independent of the total amount of DMPG per cytochrome oxidase used in a particular sample. Cytochrome c alone did not induce a second component in 14-PGSL spectra in pure DMPG bilayers at 36 °C. However, when cytochrome c was added to reconstituted cytochrome oxidase/DMPG membranes the fraction of motionally restricted spin label increased on binding of cytochrome c indicating structural changes in the membrane. Depending on the DMPG / cytochrome oxidase ratio, up to 115 immobilized lipid molecules / cytochrome oxidase were found when cytochrome c was present. Furthermore, analysis of the DMPG, cytochrome oxidase and cytochrome c content of all samples revealed that under the chosen conditions cytochrome c binds to ~ 9 negatively charged DMPG molecules independent of the cytochrome oxidase content in reconstituted systems.

Th-Pos314

THE ORIGIN OF THE LAG PERIOD IN THE PHOSPHOLIPASE C CLEAVAGE OF PHOSPHOLIPIDS IN MEMBRANES. CONCOMITANT VESICLE AGGREGATION AND ENZYME ACTIVATION.

(**G. Basáñez, J.L. Nieva, F.M. Goñi and A. Alonso**)) Dept. Biochemistry, Univ. Basque Country, E-48080 Bilbao, Spain. (Spon. by E. Padrós).

When phospholipase C is added to a suspension of LUV of egg phosphatidylcholine, maximal rates of hydrolysis occur only after a latency period. For a given vesicle concentration, the lag time may vary as a function of different factors, but activation occurs at a fixed molar fraction of diacylglycerol produced. Lag times decrease gradually with vesicle size, and also with the amount of diacylglycerol present in the bilayers when it is mixed with phospholipid prior to enzyme addition. Parallel recordings of enzyme activity and suspension turbidity reveal that in all cases the latency period ends concomitantly with the start of a process of vesicle aggregation. Both the lag time and the amount of diacylglycerol formed before activation decrease with vesicle concentration, suggesting that enzyme activation is somehow related to vesicle aggregation. The latency period of phospholipase C may be explained in terms of a hypothesis according to which: (a) full enzyme activity requires the presence of membrane surface irregularities of defects, (b) the diacylglycerol generated in the lag phase produces some kind of phase separation, with the formation of diacylglycerol-rich 'patches' or domains, (c) vesicles aggregate through contacts between those 'patches', and (d) aggregation causes the surface inhomogeneities that allow fast enzyme activity.

Th-Pos315

INTERACTION OF AMPHOTERICIN-B WITH PHOSPHOLIPIDS: INFLUENCE OF SOLVENT COMPOSITION AND INGREDIENT CONCENTRATIONS. ((F. Bedu-Addo, S. P. Bhamidipati, E. Kaisheva, J. Pawelchak, Jim Slater* and A. Zhang)) The Liposome Company Inc., Princeton, NJ 08540 and * GeneMedicine, Woodlands, TX

The association of amphotericin-B with phospholipids in aqueous medium results in the formation of a colloidal dispersion/suspension. We have used a mixed solvent system (DMSO and $MeCl_2$) based on the solubility properties of amphotericin-B and the phospholipids to investigate the interactions between these two components at the molecular level prior to the introduction of the aqueous medium. Preliminary circular dichroism studies in the mixed solvent system established complexation of amphotericin-B with the phospholipids and suggested formation of "embryonic nuclei" or "particles" as a result of this association that may be related to the colloidal dispersion in the aqueous medium. Hence, we constructed a ternary phase diagram to understand the initial formation, stability and kinetic profiles of the particles resulting from the association of amphotericin-B with phospholipids as a function of the solvent composition , amphotericin-B and lipid concentrations using the quasielastic light scattering (QELS) and circular dichroism(CD). The kinetic profiles and initial size of the "embryonic particles" and their relation to the colloidal dispersions of amphotericin-B will be discussed.

Th-Pos316

QUANTITATIVE HPLC STUDIES OF THE LIPID COMPOSITION IMPLY NON-EQUILIBRIUM MORPHOLOGY DURING THE LAG PHASE OF PHOSPHOLIPASE A_2 HYDROLYSIS OF LIPID VESICLES

T. Hønger, K. Jørgensen, J. Klausen, and O.G. Mouritsen
Department of Chemistry, The Technical University of Denmark, DK-2800 Lyngby, Denmark

High performance liquid chromatography (HPLC) and pH-stat titration are used in combination with intrinsic phospholipase A_2 (PLA_2) fluorescence and 90° light scattering to characterize the hydrolysis reaction time course of PLA_2 catalyzed hydrolysis of di-myristoyl-phosphatidylcholine (DMPC) or di-palmitoyl-phosphatidylcholine (DPPC) in large unilamellar vesicles (LUV). We use the change in PLA_2 fluorescence to define the transition from the lag phase to the regime of rapid hydrolysis. Our results demonstrate that the pH-stat method underestimates the degree of hydrolysis in the lag phase of the reaction. HPLC analysis shows that 30 mole% of the available substrate has been hydrolyzed at the end of the lag phase while this so-called critical mole fraction of hydrolysis is less than 15 mole% by the pH-stat method. Thermodynamic properties of ternary lipid mixtures of DPPC (or DMPC) and its PLA_2 hydrolysis products indicate that 10 mole% hydrolysis products destabilize an LUV structure. Consequently, the present HPLC quantitations of the fraction of hydrolysis during the lag phase imply that the hydrolysis reaction is out of equilibrium with respect to the lipid morphology. A modelling of the PLA_2 reaction kinetics should take this finding into account.

Th-Pos317

STUDIES OF THE THERMOTROPIC PHASE BEHAVIOR AND THE MISCIBILITY OF THE POLAR LIPIDS OF THE *ACHOLEPLASMA LAIDLAWII* MEMBRANE: ((EE Loon Tham, Ruthven N.A.H. Lewis and Ronald N. McElhaney)) Department of Biochemistry, University of Alberta, Edmonton, Alberta, Canada.

We have examined the thermotropic phase behavior of aqueous dispersions of the total polar lipid of elaidate-homogeneous *Acholeplasma laidlawii* B membranes, of the monoglucosyldiacylglycerol (MGDG), diglucosyldiacyl-glycerol (DGDG) and phosphatidylglycerol (PG) components thereof, and of binary mixtures of those components by a combination of DSC, FTIR spectroscopy, and ^{31}P-NMR spectroscopy. We find that the glycolipid components readily form highly ordered, poorly hydrated, lamellar crystalline phases when cooled to gel state temperatures and that they are poorly miscible with each other in all proportions. The PG component does not form crystalline phases under the conditions examined, and seems to be freely miscible with MGDG, and with DGDG only when present excess of 20-25 mol percent. However, the incorporation of relatively small (10-15 mol %) amounts of PG into model membranes derived from an equimolar mixture of MGDG and DGDG seems to repress both aggregation and lateral phase separation. Since PG is often the dominant anionic lipid present in glycolipid-containing procaryotic membranes, we suggest that aside from functions specific to its negative charge, PG may also play an important role in maintaining the structural cohesion of those membranes.
(Supported by the Medical Research Council of Canada, and by the Alberta Heritage Foundation for Medical Research.)

Th-Pos318

STUDIES OF BINARY MIXTURES OF DIMYRISTOYL PHOSPHATIDYLCHOLINE AND DIMYRISTOYL PHOSPHATIDYLGLYCEROL: EVIDENCE FOR THE FORMATION OF MOLECULAR COMPLEXES IN MIXED PC:PG BILAYERS. ((Yuan-Peng Zhang, Ruthven N.A.H. Lewis and Ronald N. McElhaney)) Department of Biochemistry, University of Alberta, Edmonton, Alberta, Canada.

The thermotropic phase behavior of binary mixtures of dimyristoyl phosphatidylcholine (DMPC) and dimyristoyl phosphatidylglycerol (DMPG) were studied by differential scanning calorimetry, FTIR spectroscopy and ^{31}P-NMR spectroscopy. Our calorimetric studies indicate that highly cooperative gel/ liquid-crystalline phase transition endotherms are observed over the entire range of mixtures, indicating that the two lipids are freely miscible in all proportions. However, the gel/liquid-crystalline phase transition temperature is not a linear function of mixture composition and attains its maximal value with the equimolar DMPC:DMPG mixture. Also, all DMPC:DMPG mixtures form highly ordered crystal-like phases which, as judged by FTIR spectroscopy, are structurally distinct from those formed by either of the pure lipids. Our results indicate that the two lipids do not mix ideally. Instead, the data seem more compatible with the idea that phosphatidylcholines and phosphatidylglycerols form "molecular complexes" when mixed in lipid bilayers.

(Supported by the Medical Research Council of Canada and the Alberta Heritage Foundation for Medical Research.)

Th-Pos319

X-RAY STRUCTURAL CHARACTERIZATION OF THE SUB-MAIN TRANSITION IN MULTILAMELLAR PHOSPHATIDYLCHOLINE LIPOSOMES

Karin Pressl[1], Kent Jørgensen[2], and Peter Laggner[1]
[1]Institute of Biophysics and X-ray Structure Research, Austrian Academy of Sciences, A-8010 Graz, Austria
[2]Department of Pharmaceutics, The Royal Danish School of Pharmacy, DK-2100 Copenhagen, Denmark

Simultaneous X-ray small- and wide-angle (SWAX) diffraction was used to characterize the structural changes involved in the sub-main transition taking place in fully hydrated $DC_{17}PC$ and $DC_{18}PC$ lipid bilayers (Jørgensen, K., BBA, (1995) 1240, 111). The SAX diffraction patterns show a clear increase in long-range multilamellar lattice order. At the same time the WAX data indicate a positional averaging of the orthorhombic hydrocarbon chain packing demonstrated to exist below the sub-main transition, towards a hexagonal symmetry above the transition. The effects of salt (KCl) on the appearance of the sub-main transition were investigated and revealed an enhancement of the transition features. This is most clearly seen by a sharper discontinuity in the multilamellar packing. The concomitant changes in the hydrocarbon lattice are enhanced due to a more ordered orthorhombic symmetry in the ripple phase below the sub-main transition. The sub-main transition does not abolish the characteristic features of a rippled phase.

Th-Pos320

ON THE MAIN TRANSITION OF FULLY HYDRATED DIACYL PEs - AN X-RAY DIFFRACTION STUDY ((F. Richter, M. Rappolt, **G. Rapp**)) EMBL Outstaton at DESY, Notkestr. 85, D-22603 Hamburg

The main transition of phosphoethanolamines reveals several steps (1-3). In X-ray diffraction experiments three steps on heating and four on cooling have been distinguished. A model explaining this sequence, their relative width and cooperativity and the hysteresis observed was given (4). In the present study reflections up to the 6th order were recorded in aqueous dispersions of DMPE in the gel (L_β) and liquid crystalline phase (L_α) and during the transition. In the L_α phase the reflections broaden with increasing temperature, in the L_β phase the peak width does not depend on temperature. In the transition region the reflections are only slightly broader than in the pure phase region. Only in the L_α, but not in the L_β phase, an increase in peak width with increasing order of the Bragg reflections is observable which is an indication of disorder of the 2nd kind. The sum of correlations lengths of the two phases during the transition is larger than the correlation length in the pure phase regions. This is evidence that the transition does not proceed shell by shell and it is suggested that at the onset of the transition the rising phase grows radially (most likely along defects) followed by a tangential growth in the multilamellar vesicle. [1] Chowdhry et al. (1984) Biophys. J. 45, 901 [2] Yao et al. (1992) Biophys. J. 61, 683 [3] Tenchov et al. (1989) Biophys J. 56, 757 [4] Rappolt & Rapp (1996) Ber Bunsenges. Phys. Chem. 100, 1153

Th-Pos321

PHASE TRANSITION TEMPERATURES AND SIMULATED STRUCTURES OF DIENOIC PHOSPHATIDYLETHANOLAMINES. ((C. Huang, G. Wang, H-n. Lin and **S. Li**)) Dept. Biochem., Univ. of Virginia, Charlottesville, VA 22908.

The chain melting temperature (T_m)-structure relationships are sought for lipids in which the positions of the two *cis* double bonds ($2\Delta^{n,m}$) are varied systematically along the *sn*-2 acyl chain of phosphatidylethanolamines (PE). Specifically, three series of *sn*-1 saturated/*sn*-2 diunsaturated C(X):C(Y:$2\Delta^{n,m}$)PE were first semisynthesized, where X=16, 18, 20, 22, and 24 carbon atoms, and Y(n,m)= 18(9,12),20(11,14),and 22(13,16). The T_m was determined by differential scanning carlorimetry. For the series of C(X):C(20:$2\Delta^{11,14}$)PE where X=16,18,20,22, and 24, the T_m values are 13.0, 18.5, 22.2, 23.8, and 25.6°C, respectively.The structures of the various dienoic PEs in the gel-state bilayer were simulated by the molecular mechanics method (Li, S. and Huang, C. (1996) J. Comput. Chem. 17, 1013),giving rise to a general structure model of a crankshift-like kink motif for the *sn*-2 acyl chain. Consequently,the unsaturated dienoic PE can be characterized by the following structural parameters: ΔC=X-Y+3.5, US=m-3.5, LS=Y-1-m, and N=X+Y-2.5. The definitions of these structural parameters are similar to those used in monoenoic lipids (Wang *et al.*(1995) JBC 270, 22738). The variation in T_m with changes in the structural parameters for the 15 dienoic PE species under study was analyzed by multiple regression analysis, yielding T_m=184.3-5746.4(1/N) + 46.0(ΔC/(N+ΔC)) - 19.3(ΔC/LS). This equation thus extends the general T_m-structure relationships derived earlier for saturated and monoenoic lipids. In addition, this equation also implies that the simulated lipid conformation with a kinked *sn*-2 acyl chain is a valid approximation for the molecular structure of dienoic PE packed in the gel-state bilayer. (Supported by NIH Grant GM-17452)

Th-Pos322

TWO-PHOTON FLUORESCENCE MICROSCOPY OF LAURDAN GP DOMAINS IN BIOLOGICAL MEMBRANES USING POLARIZED LASER EXCITATION. ((**Tiziana Parasassi**, Moshe Levi, Weiming Yu and Enrico Gratton)) CNR, Roma, Italy; U of Texas SW Med Ctr and DVAMC, Dallas, TX; and LFD, U of Illinois at Urbana-Champaign, IL.

Two-photon microscopy images of membranes of whole red blood cells, renal tubular cells (OK cells) and purified rat renal brush border and basolateral membranes labeled with LAURDAN show a fine texture of coexisting regions of different generalized polarization (GP) values. By measuring the relative water content of the membrane, LAURDAN GP function also monitors the lipid molecular dynamics or "fluidity". We have used polarized laser excitation. In images with well defined membrane orientation, such as the erythrocyte cell sections, the association of high GP with high polarization photoselection allows the attribution of coexisting GP values to lipid domains of different dynamical properties. Due to the presence of strong fluorescence from the cytoplasmic membranes, the interpretation of the membrane GP texture in images of renal tubular cells is more complex. After masking the cytoplasmic membranes, analysis of the images of red blood cells and of renal tubular cells lead to the conclusion that the coexisting regions of different GP values, i.e., of different "fluidity", have dimensions comparable to the microscope resolution in red blood cells and smaller than the microscope resolution (about 200 nm) in renal tubular cells. For their complex and mostly unknown morphology, the presence of GP domains in rat renal brush border and basolateral membranes is of difficult interpretation. Nevertheless, by plotting selected GP values, different membrane structures become apparent. (Supported by grants from NIH, VA, and CNR).

Th-Pos323

TEMPERATURE AND IONIC STRENGTH DEPENDENT SURFACE IONIZATION IN DMPG LIPOSOMES. ((K.A. Riske[1], M.J. Politi[2], W.F. Reed[3] and **M.T. Lamy-Freund**[1])) Institutes of [1]Physics and [2]Chemistry, Universidade de São Paulo, CP 66318, CEP 05389-970, SP, Brazil, and [3]Department of Physics, Tulane University, New Orleans, LA, USA.

The thermotropic behavior of aqueous suspensions of the anionic lipid DMPG (dimyristoyl phosphatidylglycerol) was studied by EPR of spin labels incorporated in the liposomes and by static light scattering. As expected, spin labels placed at different positions of the lipid bilayer monitor the gel to liquid crystal transition. The temperature of the main transition (Tm) was found to increase with the increase of the ionic strength. Light scattering indicated that bellow Tm the liposomes aggregate, yielding a negative second virial coefficient A_2, and particles of large molecular weight. At the phase transition, the conductivity was found to increase markedly, A_2 became positive and the particle molecular weight decreased, indicating a non-aggregated state. For low ionic strength, a DMPG second temperature transition could be monitored by both light scattering and conductivity. At the post-transition (Tp), the conductivity decreased, A_2 became negative and the molecular weight increased again. Both the main and the post transitions were found to be reversible. While the results obtained at the main transition could be understood by considering an increase in headgroup ionization triggered by the melting of the hydrocarbon chains, the mechanism for recondensation of headgroup ions at the upper temperature is still unclear. (Financial support: FAPESP, CNPq and FINEP).

Th-Pos324

EVIDENCE FOR SUPERLATTICE-LIKE LATERAL ORGANIZATION IN FLUID PHOSPHATIDYLCHOLINE-PHOSPHATIDYLETHANOLAMINE BILAYERS. ((**K.H. Cheng**, M. Ruonala, J. Virtanen and P. Somerharju)) Texas Tech U., Lubbock, TX, UC-Irvine, CA, and U. Helsinki, Finland.

Recently, evidence for cholesterol molecules to adapt regular superlattice-like distributions in fluid phosphatidylcholine (PC) /cholesterol bilayers has been provided (*Chong, 1994; Tang et al., 1995, Parasassi et al., 1995, Virtanen et al., 1995*). To study whether such superlattice like arrangements of lipids would be present also in other lipid bilayers, we studied the physical property of mixed PC and phosphatidylethanolamine (PE) membranes as a function of the PE composition by using an intramolecular dynamic probe, dipyrenylphosphatidylcholine, as a reporter. Significant deviations in the fluorescence excimer-to-monomer intensity ratio were observed at particular PE mole fractions. Most of those fractions, such as 0.04, 0.11, 0.16, 0.26, 0.33, 0.66, 0.75, 0.86, 0.90 and 0.94, coincide with the critical mole fractions predicted by a headgroup hexagonal superlattice model. Minimization of packing defects due to inbalance between the (intrinsic) headgroup and acyl-chain cross-sectional areas of PE and PC and dipolar repulsion between PC headgroups are probably some of the factors driving the components towards the regular superlattice-like arrangement of PE in the PC host matrix. The PE/PC superlattices are suggested to be spatiotemporal structures, i.e. they cover only a limited area (domain) of the bilayer at any time. Intriguingly, such head-group-dependent superlattice formation could play a crucial role in the regulation of phospholipid composition of biological membranes.

Th-Pos325

POLYMORPHISM OF PHOSPHATIDYLETHANOLAMINE/ CHOLESTEROL MIXTURES.
((M. Lafleur and C. Paré)) Chemistry Department, Université de Montréal, Montréal, Québec, H3C 3J7.

It is well established that cholesterol induces the formation of a liquid ordered (*lo*) phase in phosphatidylcholine (PC) bilayers. The goal of this work is to examine the influence of cholesterol on phosphatidylethanolamine polymorphism. The behaviour of 1-palmitoyl-2-oleoyl-phosphatidylethanolamine (POPE) /cholesterol mixtures was characterized using infrared and ^{2}H NMR spectroscopy (using POPE bearing a perdeuterated palmitoyl chain in the latter case). Our results reveal that cholesterol induces the formation of an *lo* phase in POPE membranes, similar to those observed for various PC/cholesterol systems. The chain ordering property of cholesterol is less pronounced for POPE than for the PC equivalent but it seems to be related to the greater orientational order of the POPE chains relative to the POPC ones in pure phospholipid bilayers. Regarding the lamellar-to-hexagonal (L_α-H_{II}) phase transition, cholesterol shifts the transition towards the low temperatures; the transition is observed at 55 °C when the POPE bilayer contains 20(mol)% cholesterol or more (the transition is at 70 °C for pure POPE). Cholesterol still displays a chain ordering effect in the hexagonal phase.

Th-Pos326

RELATIVE SURFACE CHARGE DENSITY MAPS OF BACTERIORHOPOSIN MEMBRANES DETERMINED FROM THE INTERACTION FORCE FIELD. ((**W.F. Heinz**, J.H. Hoh)) Dept. Physiology, The Johns Hopkins University School of Medicine, Baltimore, MD, 21205.

The local electrostatic properties, such as charge density and the resultant field, of biological membranes have a profound impact on the behaviour of these systems. The atomic force microscope (AFM) can be used to investigate surface electrostatics by exploiting the interaction force that arises from the overlap of electrostatic double layers, one from the tip and one from the sample, as the tip is approached toward the sample. Here we report relative surface charge density maps from bacteriorhodopsin determined from the interaction force field (IFF). An AFM was used to collect an array (typically 64x64) of force versus seperation distance curves on BR membranes adsorbed to a mica surface. These curves describe the tip-sample IFF in the space above the sample. For these initial measurements we used the intrinsic charge in the silicon nitride tip, which possses a silicon oxide-like surface and is negatively charged at a pH above ~3. The curves were fitted to a simple electrostatic model for double layer interactions using home grown fitting software, and a relative charge density parameter for each point on the surface was obtained. Preliminary 2D plots of the relative surface charge densities clearly distinguish the BR membranes from the mica substrate. These are the first results in our effort to use the AFM to characterize the IFFs that biological structures exhibit relative to each other.

Th-Pos327

DIACYLGLYCEROL-RICH DOMAIN FORMATION IN SOPC/SOPS/PO VESICLES AND ITS INFLUENCE ON PROTEIN KINASE C ACTIVATION ((A.R.G. Dibble, A.K. Hinderliter, J.J. Sando and R.L. Biltonen)) Dept. of Pharmacol., Univ. of VA, Charlottesville, VA 22908.

To test our working hypothesis that the activation of protein kinase C (PKC) is strongly influenced by the formation of lipid domains enriched in diacylglycerol (DAG), the thermotropic phase behavior of the ternary lipid mixture 1-stearoyl-2-oleoyl-*sn*-glycero-3-phosphocholine (SOPC)/1-stearoyl-2-oleoyl-*sn*-glycero-3-phosphoserine (SOPS)/1-palmitoyl-2-oleoyl-*sn*-glycerol (PO) was compared with the ability of this system to activate the enzyme. Differential scanning calorimetry (DSC) was used to monitor the gel-to-liquid crystalline phase transition as a function of mole fraction PO (χ_{PO}) in [SOPC/SOPS (1:1, mol/mol)]/PO multilamellar vesicles. The results are consistent with the coexistence of PO-poor and PO-rich domains from χ_{PO} = 0-0.02 to χ_{PO} = 0.30-0.35. With this system, the DAG-rich domains begin to form at a lower overall DAG content (χ_{PO} = 0-0.02) than with systems having a greater mismatch between the acyl chains of DAG and those of the phospholipid components. Furthermore, the DAG-rich domains of the SOPC/SOPS/PO system have a DAG:phospholipid mole ratio near 1:2, significantly less than the 1:1 DAG:phospholipid mole ratio found with systems having all acyl chains saturated. We propose that this difference is due to a stabilization of the DAG-rich domains by intermolecular hydrogen bonding, which in the 1:1 case involves the hydroxyl group of DAG and the headgroup of a phospholipid (probably at the *sn*-2 carbonyl group), while in the 1:2 case a water molecule accepts the hydrogen bond from DAG and donates to *two* phospholipid headgroups; the intervening water may be necessary when the lipid headgroups are spaced relatively far apart due to acyl chain unsaturation. PKC activity was measured as a function of χ_{PO} using [SOPC/SOPS (1:1, mol/mol)]/PO vesicles as the lipid activator. At temperatures below and above the gel-to-liquid crystalline phase transition, PKC was activated from χ_{PO} = 0.02 to χ_{PO} = 0.3, consistent with a relationship between PO-rich domain formation and PKC activation. (Supported by NIH grants F32 GM17831, RO1 GM31184, and PO1 GM47525.)

Th-Pos328

INFLUENCE OF THE DIPOLE DISTRIBUTION AT THE INTERFACE OF LIPID MIXTURES ON THE ELECTROKINETIC POTENTIAL OF VESICLES.
((G. Peltzer, M. C. Luzardo and E.A. Disalvo)) Química General e Inorgánica, Facultad de Farmacia y Bioquímica, University of Buenos Aires, Argentina.

The dipole potentials of monolayers of different DMPC/DPPC; DMPC/DSPC and DSPC/DOPC ratios show a non-regular pattern with the composition. At the specific ratios of 0.33 and 0.66 of mixtures of lipids of different chain length in the gel state, the dipole potential is much higher than that predicted from the mixtures of the pure components. The irregularities are attenuated when the lipid of longer chain prevails in the mixture. The mixtures in which gel and fluid phase coexist or of lipids with similar chain length show a continuous increase in the dipole potential when the component of the higher transition temperature prevails. The electrokinetic potentials of vesicles show also singularities at the same compositions and conditions. A model is proposed in which the dipole distribution affects the electrokinetic potential of vesicles. The results suggest that when bilayers of short lipid chains are dopped with lipids of a longer chain (or viceversa) the topography of the surface promotes a defined water and ion distribution at the shear plane.
With funds from UBACyT and Fundacion Antorchas

Th-Pos329

EQUATION OF STATE OF A CHARGED-BILAYER SYSTEM: THE MEASURED ENTROPY OF THE LAMELLAR-LAMELLAR TRANSITION IN DDAB.
((M. Dubois, Th. Zemb, N. Fuller, R. P. Rand and **V.A.Parsegian**)) SCM/CEA/Saclay, France, Brock Univ. Canada, NIH, USA

Charged bilayers repel by hydration forces near contact and by electrostatic double layer repulsion at distances ≥ 1 nm. There is a critical admixture of van der Waals attraction and, often, powerful enhancement of repulsion by undulatory "steric" forces. We have worked with didodecyldimethylammonium Br$^-$, a lipid that has two distinct lamellar phases: a dilute L_α phase dominated by electrostatic forces, and a condensed $L_{\alpha'}$ phase governed by hydration forces. By applying osmotic stress over a wide range of temperatures, we have measured the free energy of creating these phases and have mapped the phase diagram with an equation of state. The Entropy of lamellar-lamellar transition is a strong function of temperature. Above 40 C, condensation from the dilute phase incurs a negative entropy as might be expected; below 40 C, the entropy of condensation is *positive*. These data allow us to think far more critically about the forces that stabilize bilayer systems. In particular, the entropy of condensation allows us to evaluate the roles of ion condensation and of ordered-water release in bilayer interaction.

Th-Pos330

CLOSING IN ON THE VAPOR PRESSURE PARADOX.
((V.A.Parsegian and **R. Podgornik**)) NIH, USA and IJS, Slovenia

Multilayers of charged lipids immersed in distilled water swell to whatever dilution allowed them by the available volume of solvent. Multilayers of the same lipids on a solid surface will imbibe only a small amount of water even from a 100% relative-humidity vapor. We argue that the essential difference is in the extra work needed to create a vapor/multilayer interface. For stiff, tightly packed multilayers, this interfacial energy is an additive constant of little consequence. But, in water, multilayers swell to a softness where thermal excitation creates an undulating surface; the surface energy goes as the contour area not as the flat area of projected surface. The contour area grows as the multilayer swells. Surface tension against vapor quells ripples and pulls the multilayer back to tighter packing. Tension can even act to enhance attractive forces between membranes to create energy minima at very close spacings. What is remarkable is the long range and strength of surface-tension perturbation. When we think of the undulations as waves on bilayer sheets, then we see that these disturbances can reach inward to distances comparable to the lateral extent of the sheets themselves. Quantitative analysis of the vapor paradox is not merely academic. The flexibility of bio-molecules is intrinsic to their organization. Any long-range effect of surfaces on molecular packing immediately makes us ask if we may apply to micron-sized cells and viruses the rules of macromolecular assembly learned in cm-sized test tubes.

Th-Pos331

OCTYL-β-D-GLUCOPYRANOSIDE PARTITIONING INTO LIPID BILAYERS. THERMODYNAMICS OF BINDING AND STRUCTURAL CHANGES OF THE BILAYER.
((**M. R. Wenk**, T. Alt, A. Seelig, and J. Seelig)) Biocenter, University of Basel, 4054 Basel, Switzerland.

The interaction of the nonionic detergent octyl-β-D-glucopyranoside (OG) with lipid bilayers was studied with high-sensitivity titration calorimetry, monolayer methods, and ^{2}H-NMR solid state spectroscopy. Employing detergent below the critical micellar concentration the transfer of OG from the aqueous phase to lipid bilayers composed of 1-palmitoyl-2-oleoyl-*sn*-glycero-3-phosphocholine (POPC) can be explained by a surface partition equilibrium with a partition coefficient of $K \approx 170\ M^{-1}$, a molar binding enthalpy of $\Delta H \approx +1$ kcal / mol, and a free energy of binding of $\Delta G \approx -5.5$ kcal / mol. The heat of transfer is temperature dependent with a molar heat capacity of $\Delta C_p = -72$ cal / (mol · K), typical for a hydrophobic binding equilibrium. The surface area requirement of OG at the air-water interface, A_S, was determined from a measurement of the Gibbs adsorption isotherm, yielding $A_S \approx 51 \pm 2$ Å^2. The cross-sectional area of OG in a POPC monolayer, A_I, was determined by a monolayer expansion technique and was found to be $A_I \approx 59 \pm 10$ Å^2. Structural changes of the bilayer due to the presence of OG were investigated with solid state ^{2}H-NMR. POPC selectively deuterated at the headgroup region or the fatty acyl chains was used to obtain information on the conformation and the order of the bilayer membrane in presence of OG. The addition of OG had almost no influence on the conformation of the choline headgroup of POPC. However, the quadrupolar splittings of the chain deuterated segments decreased strongly with increasing OG. It can be concluded that OG induces a disordering of the acyl chains of the lipid molecules, but leaves the headgroup conformation essentially unchanged.

Th-Pos332

THE FRACTIONAL OCCURENCE OF DEFECTS IN MEMBRANES. ((**Robert M. Raphael** and Richard E. Waugh)) Dept. of Biomedical Engineering, Johns Hopkins University School of Medicine, Baltimore, MD 21205 and Dept. of Pharmacology and Physiology, School of Medicine and Dentistry, University of Rochester, Rochester, NY 14642.

The picture of biological membranes as uniform, homogeneous bileaflet structures has been revised in recent years due to the growing recognition that these structures can undergo significant fluctuations both in local curvature and in thickness. In particular, evidence has been obtained that a temporary localized disordering of the lipid bilayer structure (defects) may serve as the principal pathway for movement of lipid molecules from one leaflet of the bilayer to the other. How frequently these defects occur and how long they remain open are major unresolved questions. In this report we calculate the rate of molecular transport through a transient defect in the membrane and compare this result to measurements of the net transbilayer flux of lipid molecules measured in an experiment in which the lipid flux is driven by differences between the mechanical stress in the two leaflets of the bilayer membrane. Based on this comparison we estimate the frequency of defect occurrence in the membrane. The occurrence of defects is rare: the probability of finding a defect in 1.0 μm^2 of a phosphatidylcholine membrane is estimated to be 5.75×10^{-6}, assuming the lifetime of the defects is on the order of 1 μs. Based on this fractional occurrence of defects, the free energy of defect formation is estimated to be $\sim 1.0 \times 10^{-19}$ J.

Th-Pos333

INFLUENCE OF SHINGOMYELIN ON LIPID DYNAMICS AS DETECTED BY LAURDAN FLUORESCENCE.((V. Kumar, P. Wilson, T. Parasassi, E. Gratton, and M. Levi)) U of Texas Southwestern Med Ctr and DVAMC, Dallas, Texas; LFD, U of Illinois at Urbana-Champaign, Urbana, Illinois; and CNR, Rome, Italy.

Sphingomyelin is a major constituent of cell membranes. In renal proximal tubular apical brush border membranes(BBM) sphingomyelin accounts for 40 to 60 mole % of membrane phospholipids. The purpose of this study was to determine the effect of sphingomyelin on lipid dynamics as determined by the Generalized Polarization of Laurdan (GP Laurdan) which reflects the relative water content of the lipid bilayer. In DOPC and in DOPC-DPPC (1:1) bilayers brain, egg, or milk sphingomyelin caused a dose-dependent blue shift in the emission spectra and an increase in the excitation GP, i.e. a decrease in lipid fluidity. The dose-dependent effect of sphingomyelin to cause a progressive increase in the GP was also seen in the presence of cholesterol (25 mole % CHOL) in CHOL-DOPC-DPPC bilayers. In contrast, in total lipid extract from the renal BBM, selective removal of sphingomyelin caused a red shift in the emission spectra and a decrease in the excitation GP, i.e. an increase in lipid fluidity. Alterations in shingomyelin content therefore plays an important role in modulating lipid molecular dynamics in model membrane systems as well as in biological membranes.

Th-Pos334

DIFFRACTION FROM MAGNETICALLY ALIGNED STACKS OF L_α UNILAMELLAR LIPID BILAYERS. ((**J. Katsaras**,[1] Z. Tun,[1] R.S. Prosser[2])) [1]Atomic Energy of Canada Limited, Chalk River, Ont. K0J 1J0, [2]Department of Chemistry and Biochemistry, University of California, San Diego, La Jolla, CA 92093-0359.

For close to two decades, it has been recognized that a variety of biomolecules possess sufficient diamagnetic anisotropy to align in the presence of a magnetic field. One strategy for studying aligned biomolecules (e.g., peptides, proteins), regardless of their intrinsic magnetic properties, is to introduce them to magnetically alignable "substrates". We present neutron diffraction data of a novel, biologically relevant membrane system which is highly alignable ($\leq 1.0°$ mosaic) in a magnetic field and gives rise to well-defined higher-order Bragg reflections (n=5) necessary for detailed structural studies. These magnetically alignable unilamellar bilayer stacks, composed of dimyristoylphosphatidylcholine, dihexanoylphosphatidylcholine and Tm^{3+}, at molar ratios of 3.2:1:0.43, in 75% water (w/w), have proven to mimic the essential physical properties of biological membranes while remaining stable over a wide range of temperature, pH and ionic strength (C.R. Sanders and J.P. Schwonek, Biochemistry **31**, 8898)

Th-Pos335

FOURIER TRANSFORM INFRARED SPECTROSCOPY STUDIES OF MODEL STRATUM CORNEUM LIPIDS ((**David J. Moore**[1], Mark E. Rerek[1] and Richard Mendelsohn[2])) [1]International Specialty Products, Skin R&D, 1361 Alps Road, Wayne, N.J. 07470 and [2]Department of Chemistry, Rutgers University, Newark, N.J. 07102

The outermost layer of human skin, the stratum corneum (SC), is composed of corneocytes in a lipid matrix of ceramides, cholesterol, and free fatty acids. NMR, X-Ray and DSC studies have indicated that at physiological temperatures the SC lipids are organized in a complex heterogenous matrix of lamellar sheets containing some highly ordered lipids. The current FTIR experiments are designed to directly probe the lipid conformational order and organization of the ceramide and fatty acid components in a model stratum corneum system. Using a deuterated fatty acid the conformation of both the fatty acid and ceramide species has been simultaneously monitored in the model SC. The results of our first series of experiments indicate that both the ceramide and fatty acid components are conformationally ordered at physiological temperature. Furthermore, the CD_2 bending mode of the fatty acid is split indicating the presence of all-*trans* orthorhombic fatty acid domains at physiological temperature. A quantitative analysis of these results, including estimations of domain size, will be presented. Experiments examining the effect of pH upon this model SC are currently underway.

TRANSPORT ACROSS BILAYERS

Th-Pos336

INHIBITION OF THE AMINOPHOSPHOLIPID TRANSPORTER BY A POLYCLONAL ANTI-Mg^{2+}-ATPase SERUM.
((M.Julien and **D. L. Daleke**)) Department of Biochemistry and Molecular Biology, Indiana University, Bloomington, IN 47405 USA.

The human erythrocyte possesses an inwardly directed, ATP-dependent aminophospholipid transporter that contributes to the maintenance of an asymmetric distribution of phospholipids across the plasma membrane. A Mg^{2+}-ATPase has been purified from human erythrocytes and has been implicated in having an intimate role in aminophospholipid transport activity. When mice were immunized with the Mg^{2+}-ATPase partially purified from human erythrocyte membranes, the polyclonal serum obtained inhibits the activity of both the purified Mg^{2+}-ATPase and the aminophospholipid translocase in the erythrocyte membranes (ghosts), when added prior to resealing. The antibody fraction, purified from the polyclonal serum, also inhibits both the Mg^{2+}-ATPase and the aminophospholipid translocase. When added to the external surface of intact erythrocytes or resealed ghosts, the polyclonal sera had no effect on translocase activity, indicating that the anti-translocase antibody(ies) recognizes epitopes on the cytosolic face of the membrane. These data result strongly suggests that the Mg^{2+}-ATPase activity is associated with the aminophospholipid translocase activity.

Th-Pos337

EVIDENCE FOR TWO DISTINCT MAGNESIUM TRANSPORT MECHANISMS IN ISOLATED RAT LIVER PLASMA MEMBRANES ((C. Luca, A. Romani, A. Scarpa)) Dept. Physiol. & Biophys., Case Western Reserve University, Cleveland, OH, 44106-4970. The plasma membrane of several cell types operates very active mechanisms of Mg^{2+} uptake and extrusion. In order to define the operation and selectivity of the mechanism(s) by which hepatocytes extrude Mg^{2+}, isolated, purified, and sealed liver plasma membrane vesicles (LPM) were preloaded to contain a variety of trapped ions and phosphonucleotides. An extrusion of Mg^{2+} from loaded vesicles can be induced in a temperature and dose-dependent fashion by addition of NaCl and/or $CaCl_2$. Mg^{2+} extrusion was already detectable following the addition of 50uM or 100uM $CaCl_2$ (123.8±16.6 and 179.9±17.4 nmol Mg^{2+}/mg protein, respectively). By contrast, the concentrations of NaCl required to stimulate Mg^{2+} efflux were three orders of magnitude higher (Mg^{2+} efflux by 25mM NaCl was 94.8±14.1 nmol Mg^{2+}/mg protein). The efflux induced by the maximal concentration of $CaCl_2$ was 50% greater than the maximal Mg^{2+} efflux prompted by NaCl. In addition, the coaddition of Na^+ and Ca^{2+} elicited an additive efflux greater than that prompted by either ion alone. Replacement of Cl^- with gluconate inside or outside the vesicles did not affect the amplitude of Mg^{2+} release. Both the Na^+ and Ca^{2+} induced Mg^{2+} movements were inhibited to different extents by 200uM imipramine, 200uM quinidine, or 1mM amiloride. Approximately 35% of the total entrapped Mg^{2+} was mobilized by extravesicular addition of 25mM NaCl and 50% by the addition of 50uM Ca^{2+}. The subsequent addition of A23187 mobilized all but 15% of the total entrapped Mg^{2+}. Since unloaded vesicles contained no HPLC detectable endogenous ATP, Mg^{2+} efflux was investigated in vesicles loaded with 20mM Mg^{2+} plus 5mM of different phosphonucleotides or phosphate derivatives. The presence of Pi inside the vesicles appears to selectively enhance the operation of the Ca^{2+} activated transporter. The additive effect of Na^+ and Ca^{2+} coaddition on Mg^{2+} efflux was considerably increased in these vesicles as compared to that observed in liver plasma membrane vesicles loaded with Mg^{2+} alone. Taken together these results pose for the operation of two distinct Mg^{2+} transport mechanisms in liver plasma membrane vesicles, activated by Na^+ and Ca^{2+}, respectively. [Supported by NIH-HL18708].

Th-Pos338

DOXORUBICIN-CITRATE INTERACTIONS: THE EFFECT OF DOXORUBICIN AGGREGATION UPON ITS RELEASE FROM LIPOSOMES.

((**Xingsong Li**, Eric Mayhew, Andrew S. Janoff, and Walter R. Perkins))
The Liposome Company, Inc., One Research Way, Princeton, NJ 08540

The effect of citrate upon doxorubicin's (DXR) physical state in solution and inside liposomes has been examined using turbidity, confocal microscopy, and circular dichroism (CD) spectroscopy. We found that citrate, like sulfate, induced DXR precipitation in solution at concentrations (~0.5 mM) significantly below its aqueous solubility limit (60 mM). CD spectra of citrate-DXR and sulfate-DXR aggregates were identical suggesting that the two aggregated species have similar molecular arrangements. To assess the impact of DXR aggregation upon its release from liposomes, we designed liposomes such that the entrapped DXR (loaded to 20-30 mM DXR) was either aggregated [citrate as buffer] or disaggregated [lactobionic acid (LBA) as buffer] and compared leakage. For citrate liposomes, leak upon dilution into buffered saline was <4% after 60 min, while the leak profiles for LBA preparations were biphasic with as much as 20% DXR released within the first 20 min. When dilutions were made into a hyperosmotic solution the rapid component was avoided and leakage was similar to that for the citrate system; this indicated that an osmotic stress induced vesicle rupture had occurred and disaggregated DXR was lost. For both citrate and LBA liposomes loaded to high internal DXR concentrations (>200 mM), DXR formed aggregates and their leak in buffered saline was similar to that for citrate liposomes loaded with 20-30 mM DXR. Aggregated DXR was retained because those vesicles did not experience vesicle rupture or because aggregates were too big to be released. These data suggest that DXR deaggregation per se may not be rate limiting to its outward redistribution in vitro. For in vivo drug delivery, however, DXR aggregation would prevent leak due to osmotic stress and may reduce release in blood where membrane disruption (e.g., lipoprotein binding) is expected.

Th-Pos339

TRANSPORT OF LONG CHAIN FATTY ACIDS ACROSS LIPID VESICLES IS RATE LIMITED BY SLOW TRANSBILAYER FLIP-FLOP. ((**A.M. Kleinfeld**, P. Chu, and C. Romero)) Medical Biology Institute, La Jolla, CA 92037.

A key issue of fatty acid (FA) metabolism is whether transport of FA across cell membranes is protein mediated. Determination of the rate limiting steps for transport of FA across lipid membranes should help resolve this issue, but considerable disagreement remains even for these simple membranes. In the present study we have measured *transport* of long chain native FA from the aqueous phase on one side to that on the other side of unilamellar lipid vesicles. These measurements were done by trapping ADIFAB, the fluorescent probe of free FA, within the vesicles to monitor transport of FA across the bilayer and, by using ADIFAB in the extravesicular phase, we determined FA dissociation from the bilayer. The results reveal that in 2000 Å diameter vesicles, flip-flop rate constants (k_{ff}) for oleate (18:1) were about 0.1 s^{-1} at 20°C and increased to 0.3 s^{-1} at 37°C. Off rate constants (k_{off}) were about 1.5 s^{-1} and were relatively invariant with temperature. Rate constants for linoleate (18:2) were generally about 3 to 5 fold greater than those for oleate. For 1000 Å vesicles rate constants were about 10 fold greater. We conclude, in contrast to Kamp et al. (Biochemistry 1995, 34:11928), that 1) flip-flop is the rate limiting step for transport of long chain FA across lipid bilayers, 2) k_{ff} is sensitive to the molecular structure of the FA, and 3) k_{ff} may be too small to support observed rates of cellular metabolism of FA. Supported by NIH grant GM44171.

Th-Pos340

SALMETEROL PERMEABILITY ACROSS LIPID BILAYERS WITH COMPOSITION SIMILAR TO THAT OF LUNG EPITHELIAL CELL MEMBRANES. ((Danielle M. Wright[1], Nicole Incanno,[2] and David G. Rhodes[2*]))
(1) College of Pharmacy, Xavier University, New Orleans, LA and (2) Department of Pharmaceutical Sciences, School of Pharmacy, Univ. Connecticut Storrs, CT

Salmeterol, a long-acting sympathomimetic amine used in asthma therapy, has a very long duration of action (15-17 h) compared to more widely used analogs like albuterol (4-5 h), but has a much slower onset time (20 min) than albuterol (<2 min). In previous studies with salmeterol, we found lower membrane partition coefficients when salmeterol was added externally to multilamellar vesicles and that salmeterol incorporated into large multilamellar vesicles was retained for several hours. Both observations suggested that this salmeterol did not easily cross lipid bilayers. The purpose of this project was to *directly* measure the rate of trans-bilayer diffusion of salmeterol using membranes with lipid composition designed to mimic that of lung epithelial cells. The lipid mixture included saturated and unsaturated PC, PG, PE, PI, cardiolipin, and cholesterol. Salmeterol was entrapped in unilamellar vesicles, and the amount that leaked was monitored over time using a fluorescence assay sensitive to nanomolar quantities of the drug. The decay constant for salmeterol release (leaking) was approximately 36 hours. These data are consistent with previous qualitative results and may have important implications concerning the microscopic mechanism of salmeterol interaction with the β_2-receptor. We are now investigating the effect of variations in the lipid composition.
Supported by the UConn. Research Foundation (DGR) and a fellowship program jointly sponsored by UConn and Bayer Pharmaceutical Division (DMW).

Th-Pos341

PERMEATION OF CHLORIDE, BROMIDE, AND IODIDE ACROSS PHOSPHOLIPID BILAYERS

((**S. Paula** and D.W. Deamer)) Department of Chemistry and Biochemistry, University of California, Santa Cruz, CA, 95064.

The permeation process of the anions chloride, bromide, and iodide across phospholipid bilayers was studied using a fluorescence technique. The fluorescent dye MQAE was trapped inside liposomes which were then diluted into buffers containing one of the anions. The time dependent fluorescence quenching of the dye caused by the anions entering the liposomes was recorded and the corresponding permeability coefficients were calculated. Experiments were carried out with liposomes composed of phosphatidylcholines with chain lengths ranging from sixteen to twenty-four carbon atoms. The permeability coefficients ranged from 10^{-9} to 10^{-7} cm/s and increased as the thickness of the bilayers was reduced. A difference in permeability coefficients of less than one order of magnitude was observed between the longest and the shortest lipid. Bromide was found to permeate approximately eight times faster than chloride. Iodide was found to permeate even faster than bromide (about four times) and could be measured reliably only in the thicker bilayers. These experimental findings were compared to predictions made by two permeation mechanisms: the solubility-diffusion model and the pore model. The modest dependence of permeability coefficients on bilayer thickness and the marked dependence on ionic size point to a solubility-diffusion mechanism and argue against permeation through pores. In contrast, cation permeation has been accounted for by a combination of the two mechanisms: permeation through pores in thin bilayers and permeation by solubility-diffusion in thicker bilayers.Supported by NASA grant 4235

MEMBRANE TRANSPORT

Th-Pos342

A MODEL DESCRIBING THE POTENTIAL DEPENDENCE OF SODIUM-COUPLED ALANINE TRANSPORT. ((J.J. Wilson, J. Randles, G.A. Kimmich))
Department of Biochemistry and Biophysics, University of Rochester School of Medicine and Dentistry, Rochester, NY 14642.

Sodium-coupled alanine transport in LLC-PK_1 cells occurs via a simultaneous and ordered mechanism in which sodium binds to the cotransporter prior to alanine at the extracellular surface of the membrane. Alanine and sodium are cotransported with 1:1 coupling and glide symmetry. The relative simplicity of this six state model makes it a useful system for analysis of the molecular mechanism by which the membrane potential regulates transport kinetics.

We previously reported that neither translocation of the free-form of the cotransporter nor binding/dissociation of extracellular sodium are potential dependent. Consequently, at least one of the remaining four steps in the transport cycle must be potential dependent.

Using isotope influx studies at two different membrane potentials, -56mV and +29mV, we analyzed the kinetic parameters for sodium as a function of membrane potential and substrate concentration. Although the K_m for sodium at low alanine concentrations (5μM) is independent of membrane potential the same K_m at high alanine concentrations (2mM) is dependent on potential. Conversely, the V_{max} for sodium at low alanine concentrations is modified by membrane potential whereas the V_{max} at high alanine is not. Using rate equations derived from the six state model, these results are best described by a minimal model with a single potential dependent step, translocation of the fully-loaded transport protein/substrate complex. Similar analysis of the kinetic parameters for alanine at high and low sodium concentrations confirms this result.
Supported by PHS DK 15365-22

Th-Pos343

ATR-FTIR SPECTROSCOPY ON THE LACTOSE PERMEASE OF *ESCHERICHIA COLI*. ((**Johannes le Coutre**[1,2], L. Ravi Narasimhan[2], C. Kumar N. Patel[2], H. Ronald Kaback[1])) [1] Howard Hughes Medical Institute, University of California Los Angeles; [2] Department of Physics, University of California Los Angeles.

A continous flow ATR-FTIR setup is being used to understand mechanistic and structural properties of the lactose permease. By titrating the protein over a broad pH range, protonation of different carboxylic groups in different micro environments is observed. The data show titration of several carboxylates at low pK_a (4-5) with an IR band at 1715 cm^{-1} which most likely represent the carboxylates in the loops of the protein. However, another group titrates with a pK_a around 10 and a higher C=O stretching frequency at 1740 cm^{-1}, suggesting the existence of a protonated carboxylic group inside the membrane. Comparison of site-specific mutants will allow identification of this carboxylic group with respect to its function in the transport mechanism. Spectral shifts induced by addition of substrate indicate changes in accessibility of certain carboxylic groups and conformational changes in the protein due to ligand binding.

Th-Pos344

ELECTRICAL ACTIVITY CHANGES OF *HYDRA OLIGACTIS PALLAS* ECTODERM CELLS UNDER INFLUENCE OF HEAVY METALS IONS

((R.TYZIO, O.GOIDA))
Lviv State University, Grushevsky 4, 290000 L'viv, Ukraine (Spon. by Dr. I.Oleksiv)

The purpose of this investigation is to research the toxical influence of heavy metals (HM) ions on freshwater hydra by the changes of its ectoderm membrane electrical activity using microelectrod technics under voltage clamp. It have been received data about rhythmic spike activity of hydra ectoderm cells and some conformities and specific changes of their rhythmics under the influence of Cu^{2+}, Zn^{2+}, Cr^{3+}, Fe^{3+}. There has been elaborated biotesting method of toxical influence of HM ions on the hydra cells by their inhibition on the electrical activity and decreasing of conductivity of plasmatic membranes. It has been proved that HM ions cause unordinary action on membrane potential dynamics by means of plasmatic membrane Ca^{2+} transport systems.
The influence of HM ions in the limits of the adaptive ability under subtoxic press take place by means of membrane ATPases activity modulation and conductivity changes. Membrane potential dynamics distinctly reflects cell gomeostasis state under toxical press of incubation medium by HM ions. It has been proposed new express-method of toxicity assessment of surplus HM ions concentrations in water environment.

Th-Pos345

PHOSPHOARGININE (PA) MAY SUPPORT Na,K,Cl COTRANSPORT (NKCC) IN SQUID GIANT AXONS. ((A.A. Altamirano, G.E. Breitwieser & **J.M. Russell**)) Universidad de Buenos Aires, Buenos Aires, Argentina; Johns Hopkins U. School of Medicine, Baltimore, MD 21205; Allegheny University of the Health Sciences, Philadelphia, PA 19129.

While assaying for effects of protein kinase inhibitors on NKCC-mediated Cl influx into internally dialyzed squid axons, we found that A-3, an inhibitor of several protein kinases, including casein kinase, had an inhibitory effect on the influx in the absence, but not in the presence, of PA. Thus, when [ATP] = 200 μM, PA = 3 mM, 75 μM A-3 had no effect on bumetanide-sensitive (BS) Cl influx. However, when PA was omitted, A-3 reduced the BS Cl influx by about 35%. DiPolo and Beaugé (J. Physiol. 487: 57, 1995) have reported that PA stimulates Na/Ca exchange in the absence or presence of cellular ATP. Therefore, we examined the effects of 5 mM PA on BS Cl influx into internally dialyzed squid giant axons. After dialyzing the axons for 120 minutes with an ATP-depleting dialysis fluid (200 mM K, 0 mM Na and Cl + 1 mM cyanide) we measured the Cl influx into axons in the absence and presence of 5 mM PA. When both ATP and PA were absent, the Cl influx averaged 24 pmol/cm²sec (p/cs); addition of 5 mM PA increased the Cl influx to 52.5 p/cs. Finally, treatment with 10 μM bumetanide reduced the Cl influx to 33.4 p/cs. These results suggest that PA may serve to activate the NKCC in the nominal absence of ATP. Supported by NS 11946 (JMR)

Th-Pos346

CONSTRUCTION AND FUNCTIONAL CHARACTERIZATION OF CYSTEINE-LESS YEAST MITOCHONDRIAL CITRATE TRANSPORT PROTEIN VARIANTS ((Y. Xu, J.A. Mayor, D. Kakhniashvili, D.A. Gremse, D.O. Wood, and R.S. Kaplan)) Dept. of Pharmacology, University of South Alabama, Mobile, AL 36688

In order to probe the role of native cysteines in the function of the yeast mitochondrial citrate transport protein (CTP) we have utilized site-directed mutagenesis to initially replace each of the four endogenous Cys residues with Ser. The initial Cys-less CTP construct was abundantly expressed in *E. coli*, purified, and upon subsequent incorporation into phospholipid vesicles catalyzed a 1,2,3-benzene-tricarboxylate-sensitive citrate/citrate exchange. Competition studies indicate a substrate specificity that is similar to the wild-type profile. Kinetic characterization indicates that the Cys-less CTP displays a moderately reduced K_m and a substantially reduced V_{max} value (i.e., 8% of the wild-type value). Alternative Cys-less CTPs, which contained replacement residues other than Ser, were then developed in an attempt to obtain a construct with improved kinetic properties. We observed that two constructs display significantly enhanced V_{max} values relative to the initial Cys-less CTP construct (i.e., approx. 60% of the wild-type value). In conclusion, the construction of a functional CTP that is devoid of cysteine residues, now provides the template for the reintroduction of Cys at specific sites which can be tagged with a variety of chemical and biophysical probes in order to map the substrate translocation pathway through this transport protein. Supported by NIH grants GM54642 and DK44993 to R.S.K.

Th-Pos347

OVEREXPRESSION, PURIFICATION, AND CHARACTERIZATION OF THE YEAST MITOCHONDRIAL DICARBOXYLATE TRANSPORT PROTEIN ((R.S. Kaplan, D. Kakhniashvili, J.A. Mayor, Y. Xu, and D.A. Gremse)) Dept. of Pharmacology, University of South Alabama, Mobile, AL 36688

The gene encoding the yeast mitochondrial dicarboxylate transport protein (DTP) has been identified, for the first time from any organism, and its protein product overexpressed in *E. coli*. The expressed DTP can be solubilized from isolated inclusion bodies with sarkosyl. 28 mg of DTP is obtained per liter of culture at a purity of 75%. The function of the solubilized DTP was reconstituted in a liposomal system where both its kinetic properties (i.e., K_m = 1.55 mM; V_{max} = 3.0 μmol/min/mg protein) and its substrate specificity were determined. The intraliposomal anions malonate, malate, succinate, and phosphate supported [^{14}C]malonate uptake, whereas other anions did not. External substrate competition studies revealed a similar profile. Analysis of the DTP sequence reveals that it displays the mitochondrial transporter signature motif, three homologous 100 residue domains, and six predicted membrane-spanning regions. In combination, the above findings indicate that based on both structural and functional considerations, the yeast DTP can be assigned membership to the mitochondrial carrier family. In conclusion, identification of the yeast DTP gene, and the expression and purification of large quantities of its functional protein product, provides the foundation for comprehensive investigation into the structure/function relationships within the DTP. Supported by NIH grants GM-54642 and DK-44993 to R.S.K.

Th-Pos348

H^+ PERMEATION AND PH REGULATION AT A MAMMALIAN SEROTONIN TRANSPORTER. ((Yongwei Cao, Sela Mager, Henry A. Lester)) Division of Biology, 156-29, California Institute of Technology. Pasadena, CA 91125

The rat serotonin transporter expressed in *Xenopus* oocytes displays an inward current when external pH is lowered to 6.5 or below. The new current differs from the previously described leakage current in two ways: (1) it is roughly 10 fold larger at pH 5 and reaches 1000 H^+/s per transporter at extremes of voltage and pH with no signs of saturation; and (2) it is selective for H^+ by reversal potential measurements. Similar H^+-induced currents are also observed in several other ion-coupled transporters, including the GABA transporter, the dopamine transporter, and the Na^+/glucose transporter. The high conductance and high selectivity of the H^+-induced current suggest that protons may be conducted via a hydrogen-bonded chain (a "proton-wire mechanism") formed at least partially by side chains within the transporter. In addition, pH affects other conducting states of the serotonin transporter. Acidic pH potentiates the 5-HT-induced transport-associated current and inhibits the hyperpolarization-activated transient current. The dose-response relations for these two effects suggest that two H^+ binding sites, with pK_a values close to 4.8 and close to 6.3, govern the potentiation of the 5-HT-induced current and the inhibition of the transient current, respectively. These results are important for developing structure-function models that explain permeation properties of neurotransmitter transporters.

Th-Pos349

ELECTROPHYSIOLOGICAL CHARACTERIZATION OF THE *DROSOPHILA* SEROTONIN TRANSPORTER. ((C.I. Petersen, A. Galli, M. deBlaquiere, R.D. Blakely and L.J. DeFelice)) Dept. of Pharmacology, Vanderbilt University, Nashville, TN 37232.

Neurotransmitter transporters play an essential role in clearance of neurotransmitters from the synapse. Serotonin transporters (SERTs) transport serotonin against its concentration gradient by coupling to Na^+ and Cl^- ions. The current model for transporter function states that there is a fixed stoichiometry of coupled ions to neurotransmitter for each transport cycle; specifically, one molecule of serotonin is believed to cross the membrane with one Na^+ and Cl^- ion. This is modeled physically with the alternating access model, where binding sites are sequentially exposed intra- and extracellularly. Previous work on the serotonin transporter, as well as other neurotransmitter transporters, have begun to challenge the fundamental tenets of this model. Currents recorded from these transporters far exceed those predicted from a fixed stoichiometry of ions/neurotransmitter. This has led to the proposal that, under some conditions, these transporters may have ion-channel-like modes of conductance where an actual pore is present in the transporter molecule. Using the cloned *Drosophila* SERT (dSERT) for electrophysiological study, we have performed two-electrode voltage clamp on dSERT-transfected *Xenopus* oocytes. There is a non-stoichiometric ion influx that is voltage dependent, with larger currents present at more negative membrane potentials. By measuring 5HT-dependent current and radioactive 5HT flux in the same oocyte, we have determined that 5HT uptake through dSERT is also voltage dependent, with greater influx at more negative membrane potentials. This has led us to conclude that dSERT displays ion-channel-like properties. Additionally, our data suggest that 5HT flux and 5HT current are coupled in dSERT. Further, experiments using variance analysis suggest that the idea of one 5HT molecule transported per cycle may not hold true for dSERT, but instead hundreds of 5HT molecules may cross the membrane per transport event. Supported by NIH NS-34075, NS-33373, NARSAD estab. invest. L.J.D..

Th-Pos350

PROTON (H) MODULATION OF K-CL COTRANSPORT THROUGH BOTH INTERNAL AND EXTERNAL SITES IN DIDS-pH-CLAMPED LOW MAGNESIUM LK SHEEP ERYTHROCYTES. ((P.K. Lauf and N.C. Adragna)) Wright State University, School of Medicine, Dayton, OH 45401

The just cloned K-Cl cotransporter (KCC, Gillen et al. JBC 271:16237-44. 1996) is functionally present in low K sheep red blood cells (LK SRBCs) (Lauf et al. Amer. J. Physiol. 263:C917-32, 1992). In a recent thermodynamic study (Lauf & Adragna, J. Gen. Physiol 108:341-350, 1996) we reported that, at constant cell volume, V_{max} of K-Cl influx decreased with external pH (pH_o) in LK SRBCs, with internal Mg (Mg_i) stripped by A23187, and DIDS-clamped at internal pH (pH_i) 8.6, but not at pH_i <7.4, suggesting that H affect KCC at both membrane sides. In controls, H inhibited only inside. We attempted to functionally separate the two H sites. LK SRBCs were titrated to $pH_i = pH_o = \sim 9$, Mg_i stripped by A23187 and EDTA, and subsequently DIDS-pH clamped between $pH_i \sim 8.6$ and <6. Bidirectional K fluxes were measured in Cl and NO_3 at internal K and external Rb concentrations of ~24 and 10 mM, respectively, either at constant pH_o for cells with variable pH_i (8.6 to 6), or at variable pH_o for $pH_i \sim 8.6$ only. Although both K and Rb influxes increased marginally at $pH_i \sim 9$, bidirectional KCC, the calculated K flux differences between the two anions, was insensitive to pH_o. However, lowering pH_i from ~8.6 to 5.8 inhibited both K and Rb fluxes in Cl but also to some extent in NO_3. The shape of the H inhibition curves were different for K and Rb fluxes. Internal protonation caused a distinct hyperbolic inhibition of K-Cl efflux with an IC_{50} for protons at about pH 6.5, whereas Rb-Cl influx fell asymptotically to <1/10 of its activity at pH_i 5.8 not permitting an exact IC_{50} determination. Hence, external and internal H affinities modulating KCC in low Mg_i cells are different with different effects on function. For K-Cl efflux, the IC_{50} for the internal H effect is close to the pK_a for histidine, whereas that for RbCl influx seems to be shifted to higher pH values commensurate with a pK_a shift or a different chemical group. These data are consistent with our three state RAI model for volume-clamped low Mg_i LK SRBCs (Lauf et al., Am. J. Physiol. 266:C95-C103, 1994) in which deprotonation recruits transporters from the R into the active A state and need evaluation in terms of our kinetic asymmetry model (Delpire & Lauf, J. Gen. Physiol. 97:173-193, 1991) and Dunham's ABC activation model (J. Gen. Physiol. 101:733-766, 1993). NIH DK 37,160.

Th-Pos351

ION PERMEATION IN GLUTAMATE TRANSPORTERS
((J. Wadiche, N. Zerangue, B. Kanner*, and M. Kavanaugh)) Vollum Institute, Portland, OR 97201 and *Hebrew University, Jerusalem, Israel

Glutamate transporter-mediated uptake is associated with a Cl^- conductance increase, but unlike the gradients for Na^+, K^+, and H^+, the Cl^- gradient is not measurably coupled to that of glutamate. This conductance is not activated by external binding of the non-transported competitive antagonist kainate. The temperature coefficient (Q_{10}; 20°/10°) for D-aspartate transport mediated by the human subtype EAAT1 was 3.2 ± 0.2, while that of the anion current was 1.0 ± 0.1 (n=5), indicating that the macroscopic anion conductance is independent of the transport rate. The NO_3^- and SCN^- permeabilities of the anion channel (relative to Cl^-) were 11 and 58, respectively. No anomalous mole fraction effect was observed with mixtures of anions. The anion conductance was also activated during reverse transport induced by raising extracellular K^+ (EC_{50} = 35.3 ± 5.7mM; n=5). A macroscopic anion current with a similar permeabilty profile (P_{SCN}/P_{Cl}=61) was observed in excised inside-out patches from oocytes expressing the transporter when excitatory amino acids and Na^+ were applied to the intracellular membrane face with K^+ in the pipette. This current was not observed when K^+ was replaced by choline (n=6). A mutant EAAT3 transporter (E374D) was constructed which mediated K^+-independent obligate amino acid exchange; this mutant exhibited a similar anion conductance. The results suggest that an anion conducting state is associated with a glutamate- and Na^+-occupied state of the transporter rather than a state in the K^+-transporting limb of the cycle.

Th-Pos352

REGULATION OF INTRACELLULAR FREE MAGNESIUM IN HELIX ASPERSA NEURONS STUDIED WITH ION-SELECTIVE MICROELECTRODES
((A. Nani, S. Márquez and F.J. Alvarez-Leefmans)) Depto. de Farmacología, CINVESTAV-IPN, Ap. Postal 14-740, MEXICO 07000 D.F.; Depto. de Neurobiología, IMP, Calzada México-Xochimilco 101, MEXICO 14370, D.F. and Dept. Physiol. and Biophys. UTMB, Galveston, TX 77555-0641, U.S.A.

Double-barrelled ion-selective microelectrodes were used to measure transmembrane voltage (Vm) and intracellular free magnesium concentration, $[Mg^{2+}]_i$, in identified neurons (1F,2F and 77F) of the suboesophageal ganglia of *Helix aspersa*. The Mg^{2+} selective barrel contained the neutral ionophore ETH 7025 mixed with PVC, and cyclohexanone (Schaller et al. Pflügers Arch. 423:338, 1993), giving more stable and selective electrodes than previous ones (e.g. ETH 5214). They were calibrated in solutions containing (in mM): KCl, 95; NaCl, 5; Na-Hepes, 5; pH 7.2 and variable concentrations of $MgCl_2$ (0, 0.2, 0.5, 1.0, 2.0, 5.0, 10). The basal $[Mg^{2+}]_i$ was 0.74 ± 0.06 mM (cf. Alvarez-Leefmans et al. J. Physiol. 354: 303, 1984). Replacement of external Na^+ with n-methyl-D-glucamine, produced an increase in $[Mg^{2+}]_i$ from 0.8 ± 0.3 mM up to 1.7 ± 0.4 mM at an initial rate of 0.02 mM/min. Mole by mole replacement of 20 mM external Na^+ with NH_4Cl, produced a transient intracellular alkalinization, followed by an acidification upon removal of NH_4Cl. During the alkalinization, basal $[Mg^{2+}]_i$ decreased from 0.9 mM to 0.1 mM. Upon removal of NH_4Cl, $[Mg^{2+}]_i$ recovered even in the absence of external Mg^{2+}, indicating that the changes in $[Mg^{2+}]_i$ were due to intracellular redistribution. The data suggests that pH_i modulates intracellular Mg^{2+}, probably by affecting cytosolic Mg^{2+} binding or transport. (Supported by NINDS USA Grant NS29227 to FJAL).

Th-Pos353

FUNCTIONAL ANALYSIS OF hu MDR 1 PROTEIN EXPRESSED IN YEAST
((F. Fritz, L.Y. Wei and P.D. Roepe)) Program in Molecular Pharmacology and Therapeutics, Memorial Sloan - Kettering Cancer Center, 1275 York Ave., New York, NY 10021

A truncated hu MDR 1 cDNA (missing the first 17 amino acid codons of the open reading frame) fused to the Ste 6 promoter of S. cerevisiae (generously provided by Drs. K. Kuchler and J. Thorner [P.N.A.S. 89, 2302 - 2306]) was cloned into the yeast expression vector pVT102. The resulting construct (pMDR1) places both the Ste 6 and alcohol dehydrogenase (ADH) promoters upstream of the hu MDR 1 cDNA. Colonies of pMDR1 stable transformants were found to exhibit high levels of hu MDR 1 protein expression. The strains are resistant to valinomycin, indicating the expressed protein is functional. The expressed protein migrates at about 140 kDa on SDS gels, due to inefficient glycosylation, and we estimate hu MDR 1 protein is about 0.1 % - 0.5 % of the total membrane protein in our highest - expressing clones. Isolated plasma membranes exhibit about a 2 - fold higher rate of ATP hydrolysis in Tris buffer (pH 7.50, 5 mM Mg^{++}) relative to control, and the increased ATPase activity can be further modulated by 10 - 100 μM levels of a variety of hydrophobic compounds. A summary of rates of growth in media of various tonicity and ionic composition, cell volume, intracellular pH, plasma membrane potential, and ion transport for these strains will be presented. Similar data for hu MDR 1 expressing yeast strains created in erg6 and K^+ uptake mutants will also be presented. *This work was performed in the Sackler Laboratory of Membrane Biophysics and was supported by grants from the NIH (GM54516, GM55349) and a Cancer Center Support Grant (NCI-P30-CA-08748). P.D.R. is a Sackler scholar at MSKCC. pV102 was generously provided by the NRC, Canada.*

Th-Pos354

ALTERED pHi REGULATION in 3T3 / CFTR CLONES AND THEIR CHEMOTHERAPEUTIC DRUG - SELECTED DERIVATIVES
((L. Y. Wei, M. M. Hoffman and P. D. Roepe)) Program in Molecular Pharmacology and Therapeutics, Memorial Sloan - Kettering Cancer Center, 1275 York Ave., New York, NY 10021

Recently (Wei et al., Biophys. J. 69: 883 - 895, 1995) we found that 3T3 cells overexpressing the CFTR exhibit traits of multidrug resistant (MDR) cells. In this work, 3T3 / CFTR clones were selected with either doxorubicin or vincristine to generate series of stable cell lines that exhibit increasing levels of multidrug resistance. Thus, C3D6 (grown in the presence of 600 nM doxorubicin) was selected from C3D4 (grown in 400 nM), which was selected from C3D1 (grown in 100 nM), which was selected from the original 3T3 / CFTR clone C3 (M.J. Stutts *et al., J.B.C. 268,* 20653 - 20658) that was not grown in the presence of drug. A similar series was generated via selection with vincristine. Initial low - level drug selection increases CFTR expression without promoting MDR 1 or MRP expression. Upon continued selection at higher drug concentrations, CFTR mRNA levels decrease while MDR 1 mRNA levels concomitantly increase. At each incremental step of selection intracellular pH (pHi) increases. Cl^-/HCO_3^- exchange (AE) activity is significantly reduced in derivatives overexpressing MDR 1, but not the parental CFTR clones. The set point of Na^+/H^+ exchange (NHE) activity is significantly lower for the non drug - selected 3T3 / CFTR clones, relative to controls, but then increases upon initial drug selection. Overexpression of MDR 1 in the higher level selectants does not appear to further perturb apparent NHE. These data further describe how CFTR and MDR proteins may affect pHi regulation. *This work was performed in the Sackler Laboratory of Membrane Biophysics and was supported by grants from the NIH (GM54516, GM55349) and a Cancer Center Support Grant (NCI-P30-CA-08748). P.D.R. is a Sackler scholar at MSKCC.*

Th-Pos355

ALTERED pHi REGULATION IN hu MDR 1 TRANSFECTANTS
((M.M. Hoffman, L.Y. Wei and P.D. Roepe)) Program in Molecular Pharmacology and Therapeutics, Memorial Sloan - Kettering Cancer Center, 1275 York Ave., New York, NY 10021

We recently reported on the characteristics of stable LR73 / hu MDR 1 transfectants created without any exposure to chemotherapeutic drugs (M.M.H. *et al., J. Gen. Physiol. 108,* 295 - 313). These clones define the phenotype unequivocally mediated by MDR protein overexpression alone, without any complications associated with exposure to chemotherapeutic drugs. The clones exhibit increased pHi and decreased membrane potential. We have analyzed pHi regulation in detail for these clones, as well as other clones created in Cl^-/HCO_3^- exchanger (AE) - deficient and Na^+/H^+ exchanger (NHE) - deficient backgrounds. Based on Cl^- substitution experiments for clones under constant perfusion with CO_2 / HCO_3^- - buffered media, we conclude that overexpression of hu MDR 1 protein inhibits AE isoform 2 (AE2) function. Conversely, ammonium pulse experiments show that MDR protein overexpression does not perturb NHE function. Cl^- - substitution experiments have been performed under conditions that deplete cellular ATP, in hypotonic and hypertonic media, in the presence of altered Cl^- and HCO_3^- gradients (e.g. altered AE driving force), as well as under Na^+ - free and K^+ - free conditions. In addition, we have performed HCO_3^- - pulse experiments under a variety of conditions. The data describe how MDR protein overexpression perturbs pHi regulation in LR73 cells. *This work was performed in the Sackler Laboratory of Membrane Biophysics and was supported by grants from the NIH (GM54516, GM55349) and a Cancer Center Support Grant (NCI-P30-CA-08748). P.D.R. is a Sackler scholar at MSKCC.*

Th-Pos356

HOMEOSTASIS OF Mg2+ IN ISOLATED RAT HEPATOCYTES UNDER VARIOUS METABOLIC CONDITIONS. ((P. Dalal; A. Romani; and A. Scarpa)) Department of Physiology and Biophysics C.W.R.U., Cleveland OH, 44106-4970.

Chemically induced hypoxia has been shown to induce a depletion of ATP and thereby increase in cytosolic *free* Mg2+. Since cytosolic *free* Mg2+ is tightly regulated, we hypothesized that the increase of cytosolic *free* Mg2+ would result in Mg2+ extrusion from the cell or an uptake by intracellular compartments. To determine the mechanism(s) of Mg2+ transport total Mg2+ content and cytosolic *free* Mg2+ were measured in collagenase dispersed hepatocytes resuspended in a Krebs-Henseleit medium containing only contaminant traces of Mg2+. At selected times after the addition of various drugs, aliquotes of the incubation mixture were sedimented in microfuge tubes, and Mg2+ content in the supernatant and in the pellet were measured by using Atomic Absorption Spectrophotometry (AAS). Upon stimulation with 2mM NaCN (chemical hypoxia), a sizeable amount of Mg2+ started being extruded from isolated hepatocytes after 10 min lag phase, and reached the maximum within 40 min of hypoxia treatment (35-40 nmol/mg protein). A quantitatively similar extrusion was also induced by 5 ug/ml FCCP, an uncoupler which collapses the mitochondrial proton gradient and thereby ATP generation, but not by 2 mM iodoacetate, a glycolysis inhibitor. After 60 min of NaCN treatment, the addition of digitonin did not significantly increase the amount of Mg2+ released into the supernatant, suggesting that most of cytosolic Mg2+ has been already extruded or compartmentalized in intracellular organelles. The determination of Mg2+ content in the pellet complemented the amount of Mg2+ mobilized into the extracellular medium. Previous observations from this and other laboratories indicate that Mg2+ can be extruded across the cell membrane via a Na+ dependent and a Na+ independent mechanisms. In order to ascertain as to which pathway was involved in the observed Mg2+ extrusion, the experiments described above were performed on hepatocytes incubated in a medium devoid of Na+ or Ca2+. Under these experimental conditions, Mg2+ extrusion occured irrespectively of the absence or presence of Ca2+ in the incubation medium while it was completely prevented by the absence of extracellular Na+. The Mg2+ extrusion was unaffected by 1mM amiloride, an inhibitor of the Na+/Mg2+ exchanger, but was markedly inhibited by (~75% inhibition) by 1 mM quinidine, an inhibitor of the alternative Mg2+ transport mechanism. These data suggest that Mg2+ is transported via a Na+ dependent mechanism sensitive to quinidine and insensitive to amiloride which is distinct from the previously described Na+/Mg2+ antiporter. In order the measure change in cytosolic *free* Mg2+, the cells were loaded with mag-fura-2 and ratio of 340/380 excitation was detected at 510 nm. The addition of NaCN was followed by an initial rise (few mins) in cytosolic *free* Mg2+ which progressively decreased, at time points in which AAS measurements indicate an extrusion of Mg2+ out of the cells. When these experiments were repeated in a Na+ free buffer, both the initial rise and the subsequent decrease in cytosolic *free* Mg2+ were markedly reduced until 120 mM NaCl was reintroduced into the system. These data suggest, the operation of a Na+ dependent Mg2+ transport mechanism under condition of ATP depletion which is sensitive to quinidine but insensitive to amiloride. This transported may be activated by a rise in cytosolic *free* Mg2+ and might be regulated by the presence of physiological concentrations of ATP*Mg in the cytosol of liver cells. [Supported by NIH-HL 18708]

Th-Pos357

PHARMACOLOGICAL AGENTS AS FUNCTIONAL PROBES OF THE HUMAN DOPAMINE TRANSPORTER.

((**Mark S. Sonders** and Susan G. Amara)) Howard Hughes Medical Institute and the Vollum Institute, Oregon Health Sciences Univ., Portland OR 97201

The human dopamine transporter (hDAT) is a plasma membrane Na/Cl/substrate cotransporter which serves as the principal means of terminating DA signals in neural tissue. We have previously described two steady-state ionic currents associated with hDAT expression in *Xenopus* oocytes: 1) a transport-associated current elicited by substrates (e.g. DA, amphetamine) that is dependent upon external Na^+ and Cl^-, and 2) a constitutive proton-selective leak current that is inhibited both by substrates and non-substrate translocation inhibitors (e.g. cocaine). Blockade of the leak current by any organic hDAT ligand can be utilized as a functional index of ligand binding affinity and also of the ligand's affinity in inhibiting [^{3}H]DA uptake. On the other hand, the magnitude of the substrate-elicited transport-associated current principally reflects the rate of translocation.

The V_{max} and transport I_{max} vary markedly among substrates, the neurotoxin MPP^+ being the most efficacious substrate identified to date. In order to better understand the substrate translocation process and its molecular determinants, we have examined a variety of congeners of β-phenethylamine and of MPP^+ in electrophysiological and biochemical assays. The structure-activity data help reveal the molecular requirements for substrates and for translocation (uptake) inhibitors. Furthermore, they provide insights into the relation between the transport and leak currents, and should prove useful for elucidating the consequences of site-directed mutagenesis of hDAT.

This work was supported by grant DA07595.

Th-Pos358

Further Characteristics of the Rapid Mechanism of Mitochondrial Calcium Uptake in Heart Mitochondria

((L. Buntinas, K.K. Gunter, G.C. Sparagna, T.E. Gunter))
Univ. of Rochester Dept. of Biophysics, Rochester, NY 14642

We have used our pulse-generating system, fluorescence spectroscopy, and dual label isotope techniques to show the existence of a rapid mode of Ca^{2+} uptake into heart mitochondria similar to that shown earlier in liver mitochondria. The rapid mode is most easily demonstrated by showing that a plot of Ca^{2+} uptake vs. pulse duration always extrapolates to an intercept with the ordinate that is significantly above 0 uptake at 0 time. We have found, as was the case with liver mitochondria, that ending the pulse by addition of EGTA so as to bring the $[Ca^{2+}]$ to near 1 nM does not eliminate this type of uptake. Depletion of endogenous calcium and depletion combined with loading of radioactive calcium has no effect on this uptake. This suggests that what is being observed is not exchange of cold endogenous Ca^{2+} for external labeled Ca^{2+} but net Ca^{2+} uptake. In contrast to RaM behavior in liver, RaM uptake in heart is not inhibited by ruthenium red and is inhibited by spermine and AMP. The RaM mechanisms in heart and liver mitochondria seem quite different.

Gunter, T.E., K.K. Gunter, S.-S. Sheu, and C.E. Gavin, "Mitochondrial calcium transport: Physiological and pathological relevance." *Am. J. Physiol.* 267:(Cell Vol. 36) C313-C339 (1994)

Sparagna, G.C., K.K. Gunter, S.-S. Sheu and T.E. Gunter, "Mitochondrial Calcium Uptake from Physiological-type Pulses" *J. Biol. Chem.* 270 No.46 pp.27510-27515(1995).

(Supported by NIGMS Grant GM-35550 and AHA Grant 960166)

Th-Pos359

SIMPLE & COMPLEX BEHAVIORS OF THE GAT1 TRANSPORTER. (C. Lu & D.W. Hilgemann), Dept. of Physiology, UTSW Med. Ctr., Dallas, TX 75235

The cloned GABA:Na:Cl cotransporter, GAT1, was expressed in *Xenopus* oocytes and studied in excised giant membrane patches. Dependencies of the reverse-mode steady-state transporter current (I_{GABA}, defined by intracellular GABA) on cytoplasmic and extracellular substrate concentrations were determined. Results obey predictions for a simple alternating-access model with empty GAT1 binding Na^+ first from the outside and Cl^- first from the inside. This is also supported by: (1) Cl^-_{in} suppresses the forward-mode I_{GABA} and decreases the capacitance of the empty GAT1. (2) These effects show similar concentration dependencies on Cl^-_{in}. And (3), neither cytoplasmic GABA nor Na^+ inhibits the forward-mode I_{GABA}. Other observations have revealed more complexities: (1) The concentration dependence of GAT1-specific capacitance on Cl^-_{in} is not affected by varying *cis*- or *trans*- Na^+. (2) The Cl^-_{in}-induced capacitance change is not inhibited by the specific inhibitor NO-711, even in the presence of Na^+_{ex}. (3) The charge-voltage (Q-V) relation of the slow, Na^+_{ex}-defined charge movement (V_{hold} = -30 mV) shows a much smaller shift by Cl^-_{in} than expected at concentrations up to 120 mM, which fully inhibits the forward-mode I_{GABA}. And (4), analysis of slow charge movement at V_{hold} = 0 mV is complicated by the presence of multiple components, anomalous Q-V relations and a Q_{on}/Q_{off} ratio smaller than unity.

Th-Pos360

MULTIPLE CYS TO SER MUTATIONS IN THE MITOCHONDRIAL UNCOUPLING PROTEIN IMPAIR H^+ TRANSPORT AND GDP INHIBITION. ((Martin Modriansky and Keith D. Garlid)) Dept. of Chemistry, Biochemistry, and Molecular Biology, Oregon Graduate Institute of Science & Technology, Portland, OR 97291-1000.

Mitochondrial uncoupling protein (UcP) facilitates proton backflux across the membrane in the presence of free fatty acids (FA). The UcP activity is allosterically inhibited by purine di/trinucleotides. Chemical studies with specific -SH reagents suggested involvement of Cys residues in both H^+ transport and GDP inhibition of the UcP. Single Cys to Ser mutants, however, refuted this hypothesis. All seven of the mutants have shown wild-type characteristics. We prepared three mutants that had three, four, and six Cys residues changed into Ser. We measured kinetic parameters on all three mutants using our sensitive fluorescence assay of proton flux in liposomes. The K_m and V_{max} for FA and the K_i for GDP were compared to a wild-type control. In contrast to the single mutants, multiple Cys mutants exhibited pronounced differences from wild-type, and those differences increased with the number of Cys mutated. Markedly decreased affinities were observed for both FA and GDP. (Supported by NIH grant GM 31086.)

Th-Pos361

CHARACTERIZATION OF ACIDIFICATION, IONIC FLUXES, AND MEMBRANE POTENTIAL GENERATION OF CLATHRIN COATED ENDOSOMES. ((Alisha Hoffpauir, Taletha C. Moore, Marcus Taylor, J. Abra Watkins, C-Y. Li, and Jonathan Glass)). Center for Excellence in Cancer Research, Treatment, and Education, Department of Medicine, LSUMC-S, Shreveport, LA, 71130-3932.

Differences between the functional properties of vesicles during the transitions involved in various processes of endocytosis have been poorly understood. Vesicles isolated from red cells provide a uniquely interesting model for the study of vesicular acidification and consequent coupling of ionic fluxes due to their extremely stable properties. The relationships between vesicular acidification, generation of membrane potential, and ionic fluxes for isolated clathrin coated (early) endosomes have been examined in order to quantitatively constrain general models developed on the basis of results obtained for uncoated endosomes. Upon the addition of 1 mM ATP, the kinetics of acidification are slightly biphasic with an apparent rate constant of $7.7\pm1.2 \times 10^{-3}$ s^{-1} and a ΔpH of 1.3 ± 0.2 while the kinetics of gradient dissipation are more difficult to detect with an apparent rate constant of $4.6\pm1.1 \times 10^{-3}$ s^{-1}. Following the addition of 1mM GTP, the kinetics of acidification are monophasic with an apparent rate constant of $4.6\pm0.06 \times 10^{-3}$ s^{-1} and a ΔpH of 0.7 ± 0.2. Membrane potential kinetics indicate an overall increase of 40 mV with an apparent rate constant of $5.4\pm0.6 \times 10^{-4}$ s^{-1}, for 1mM ATP, and 20 mV at $1.7\pm0.6 \times 10^{-4}$ s^{-1}, for 1 mM GTP. These rate parameters are about an order of magnitude slower than similar observations using uncoated vesicles. Apparent rate constants for sodium, potassium, and chloride ion fluxes are similar to those observed for uncoated vesicles although the net changes are significantly smaller. The results provide quantitative constraints on coupling and provide needed insight into modifications of our current models.

Th-Pos362

COUPLING OF CHLORIDE TRANSPORT TO PROTON AND CATION FLUXES DURING ENDOSOMAL ACIDIFICATION. ((R. Damion Hardison, Jeff S. Weeks, Emily J. Besser, Marcus Taylor, J. Abra Watkins, C-Y. Li, and Jonathan Glass)) Cancer Center, Department of Medicine, LSU Med. Ctr., 1501 Kings Highway, Shreveport, LA, 71130-3932.

The regulation and control of endosomal acidification is a rate limiting process of iron absorption/transport and has been proposed to be critically dependent on chloride transport. Rabbit reticulocyte endosomes provide a relatively simple model for investigating detailed relationships among ionic fluxes, membrane potential generation ($\Delta\Psi$), and pH gradient formation (ΔpH). Under well defined buffer conditions, chloride fluxes are observed using SPQ, a membrane permeant fluorescent probe, while cation fluxes, ΔpH, and $\Delta\Psi$ generation are monitored with PBFI, fluorescein labeled differic transferrin, or Oxonol VI respectively. Upon the addition of 1 mM ATP, the kinetics of chloride influx is primarily biphasic with an apparent rate constant of $4.2\pm0.4 \times 10^{-3}$ s^{-1} and a very fast phase of $>1 \times 10^{-1}$ s^{-1}. The kinetics of $\Delta\Psi$ generation are similarly biphasic with observed rate constants of $3.5\pm0.5 \times 10^{-3}$ s^{-1} and >10 s^{-1} as well as an increase of >80 mV indicating greater chloride influx than sodium and potassium efflux. In contrast to the other transport activities the difference between ATP and GTP is negligible. In addition, cAMP or cGMP alone stimulated significant Cl^- transport. The chloride transport inhibitor, DIDS, effectively stopped all transport activity at 100 μM concentrations. Selective use of ionophores and inhibitors of Na^+ and K^+ transport indicate that Cl^- influx is not strongly coupled to K^+ and Na^+ effluxes. However, H^+ influx is highly coupled to Cl^- influx. These observations provide kinetic evidence of Cl^- fluxes in reticulocyte endosomes and suggest that Cl^- transport may be the most important ionic flux coupled to acidification relative to Na^+ and K^+ efflux.

Th-Pos363

CRYSTALLOGRAPHIC ANALYSIS OF CORE PROTEINS OF CYTOCHROME b/c1 COMPLEX -- IMPLICATION TO THE STRUCTURE AND FUNCTION OF MITOCHONDRIAL PROCESSING PEPTIDASE. ((D. Xia[1], K. P. Deng[2], H. Kim[1], A. Kachurin[2], C. A. Yu[2], L. Yu[2], & J. Deisenhofer[1])) [1]HHMI, UT Southwestern Medical Center, Dallas, TX 75235. [2]Oklahoma State University, Stillwater, OK 47078.

Most nucleus-encoded mitochondrial proteins are synthesized with an N-terminal leader peptide that confers the signal for targeting to mitochondria. The leader peptides are cleaved by the mitochondrial processing peptidase (MPP) after translocation into the mitochondria. MPP of animals are hetrodimers of α- and β-subunits with a total molecular weight around 100 kDa, located in the mitochondrial matrix. MPPs from plants, on the other hand, have been identified as an integral part of the mitochondrial cytochrome bc1 complex (bc1), and the MPP activity was further mapped to the core proteins of bc1. Sequences of the core proteins of bovine bc1 are highly homologous to those of rat, yeast and patato MPPs, but the core proteins appear to lack enzymatic activity. The crystal structure of bovine mitochondrial bc1 complex shows that the subunits core 1 and core 2, which correspond to the β- and α- subunits of MPP, respectively, are remarkably similar to each other. Each core protein is folded into two domains of similar size, which are related by a pseudo two-fold symmetry axis. Both domains belong to the α/β folding type, but have different folding topologies. The subunits core 1 and core 2 tightly associate with each other, enclosing a hollow cavity. The association also creates a cleft between the two subunits, which is filled with a polypeptide whose identity is yet to be established. A putative catalytic site including a zinc binding motif has been identified, and is located on the interface between the two subunits. On the basis of sequence homology between the core proteins of bc1 and MPP, we assume that these two complexes also have very similar three-dimensional structure. This work is supported by grants from NIH (GM30721 to CAY) and from Welch Foundation (to J.D.).

Th-Pos364

IDENTIFICATION OF THE VOLUME SENSOR IN BARNACLE MUSCLE CELLS ((L. Trais, J.C. Summers, R. Lajvardi, K. Goharderakhshan, D. Hergan, R. Buechler, H. Chang, C. Peña-Rasgado and H. Rasgado-Flores)). Dept. Physiol. & Biophys. FUHS/The Chicago Medical Sch. N. Chicago, Il, 60064.

In animal cells, continuous exposure to a hypoosmotic environment induces an initial swelling. However, most cells subsequently shrink towards their original volume. This process is termed regulatory volume decrease (RVD) and results from at least two functional elements: a sensor that detects the increase in volume, and a sensor-activated effector responsible for restoring the original volume. Although the effector mechanisms have been extensively studied, little is known about how cells detect an increase in their volume. Two major hypotheses have been proposed to explain how cells sense volume changes: i) mechanical events, like bending or stretching of the membrane or rearrangement of structures within the cell; and ii) changes in the concentration of some intracellular component, such as water, salt, or cytoplasmic proteins. The present work was undertaken to test specific predictions of two of the major hypothesis proposed to explain how cells sense swelling: First, if an increase in membrane stretch is the volume sensor, an increase in swelling *per se* under conditions where the ionic strength, osmolality and macromolecular concentration are maintained constant, should activate RVD. Second, if a reduction in the intracellular concentration of macromolecules is the sensor, isosmotic replacement of large macromolecules by smaller ones should induce volume decreases proportional to the initial macromolecular concentration and size as well as to the magnitude of the concentration reduction. Barnacle muscle cells were used as models because these cells undergo an extracellular Ca^{2+} (Ca_o)-dependent RVD in response to continuous exposure to a hypoosmotic environment and because these cells can be internally perfused and voltage-clamped. The results show that, in the absence or presence of Ca_o, an increase in cell volume of 50% resulting from an hydrostatic pressure of 18 mm of water, did not induce volume reduction. However, the results were consistent with the predictions of the macromolecular crowding theory: isosmotic replacement of proteins or polymers with sucrose induced volume reductions but this effect was only observed when the replacement was $\geq$ 25 % and the particular macromolecule had an average molecular weight of $\leq$ 20 KD and a concentration of at least 18 mg/ml. Volume reduction was effected by a mechanism identical with that of hypotonicity-induced RVD, namely, activation of verapamil-sensitive Ca^{2+} channels.

Th-Pos365

CHARACTERIZATION OF GLYCINE EFFLUX AND VOLUME REDUCTION MECHANISMS IN BARNACLE MUSCLE CELLS ((K.McGruder, J.B. Bitner, C.Peña-Rasgado, & H. Rasgado-Flores)) Dept. Physiol. & Biophys. FUHS/Chicago Med. Sch. N.Chicago, IL 60064

Glycine (gly) is the most abundant intracellular amino acid in barnacle muscle cells (~ 90 mM). Under isosmotic or hypoosmotic conditions, an increase in the intracellular free Ca^{2+} concentration ($[Ca^{2+}]_i$) induces the synthesis of cAMP which promotes in turn the efflux of osmolytes (e.g., gly) leading to water loss and volume reduction. The present work had two aims: i) to identify the mechanism(s) by which gly exits barnacle muscle cells in response to volume reduction effectors (i.e. exposure of the cells to hypoosmotic conditions in the presence of extracellular Ca^{2+} or exposure to an isosmotic increase in $[Ca^{2+}]_i$ or cAMP); and ii) to assess if all unidirectional gly efflux induces volume reduction. The experimental strategy consisted of comparing the gly efflux accompanying volume reduction with the efflux expected from the measured volume reduction assuming that this reduction was entirely due to the gly efflux. Gly efflux was measured radiometrically from cells perfused with solutions containing gly (100-200 mM) as the predominant osmolyte able to exit the cell in response to the presence of volume reduction effectors. Calculation of the expected increase in gly efflux from a given measured volume reduction was accomplished using the following equation: gly efflux = ([gly]xR)/surface area, where R is the measured rate of volume change (μl/sec) in response to the volume reduction effector. The results show that when the cells were exposed to hypoosmotic conditions in the presence of Ca_o, the ratio of measured/expected gly efflux was very close to unity (i.e. 1.09). When 1 mM cAMP was used as the volume reduction effector the ratio was 1.77. However, this ratio was reduced to 1.1 if extracellular Cl (Cl_o) was replaced with methanesulfonate. Finally, when 20 μM $[Ca^{2+}]_i$ was used as the volume reduction effector, the ratio was 2.4 in the presence of Cl_o but only 1.1 in its absence. The Ca_o-induced volume reduction was inhibited by presence of the cAMP antagonist, Rp-cAMPS. This indicates that an increase in $[Ca^{2+}]_i$ induces the synthesis of cAMP which induces in turn gly efflux. Gly efflux is either accompanied with water or occurs in exchange for Cl_o. Three additional evidences indicate that gly efflux is difussional rather than carrier mediated and that this efflux takes place *via* anion channels: i) an increase in $[Ca^{2+}]_i$ promoted the exchange of intracellular gly for extracellular gly or taurine without promoting volume reduction; ii) presence of intracellular taurine or a mixture of amino acids did not inhibit gly efflux; and iii) the anion channel blockers SITS and niflumate inhibited gly efflux.

Th-Pos366

PERTURBATION OF THE ATPase ACTIVITY OF P-GLYCOPROTEIN BY VARIOUS HYDROPHOBIC COMPOUNDS ((S. Orlowski, F. André and **M. Garrigos**)), DBCM, CE Saclay, F-91191 Gif/Yvette, France. (Spon. by P. Ripoche).

P-glycoprotein (P-gp), which is responsible of the multidrug resistance in tumor cells, is a membrane transporter of various hydrophobic drugs. P-gp displays an ATPase activity which we measured using P-gp-containing vesicles obtained from purified total membranes from Chinese Hamster lung fibroblasts (DC-3F/ADX). Tentoxin is a hydrophobic cyclic tetrapeptide which stimulates P-gp ATPase activity in a saturable manner (activation factor: 1.5±0.1, half-maximal activating concentration: 20-30 μM). The presence of stimulating concentrations of tentoxin does not influence the activation of P-gp ATPase activity by verapamil or progesterone. Cytotoxicity experiments performed on DC-3F/ADX cells in the presence of vincristine and various concentrations of tentoxin showed no reversing effect, which suggests that tentoxin is not transported by P-gp. Compared to membrane permeabilizing agents like digitonin and saponins, tentoxin did not induce detectable detergent-like membrane perturbing effects when tested on P-gp-containing or -devoid vesicles. In addition, digitonin and saponins specifically influenced the activation of P-gp ATPase by verapamil, revealing complex effects of hydrophobic compounds on the P-gp function.

Th-Pos367

CHARACTERIZATION OF THE CALCIUM TRANSPORT MECHANISMS IN ISOLATED T-TUBULE AND SARCOPLASMIC RETICULUM MEMBRANES FROM THE DIAPHRAGM MUSCLE. Sandra I. Bajaña and Alicia Ortega. Dpto. de Bioquímica, Facultad de Medicina, Universidad Nacional Autónoma de México, 04510, México.

Skeletal muscle membranes derived from rabbit diaphragm muscle, such as the transverse tubular network and the sarcoplasmic reticulum (SR), were isolated and characterized with respect to the binding of the dyhidropyridin, [^{3}H] PN200-110 and [^{3}H] Ryanodine, as well as by its lipid composition, ATPase activities and Ca^{2+} transport. Previous experiments done by *Eberstain and Sandow (1961), Gonzalez-Serratos et al. (1978) and Bianchi and Narayan (1982),* suggest that the transverse tubular system from skeletal muscle has an important role in removing the Ca^{2+} that is released from the SR during excitation contraction coupling, where an increase in Ca^{2+} concentration in the transverse tubular system after stimulation may explain the uncoupling of the action potential from contraction during fatigue. In an attempt to reveal what could be the physiological role of the t-tubule membrane Ca^{2+} transport mechanisms in the mechanistic of fatigue, we used muscle diaphragm as a model which has a high *in* and *out* Ca^{2+} transport ratio, and contracts rhythmically and permanently. The Ca^{2+} extrusion mechanisms are more developed in this muscle than in the slow and rapid skeletal muscle may be to avoid permanent contractions.

Eberstain and Sandow (1961), Science 134: 383.
Gonzalez-Serratos et al.(1978), Proc.Natl.Acad. Sci. usa 75:1329
Bianchi and Narayan (1982), Science, 215: 295.

Th-Pos368

ZN-DEPENDENT PROTEOLYTIC CLEVAGE OF F188 GENE PRODUCT IS ASSOCIATED WITH AN INCREASE IN ZN- RESISTANCE IN BACTERIA. ((Meenakshi Noll [1], Konstantin Petrukhin [2] and Svetlana Lutsenko [1])) 1. Dept. Biochemistry and Mol. Biology, OHSU, Portland, OR 97201, 2. Dept. Psychiatry, Columbia University, New York, NY 10032.

Transformation of E.Coli cells with PROT1, a plasmid containing a 13.5 kb EcoR1 genomic fragment of Proteus mirabilis, markedly increases resistance of the cells to high concentrations of zinc (1 mM). The increase in Zn-resistance was concomittant with overexpression of a 14 kDa protein and its accumulation in periplasm. Deletion experiments showed that genes important for expression of this protein are located in the 3 kb segment downstream from Cu-ATPase gene. Identification of these genes are currently underway. Other heavy or transition metals, such as Co, Ni, Cu or Mn did not induce expression of the 14 kDa protein. N-terminal amino-acid sequencing of the 14 kDa protein yielded HGGHGMWQQN.., which corresponds to the C-terminal half of F188 gene product of E.Coli. F188 was previously proposed to encode a 20.4 kDa protein with unknown function. HGGHGM and GHMGMGH motifs in the sequence of our 14 kDa fragment indicates that this protein is involved in Zn-binding, which is consistent with the specific induction of this band in the presence of Zn. We propose that F188 gene product is involved in cellular Zn-homeostasis and that the specific Zn-dependent proteolysis (or autolysis) of the 20.4 kDa protein may be an important step leading to Zn resistance in E.coli. Supported by start-up funds for SL.

Th-Pos369

MITOCHONDRIAL PHOSPHATE TRANSPORT PROTEIN (PIC, PTP, MIR). GLU192ASP (TRANSMEMBRANE HELIX D) SUPPRESSES INACTIVE SINGLE REPLACEMENT MUTANTS ON TRANSMEMBRANE HELICES A AND C. ((E. Ligeti, L. Mincone, and **H. Wohlrab**)) Boston Biomedical Research Institute and Harvard Medical School, Boston, MA 02114.

The inability of yeast (*Saccharomyces cerevisiae*) PTP null mutant to grow on glycerol was used to identify suppressors of inactive PTP mutants. Glu192Asp [cytosolic and C-terminal end of transmembrane (TM) helix D] suppresses Asp39Asn (matrix and C-terminal end of A) and also Glu137Gln (matrix and C-terminal end of C). These revertant double mutants, expressed in *E.coli*, purified, and reconstituted, catalyze pH gradient-dependent net phosphate transport. The locations at opposite ends of the TM helices suggest interactions among the helices. This is expected since residues of the hypothetical proton cotransport path (1) are located on TM helices A (His32) and C (Glu126, Glu137) and should be nearest neighbors. Other transport-relevant residues are also on these three helices: mutations in helix D increase transport activity (1); Cys28 in helix A is the only Cys of this PTP involved in the interconversion of antiporter and uniporter activities (2) and in transport-inactivation by an intersubunit disulfide (3); mutations in the C and D connection yield uncoupled (4) and inactivated (5) PTP. (1) Phelps et al. (1996) Biochemistry 35, 10757; (2) Kraemer et al. (1997) this meeting; (3) Phelps & Wohlrab (1993) FASEB J. 7, 321; (4) Wohlrab & Briggs (1994) Biochemistry 33, 9371; (5) Phelps et al. (1996) Biophys. J. 70, A8. (Supported by NIH grant GM33357)

EPITHELIAL PHYSIOLOGY

Th-Pos370

ACTIVATION OF BOTH Ca^{2+}-ATPase AND Ca^{2+} CHANNEL BY SCORPION VENOM IN THE MICROSOMES OF PORCINE TRACHEAL EPITHELIA. ((Young-Kee Kim and Kyoung-Soo Cho)) Department of Agricultural Chemistry, Chungbuk National University, Cheung-Ju, Chungbuk, 361-763, Korea.

The effects of *Leiurus quinquestriatus hebraeus* (Lqh) venom were evaluated on the activities of microsomal Ca^{2+}-ATPase and Ca^{2+} release channel prepared from the epithelial cells of pig airway. The whole venom of Lqh (120 μg/ml) increased the activity of microsomal ATPases ~32% in the tight-sealed microsomes and ~28% in the Triton X-100-treated or ionomycin-treated leaky microsomes. Thapsigargin, a specific antagonist of Ca^{2+}-ATPase, blocked ~40% of total ATPase activity, completely diminishing the effect of Lqh venom, and this result suggests a direct activation of microsomal Ca^{2+}-ATPase by Lqh venom. The Lqh venom-induced increase in $^{45}Ca^{2+}$ uptake was ~20% and it was only obtained when heparin, an antagonist of $InsP_3$-receptor channel, was added in the uptake medium. In the absence of heparin, Lqh venom unexpectedly decreased the rate and the amount of $^{45}Ca^{2+}$ uptake and this was explained by the Lqh-induced increase in microsomal Ca^{2+} release. Lqh venom released microsomal $^{45}Ca^{2+}$ as much as the amount of $^{45}Ca^{2+}$ release by 4 μM $InsP_3$, implying that Lqh venom also activates the microsomal $InsP_3$ receptor. In order to purify the active components of Lqh venom, the whole venom was loaded onto a column of Sephadex G-50. Four fractions were obtained and the increases in microsomal $^{45}Ca^{2+}$ releases were obtained by the fractions F-I and F-II. Molecular weights of these fractions were roughly estimated to 15~20 kDa by comparing to K_{av} values of molecular weight markers. The effect of fraction F-II on microsomal $^{45}Ca^{2+}$ release was disappeared by the treatment of protease, implying that the chemical nature of the active component is a polypeptide. Meanwhile, only fraction F-I activates microsomal Ca^{2+}-ATPase and this effect was inhibited by thapsigargin. Currently, we are under further purification and evaluation of the active component on the electrophysiological characteritics of $InsP_3$ receptor.

Th-Pos371

SIMULTANEOUS HIGH RESOLUTION MEASUREMENTS OF $[Ca^{2+}]_i$ AND CILIARY BEAT FREQUENCY IN SINGLE CILIATED TRACHEAL EPITHELIAL CELLS. ((**M. Salathe** and R.J. Bookman)) Dept. of Mol. & Cell. Pharmacology and Division of Pulmonary and Crit. Care Med., University of Miami School of Medicine, Miami, FL 33101.

Despite the fact that $[Ca^{2+}]_i$ plays an important role in regulating ciliary beating, the molecular site of Ca^{2+} action is unknown. In an effort to constrain the number and type of reactions that could link changes in $[Ca^{2+}]_i$ to changes in ciliary beat frequency (CBF), we have analyzed the kinetics of coupling between $[Ca^{2+}]_i$ and CBF in response to 10 μM acetylcholine (ACh) using simultaneous recordings of both signals from single ciliated ovine tracheal epithelial cells. CBF of a single cilium was calculated from intensity data recorded by red-filtered, digital video phase-contrast microscopy. These data represented the transmitted light intensity changes of a ~200 nm^2 area as a single cilium moved in and out of the sampling area over time. Changes in $[Ca^{2+}]_i$ were followed by changes in epifluorescence emission (excitation with 380 nm) of the same, fura-2/AM-loaded cell. Using staggered FFT analyses for CBF (time resolution: 3s), we showed that tight coupling between the changes in CBF and $[Ca^{2+}]_i$ persisted throughout the 2 minute response to ACh (from initial increases in both signals above baseline through the returns to baseline; n=5 cells). To improve the CBF time resolution, instantaneous frequencies or single beat cycle durations were calculated. This allowed comparison of the kinetic changes of $[Ca^{2+}]_i$ and CBF during simultaneous measurements with a CBF time resolution of ~130 ms. Such records revealed that, in response to ACh, the CBF signal tracked the increase in $[Ca^{2+}]_i$ with a delay of 1-3 beat cycles. Given the beating frequency at room temperature (~7 Hz), CBF thus changed within 150-400 ms of a $[Ca^{2+}]_i$ change (n=20 cells). Since the noise of these CBF calculations could have influenced the kinetic comparisons, we also assessed CBF by a sliding FFT analysis of the intensity signal. This analysis confirmed the conclusions from the instantaneous CBF records: the CBF delay was >1 and ≤3 beat cycles, a time longer than expected for unopposed solution diffusion kinetics of Ca^{2+} to the ciliary target. Thus, these data suggest that either Ca^{2+} activates a multi-step cascade to change CBF or significant Ca^{2+} diffusion barriers exist near the cilium. (M. Salathe is an HHMI Physician Postdoctoral Fellow. Also supported by NHLBI-20989, ALA/Dade, & Glaser Foundation).

Th-Pos372

CALCIUM SENSING RECEPTORS ARE EXPRESSED IN INTESTINAL EPITHELIUM. ((**L. Gama**, L.M. Baxendale-Cox and G.E. Breitwieser)) Johns Hopkins University, Schools of Medicine and Nursing, Baltimore, MD 21205.

Expression of calcium sensing receptors (CaR) was demonstrated in several human intestinal epithelial cell lines (T84, HT29 and Caco-2) and rat intestinal epithelium by both RT-PCR and Northern blotting of RNA. Restriction patterns of the PCR products were the sizes predicted by the human and rat sequences. Northern blotting utilizing either a biotinylated probe prepared from a PCR fragment or from the full length human CaR yielded transcripts of several sizes consistent with CaR expression. CaR agonists (Ca^{2+}, poly-L-arginine) produced an intracellular Ca^{2+} increase in HT29-18-C1 cells (monitored with fura-2) which was dependent upon release from thapsigargin-sensitive stores. CaR agonists (Ca^{2+}, Gd^{3+}, Ni^{2+}, poly-L-arginine) increased short circuit current (and decreased trans-epithelial resistance) of T84 cell monolayers only when added to the basolateral side, and produced responses comparable to the peak response to carbachol. Taken together, these studies demonstrate that calcium sensing receptors are expressed in intestinal epithelial cells, localize to the basolateral membrane, and couple to mobilization of intracellular Ca^{2+}. The presence of CaR in intestinal epithelium presents a new locus for investigations into the role(s) of extracellular Ca^{2+} in modulating intestinal epithelial cell differentiation and trans-epithelial Ca^{2+} transport. Supported by NIH (DK 44484) and NINR (3800-02) and JHUSON.

Th-Pos373

CFTR-INDEPENDENT ATP RELEASE BY EPITHELIA TRIGGERED BY MECHANICAL STIMULI. ((**R. Grygorczyk** and J.W. Hanrahan)) Dept. Physiology, McGill University, Montreal, QC, Canada, H3G 1Y6.

Cystic fibrosis transmembrane conductance regulator (CFTR)-mediated ATP efflux has been proposed as an autocrine mechanism for regulating chloride secretion through other types of chloride channels. We found in previous studies that wild type CFTR channels do not conduct ATP at rates that can be measured using the patch clamp technique. However, those electrophysiological studies would not have detected very small or electroneutral ATP fluxes through CFTR, or ATP efflux through other pathways that might be regulated by CFTR. To examine these possibilities we have now used a sensitive luciferase luminometric assay to measure ATP efflux from epithelial and nonepithelial cell lines. cAMP stimulation did not raise external ATP concentration above the background noise in any of the cell lines tested; T84, Calu-3, 9HTEo⁻ and ΣCFTE29o⁻ (colonic and airway human epithelial cells, respectively), NIH 3T3 fibroblasts and CHO cells, nor were rates of ATP release correlated with CFTR expression. During the course of these studies we noticed that transient ATP release was exquisitely sensitive to mechanical perturbation. When cells were grown on flexible plastic coverslips, slight bending of the coverslip resulted in ATP release that was proportional to the amount of mechanical stimulus. Similar mechanically-induced release was observed from cells lacking CFTR expression. Agents that elevate intracellular calcium (A23187 1 μM; histamine 100 μM; carbachol 100 μM) were without effect, suggesting that ATP is not released by calcium-dependent exocytosis. Mechanically-induced ATP release may be a physiologically relevant mechanism of epithelial transport regulation, which has not previously been fully appreciated. *Supported by CCFF, NIH (NIDDK) and MRC.*

Th-Pos374

BIOENERGETIC PROPERTIES OF HUMAN PROSTATE CANCER CELLS LINES, DU145, PC-3 AND LNCaP, AND FIBROSARCOMA HT1080C1 CELLS. ((**A.V. Panov**[*], J.A. Petros[*], S.D. Graham[*], D.C. Wallace[**])) Division of Urology, Winship Cancer Center[*], and Department of Genetics and Molecular Medicine[**], School of Medicine, Emory University, Atlanta, GA 30322

Normal prostate epithelial cells have unique bioenergetics: unlike other tissues, they do not oxidize citrate (Costello, L.C. & Franklin, R.B. (1994) The Prostate, 25, 162.). We compared (polarographically) the rates of oxidation of glucose and various Krebs Cycle substrates by three prostate cancer (PC) cell lines: DU145, PC-3, LNCaP, and the human fibrosarcoma cell line HT1080C1. The data showed that all these cells have a capability to oxidize succinate, glutamate and citrate (in the presence of malate), pyruvate. Oxidation of glucose alone was independent of the rate of endogenous respiration. The rates (calculated per 10^6 cells) of oxidation of glutamate, pyruvate and citrate were 1.5-2-fold higher than respiration on glucose, and were the same for DU145, PC-3 and HT1080, whereas LNCaP cells respired almost 1.5 faster with all substrates. The respiratory properties of isolated mitochondria, however, displayed much larger diversity than intact cells. Mitochondria from all cell lines studied showed significant differences in the rates of oxygen consumption in State 3 and in the presence of DNP as uncoupler. PC-3 cells displayed higher rates of substrates oxidation, particularly with DNP. Measurements of electrical membrane potential with the TPP^+-sensitive electrode showed that mitochondria from all cancer cell lines have $\Delta\Psi$ in the range between -220 and -236 mV. This is 30 to 65 mV higher than in mitochondria from parenchimal organs (liver, heart). Enzymological study of the submitochondrial particles (SMP) showed relatively low activity of Complex I and Complex I+III, and relatively high activity of Complexes II+III and Complex IV (the rates were related to citrate synthase activity). Both, respiratory activities of isolated mitochondria and enzymological activities of SMP, prepared from LNCaP cells, did not differ so dramatically from those of DU145 and PC-3 cells, as was observed with the whole cells. Thus higher rates of respiration of LNCaP cells are, probably, bound to a larger number of mitochondria per cell. It is concluded that prostate cancer cell mitochondria can oxidize citrate, and thus are different from those of normal prostate epithelial cells.

Th-Pos375

EFFECT OF GLIBENCLAMIDE ON THE GROWTH OF HUMAN BLADDER TUMOR (HTB-9) CELLS. ((Meghan Cregan, Leigh Strickler, Robert Miller, Jill Suttles, and **Robert Wondergem**)) Depts. of Physiology and Biochemistry, Quillen College of Medicine, East Tennessee State University, Johnson City, TN 37614-0576.

We have found that two K^+channels predominate in the plasma membrane of HTB-9 cells: a voltage- & Ca^{2+}-dependent maxi-K channel and an inward rectifier K^+ channel. We have implicated the latter in controlling cell growth (Monen, et al., *submitted*). So, we conducted the present study to determine whether glibenclamide, an inhibitor of the sulfonylurea receptor, might impact the growth and membrane current of these cells. Glibenclamide added to HTB-9 cells for 48 h at concentrations that ranged from 1 - 500 μM reduced cell growth ($ED_{50} \approx 100$ μM), as measured either by an increase in cell number or by an accumulation of protein, compared with vehicle-treated controls. In contrast, diazoxide, an opener of K_{ATP} channels, at concentrations ranging from 0.1 to 10 μM increased protein accumulation ($ED_{50} \approx 1$ μM) and counteracted the growth inhibition of glibenclamide at 10 μM. Furthermore, addition of glibenclamide for 48 h altered the distribution of cells within stages of the cell cycle as determined by flow cytometry using 10^{-5} M bromdeoxyuridine. Glibenclamide (100 μM) increased the percentage of cells (10,000 cts) in G_0/G_1 from 27.3% (vehicle control) to 33.3%, and it reduced the percentage of cells in S phase from 38.6% to 24.0%. Finally, addition of 50 μM glibenclamide reduced whole-cell current from 0.65 $\pm$ 0.14 nS/pF to 0.27 $\pm$ 0.03 nS/pF, and it reduced channel open probability (inside-out patch) from 0.41 $\pm$ 0.01 to 0.15 $\pm$ 0.005. We conclude that the sulfonylurea receptor and the corresponding K^+ channel are involved in mechanisms controlling HTB-9 cell growth. Supported in part by the Cardiovascular Research Institute at ETSU.

Th-Pos376

IDENTIFICATION AND CHARACTERIZATION OF CHLORIDE CHANNELS IN NORMAL HUMAN BRONCHIAL EPITHELIAL CELLS. ((Z.H. Zhang, F. Jow, **J. Hinson**, R. Numann and T.J. Colatsky)), Wyeth-Ayerst Research, Princeton, NJ 08543 (Spon. J. Hinson)

Whole cell patch-clamp technique was used to study chloride channels in normal human bronchial epithelial cells (NHBE). The results show that a background outwardly-rectifying chloride current, $I_{Cl,basal}$, was present in 75 % of the cells studied (n=45). $I_{Cl,basal}$ was completely inhibited by 0.1 mM 5-Nitro-2(3-phenyl-propylamino)-benzoic acid (NPPB), partially blocked by 0.1 mM 4-acetamide-4'-isothiocyanostilbene-2,2'disulfonate (SITS) and insensitive to 0.1 mM 9-anthracene carboxylic acid (9-AC). It was also observed that the background current was significantly increased in the presence of the calcium ionophore, A23187. The calcium-induced current, $I_{Cl,Ca}$, displayed outward rectification and was completely blocked by NPPB. Using the agent 8-(4-Chlorophenylthio) adenosine-3',5'-monophosphate (CPT-cAMP), a cAMP-activated chloride current, $I_{Cl,cAMP}$, was found in only 7 of 24 cells and demonstrated strong outward rectification in some cells. $I_{Cl,cAMP}$ could be partially reversed by reperfusing the cell with CPT-cAMP-free and NPPB solution. A volume-sensitive chloride current, $I_{ClSwelling}$, was recorded in hypotonic external solution (180 vs. 280 mOs) and exhibited strong outward rectification. NPPB, but not SITS, completely blocked this current. Conclusion: background chloride current may play an important role in the maintenance of normal cell function. The results also indicate that NHBE chloride channels may be regulated by cell swelling, cAMP-dependent protein kinase, as well as intracellular Ca^{++}.

Th-Pos377

PROPERTIES OF TWO MULTISUBSTATE Cl^- CHANNELS FROM HUMAN APICAL SYNCYTIOTROPHOBLAST RECONSTITUTED ON PLANAR LIPID BILAYERS. ((Claudio Grosman and **Ignacio L. Reisin**)) Departamento de Química Analítica y Fisicoquímica, Facultad de Farmacia y Bioquímica, Universidad de Buenos Aires, Junín 956 2 p (1113), Buenos Aires, Argentina.

An apical plasma membrane-enriched vesicle fraction from human syncytiotrophoblast at term was prepared. We have already reported (Grosman & Reisin, *Biophys. J.* **70**: A199, 1996) that, unlike previous patch-clamp studies, non-selective cation channels were incorporated in most cases, a result consistent with the higher permeability for cations as compared with Cl^- and with the low apical membrane potential difference at term revealed by radiotracer-flux, microelectrode, and fluorescent probe partition studies. In the present study we report that Cl^--selective channels were incorporated in 4 % of successful reconstitutions (14 out of 353) and that their analysis revealed two types of channels. One of them was consistent with a voltage-dependent, 100-pS channel while the other was consistent with the lateral association of 47-pS conductive units, giving rise to multi-barrelled channels of variable conductance (300 to 650 pS). The latter displayed a very complex behavior which included cooperative gating of conductive units, voltage-dependent inactivation, and flickering activity. The possibility of a non-apical origin for the reconstituted Cl^- channels was taken into account given their low frequency of being observed but the frequent simultaneous co-reconstitution of maxi Cl^- and non-selective cation channels is an example of the evidences against such hypothesis. The role of the reported Cl^- channels in transplacental ion transport and/or syncytium homeostasis remains to be determined.

Th-Pos378

NITRIC OXIDE MODULATES CHLORIDE CURRENT IN A549 EPITHELIAL CELLS. ((**B. Kamosinska,** M.W. Radomski, M. Duszyk, A. Radomski and S.F.P. Man)) Departments of Medicine, Pharmacology and Physiology, University of Alberta, Edmonton, Alberta T6G 2H7, Canada

Chloride channels in epithelial cells are affected by many regulatory factors, including intracellular calcium, membrane potential, cell volume, cAMP and cGMP. Since cGMP mediates many of the physiological actions of nitric oxide (NO) we have studied both the presence of endogenous NO and the effects of exogenous NO on Cl^- currents in A549 human lung epithelial cells. We have detected Ca^{++}-dependent NO synthase activity in A549 cells. Using the perforated patch-clamp technique, we have shown that inhibition of this enzyme by N^G-monomethyl-L-arginine (L-NMMA) decreased Cl^- current, an effect that was reversed by NO donor, S-nitroso-glutathione (GSNO). In addition, the NO donors GSNO and S-nitroso-N-acetyl-D,L-penicillamine (SNAP) increased whole-cell Cl^- currents in A549 cells. This stimulatory effect of the NO donors was completely inhibited by 4,4'-diisothiocyanatostilbene-2,2-disulfonic acid (DIDS) suggesting that channels other than the cystic fibrosis transmembrane conductance regulator (CFTR) are involved in the action of NO on A549 cells. In addition, 1H-[1,2,4]oxadiazolo[4,3-a]quinoxalin-1-one (ODQ), a selective inhibitor of soluble guanylyl cyclase, decreased NO-mediated stimulation of Cl^- currents. Our results suggest that in lung epithelial cells NO regulates the non-CFTR Cl^- conductance acting via a cyclic GMP-dependent mechanism.

Th-Pos379

RAT SMALL INTESTINE ION TRANSPORT AND ATRIAL NATRIURETIC PEPTIDE (ANP). ((**L. V. González Bosc**, P. A. Elustondo, M. C. Ortiz and N. A. Vidal)) Cátedra de Biología Celular e Histología. Depto. de Ciencias Biológicas. Facultad de Farmacia y Bioquímica. UBA. PROSIVAD-CONICET. Junín 956. 1 p (1113) Buenos Aires. Argentina. (Spons. by M. Roux)

In vitro ANP not modified active ion transport in small intestine of rats, but with Na^+ concentration gradient (SCG), decreased Na^+ absorption, may be mediated by a Na^+/ glucose cotransporter (SGLT) inhibition (González Bosc et al., Med. Sci. Res. 23: 759, 1995). To confirm this hypothesis we developed the following protocol using a voltage clamp technique in Ussing's chamber with SCG: I)0.1 mM (luminal) phloridzine (Phlz) and 15' later 1 µM ANP (serosal) was added, II)ANP and 15' later Phlz, III)0.1 mM (luminal and serosal) methylene blue (MB) and 5' later ANP was added and IV)1 mM (luminal and serosal) L-NAME and 10' later ANP was added. Results (n=6): I)potential difference (PD=mV):basal=5.4±0.5 Phlz=4.1±0.5* Phlz+ANP=3.9±0.6$^{ns\ vs\ Phlz}$, short circuit current (Isc=µA/cm^2):basal=93.2±10.6 Phlz=77.4±12.4* Phlz+ANP=85.7± 18.6$^{ns\ vs\ Phlz}$ and conductance (G=mS/cm2):basal=17.8±2.2 Phlz=19.0±2.2^{ns} Phlz+ANP= 21.6±2.6$^{ns\ vs\ Phlz}$, II)PD basal=6.4±0.7 ANP=5.0±0.6* ANP+Phlz=4.8±0.7$^{ns\ vs\ ANP}$, Isc basal=127±18 ANP=105±12* ANP+Phlz=112±13$^{ns\ vs\ ANP}$ and G basal=18.3±1.7 ANP=21.0±2.8^{ns} ANP+Phlz=23.5±3.0*, III)PD=4.1±0.2 vs 3.9±0.2, Isc=56.9±2.8 vs 59.7±4.2 and IV)PD= 4.4±0.2 vs 4.3±0.2, Isc=69.0±7.2 vs 72.4±8.2 (*p<0.01 vs basal, †p <0.01 vs ANP). We think that ANP blocks the SGLT because the pretreatment with Phlz inhibited ANP effects and *viceversa* and this effect could be mediated by cGMP because MB inhibited ANP action. We suppose that this effect was mediated by NO because L-NAME abolished ANP response, but we cannot rule out that L-NAME affects other transport mechanisms.

Th-Pos380

DEPENDENCE OF AMPLITUDE OF Na-Ca-EXCHANGE CURRENT (INaCa) OF SECRETORY CELL MEMBRANE ON pH OF EXTERNAL SOLUTION. ((N. Fedirko, M. Klevets.,V. Manko)) .

Lviv State University, Universytetska 1, 290602, L'viv, Ukraine (Spon. by prof. O.Gojda)

The purpose of this investigation-elucidate of the role of aminoacids ionogenic groups in functioning of the Na-Ca-exchanger. I_{NaCa} on isolated cells of the salivary gland in Chironomus larvae was registered by mean of voltage clamp method in conditions of intracellular perfusion in response to the membrane hyperpolarization from -20 to -60 mV.

Inward I_{NaCa} decreased in the dependence of the degree of reduce of pH (pK'=3.72). At pH 3,5-3,25 insignificant outward or inward currents were registered. At pH 3,0 it always was outward. I_{NaCa} blocade is probably related with protonization of acidic ionogenic groups that take part in binding of cations by extracellular site of exchanger. On the base of pK' we assume that they are COO^- - groups of the remains of Asp or Glu.

The amplitude of inward I_{NaCa} increased in dependence of the degree of alkalization of the solution (9<pK'<10). I_{NaCa} increase during alkalization is connected with appearance of additinal negative charges in the site of cations binding. The carriers of them could be ionized SH-groups of Cys remains.

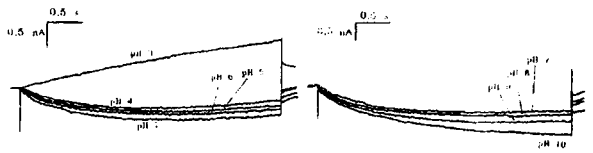

Th-Pos381

FLUID FLOWS ACROSS MDCK CELL TIGHT JUNCTIONS (TJ).

((O. Kovbasnjuk, J.P. Leader and K.R. Spring)) LKEM, NHLBI, NIH, Bethesda, MD 20892. (Spon. by S. Yoshikami)

The magnitude of fluid flow across the TJ of epithelia has not been directly determined. We developed techniques to measure fluid flow across the TJ of MDCK cells using confocal fluorescence microscopy. Fluorescein-dextran (70,000 MW) was microinjected into the subepithelial spaces of MDCK cell monolayers grown on permeable supports (Anocell). The monolayers were perfused with bicarbonate solutions (pH=7.4) at 37°C. Because of its size, the fluorescein-dextran couldn't diffuse across the TJ to the apical solution and remained confined to the lateral intercellular space (LIS). The permeable supports were treated to reduce pore size and prevent dye diffusion across the filter. Under these conditions, distribution of dye along the LIS from the TJ to basolateral surface of cells depends only on the balance between fluid convection and dye diffusion. Images of LIS fluorescence were made at 0.32μm intervals from the apical to basolateral epithelial surface using a NORAN confocal microscope. When apical and basolateral perfusion solutions were isotonic, the fluorescence intensity was diminished near the TJ and basal surface of the cells, a result consistent with high fluid flow in both regions. To increase fluid flux, one of solutions was made hypertonic by the addition of 50mM PEG (3,350 MW), and dye distribution was measured again after 2-3 min. With PEG in the apical solution, the intensity was highest near the TJ as expected for solute polarization. When the basolateral solution was made hypertonic, dye was swept away from the TJ. When TJ permeability was increased by treating the monolayer with 0.01mM Sp-cAMPS, hypertonic apical solutions caused dye to accumulate very close to the TJ. As a control, the LIS were filled with BCECF, a fluorescent dye with a high diffusion coefficient. All intensity profiles were flat and unaffected by fluid flow. We concluded that fluid flows across the TJ of MDCK cells during both isotonic and osmotically-induced fluid transport.

Th-Pos382

INVOLVEMENT OF SA-CHANNELS IN THE VOLUME REGULATION TO HYPOTONIC STIMULATION IN A6 CELLS. ((**M. Sokabe,** T. Takemoto and W. Yu)) Department of Physiology, Nagoya University School of Medicine, Nagoya 466, Japan.

We investigated changes in cell volume and intracellular calcium concentration ($[Ca^{2+}]_i$) during hypotonic stimulation in cultured amphibian renal cells (A6 cells). Upon being exposed to hypotonic solution (55% osmolarity), the A6 cells swelled in the first two minutes, which was followed by a progressive decrease in cell volume termed regulatory volume decrease (RVD). The hypotonic stimulation also induced a transient $[Ca^{2+}]_i$ increase peaked in a minute followed by a period of steady state plateau. Depletion of Ca^{2+} from intracellular stores by a pretreatment with thapsigalgin abolished the peak but not the plateau of the $[Ca^{2+}]_i$ increase. In contrast the plateau but not the peak of $[Ca^{2+}]_i$ was abolished in Ca^{2+}-free hypotonic media. RVD was not inhibited in both cases. However, in Ca^{2+}-free hypotonic media, cells pretreated with thapsigalgin showed neither $[Ca^{2+}]_i$ increase nor RVD. A similar inhibitory effect was observed when the cells were pretreated with thapsigalgin and incubated with hypotonic media containing 10 μ M Gd^{3+} (a blocker for stretch activated (SA) channels). These results suggest that during hypotonic stimulation the early peak of $[Ca^{2+}]_i$ is originated from the Ca^{2+} release from intracellular stores, whereas the later plateau of $[Ca^{2+}]_i$ is from the Ca^{2+} influx through Ca^{2+}-permeable SA-channels. The results also suggest that the Ca^{2+} influx through the SA-channels activated by cell sweilling is involved in the process of RVD.

Th-Pos383

A MODEL FOR FLUID TRANSPORT BASED ON CYCLIC CELL VOLUME OSCILLATIONS. ((**J. Fischbarg** and J.A. Hernández)). Depts. of Physiology and Ophthalmology, Columbia University, New York, NY 10032, and Dept. of Biophysics, University of the Republic, Montevideo, Uruguay.

Diverse explanations proposed for the mechanism of transepithelial isotonic fluid transport cannot completely account for it. In prevailing models, net water movement follows steady-state local osmotic gradients created by the transport of solutes across the apical and basolateral domains of the cell membrane. However, it is unclear whether such stationary osmotic gradients exist, and there is instead some recent evidence (Zhu et al., IOVS 37:1899-1906, 1996) consistent with fluid transport being linked to cell signaling and arising from *transient* osmotic gradients. Findings that epithelial cells exhibit spontaneous and/or induced oscillations in properties such as intracellular concentration of Ca^{2+} and translayer potential are consistent with the possibility that fluid transport also takes place in an oscillatory fashion. Furthermore, given the selective expression of water channels by fluid-transporting epithelia, transport of fluid may be transcellular. We therefore propose a model for pulsatile transcellular fluid transport. Its two key assumptions are: 1) an ideal osmolyte is transported in the same vectorial direction across both the apical and basolateral membranes of a polarized epithelial cell, and 2) one of these transport mechanisms is modulated by cell volume. In spite of its simplicity, this model exhibits spontaneous and sustained oscillations in cell volume and yields transepithelial isotonic fluid transport of a magnitude consistent with that of experimental findings. Support: NIH Grant EY06178 and RPB, Inc.

Th-Pos384

HETEROLOGOUS EXPRESSION AND CHARACTERIZATION OF THE 2.9 KB ISOFORM OF THE RAT RENAL UREA TRANSPORTER. ((Richard T. Timmer, Robert B. Gunn, Otto Froehlich, Serena M. Bagnasco, Janet D. Klein and Jeff M. Sands)). Departments of Physiology, Pathology, and Medicine, Emory University School of Medicine, Atlanta, GA, 30322.

The cDNA for the rat renal urea transporter was isolated by PCR based upon the sequence for the rabbit urea transporter (You, et al., 1993). We have subcloned the coding region and the flanking 100 bp of the rat urea transporter into a mammalian expression vector (pcDNA3). We have transfected this construct into HEK-293 cells in order to characterize the kinetics, pharmacology, and the response of the expressed transporter to AVP and cAMP. Transfection of HEK-293 cells with this construct results in a urea influx of 5800 nmol / g protein - min, which is a 5.8-fold increase in urea influx compared to vector-only transfected cells which had a urea influx of only 1000 nmol / g protein - min. The phloretin-insensitive (100 uM) urea influx in both transfected and vector-only transfected cells was only 800 nmol / g protein, which probably reflects the bilayer urea permeability in these cells. Western analysis indicates that there is little or no expression of urea transporter protein in vector-only transfected cells, whereas there is a new immunoreactive 43 kDa protein band in cells transfected with the urea transporter construct. The urea influx in HEK-293 cells transfected with this construct is not stimulated by arginine vasopressin (AVP). However, it has not been reported whether or not HEK-293 cells have AVP-V_2 receptors, therefore, we also treated transfected cells with the membrane permeable cAMP analogue CPT or with forskolin, an activator of adenylyl cyclase. Neither of these compounds stimulated the expressed urea transport activity, although both of these reagents are reported to activate other cAMP responses in HEK-293 cells. These data demonstrate that the urea transporter product of the 2.9 kb isoform is not regulated by AVP at a post-transcriptional level when expressed in HEK-293 cells. Therefore, we suggest that the 2.9 kb isoform of the urea transporter does not code for the AVP-regulated urea transporter as first suggested by You, et al., or alternatively that the AVP-regulation of this transporter is at the transcriptional level. (This work supported in part by grants HL28674 to RBG, HL08989 to RTT, and DK41707 to JMS).

Th-Pos385

STABILIZATION, ACTIVATION AND CONFORMATIONAL CHANGES OF YEAST HEXOKINASE UPON BINDING TO ZWITTERIONIC MICELLES. ((M.L. Bianconi and R. Guerra)) Departamento de Bioquímica Médica, ICB, Universidade Federal do Rio de Janeiro. (Spon. by M. Sorenson)

We have examined the correlation between enzyme kinetics and changes in protein structure upon interaction of yeast hexokinase (HK) and an interface. Yeast HK interacts with zwitterionic micelles of lyso-phosphatydylcholine (LPC) or N-hexadecyl-N,N-dimethyl-3-ammonium propanesulfonate (HPS) leading to a considerable increase in the enzyme stability at 35 C. After 200 min incubation in a medium containing glucose and $MgCl_2$, only 12% of the original HK activity was detected in contrast to over 80% observed when LPC or HPS were present during incubation. In the absence of glucose the micelles are not able to protect the enzyme against thermal inactivation, suggesting that the conformational change induced by glucose binding favors the interaction. Interfacial binding of yeast HK cause an increase in both the affinity for ATP and $V_{max.}$, with no significant change in the glucose binding dissociation constant. It was observed a red shift in the intrinsic fluorescence spectrum of HK upon interaction with micelles. In addition, the calorimetric enthalpy of the yeast HK reaction was increased in the presence of micelles. In conclusion, interfacial binding of yeast HK causes protein conformational changes which, in turn, lead to an increased stability and catalytic efficiency. Supported by CNPq.

Th-Pos386

ALLOSTERIC TRANSITIONS IN REVERSE MICELLES. KINETIC PROPERTIES OF GLUCOSAMINE-6P-DEAMINASE IN AOT- AND CTAB-BASED SYSTEMS. ((**Edgardo Escamilla, Rafael Dávila and Martha Contreras**)). Dept. of Microbiology, Institute of Cellular Physiology. Natl. University of Mexico (UNAM), Apdo. postal 70-242, 04510 México, D.F. México

Many surfactants in non polar organic solvents form reversed micelles, capable of solubilizing water and other polar compounds, such as enzymes that usually retain its catalytic activity and specificity. It has been found that there is an optimum value of hydration for which catalytic activity of the solubilized enzyme is maximum. The highest catalytic activity seems to occur when the entrapped enzyme molecule is forced to a close contact with the inner micellar interface.
Here we describe the kinetic behavior of an allosteric enzyme: glucosamine 6-phosphate isomerase deaminase from *E. coli* in reverse micellar systems. The nature of the surfactant used to form the reverse micelles (in isooctane) was determinant for the allosteric response obtained, i.e. with the cationic CTAB (hexadecyl-trimethylammonium bromide) the enzyme showed the normal sigmoidal response to substrate, while in the anionic AOT (sodium bis [2-ethylhexyl]) sulfosuccinate, the homotropic and heterotropic responses could be dissociated since the enzyme showed no activity in the absence of the allosteric activator. This situation let us to study the kinetics of the heterotropic response without interference of the homotropic activation. This behavior suggest that the negatively charged interface in AOT-based micelles interferes with the normal binding of the negatively charged substrate, thus the enzyme remains frozen in the T-state.

Th-Pos387

TRANSIENT KINETIC STUDIES OF PHOSPHATE-TRANSFER REACTIONS IN HUMAN-B NUCLEOSIDE DIPHOSPHATE KINASE. ((**Sabine Schaertl**[$], Manfred Konrad[$], Ioan Lascu[$] & Michael A. Geeves[¥])) MPI für biophysikalische Chemie, 37077 Göttingen, Germany., [$]IBGC Universite II, 33077 Bordeaux, France, [¥]MPI für molekulare Physiologie, 44026 Dortmund, Germany.

Nucleoside Diphosphate Kinases (NDPK) catalyze transfer of γ-phosphate from nucleoside triphosphates to diphosphates with a ping-pong mechanism via a phosphorylated His (118). We have used the changes of intrinsic tryptophan fluorescence which occurs on phosphorylation to measure the rates of enzyme phosphorylation by different nucleoside triphosphates. The second-order rate constants varied between 0.7 and 14 x 10^6 $M^{-1}s^{-1}$. By isolating the phospho-enzyme intermediate complex and mixing with nucleoside diphosphates, rates of dephosphorylation were measured. Again the second-order rate constants varied from 2.4 - 44 x 10^6 $M^{-1}s^{-1}$ for ribose and from 0.4 - 21.8 x 10^6 $M^{-1}s^{-1}$ for deoxyribose NDPs. In all cases second-order rate constants were highest for guanine followed by adenine and lowest for cytidine nucleotides. The rates of thiophosphorylation by ATPγS and GTPγS were 1/1000 of the equivalent phosphorylation rates. The observed rate constants were hyperbolically dependent on [NTP] with k_{max} of 2.7 and 1.35 s^{-1} and $K_{0.5}$ of 144 and 39 μM respectively. For de-thiophosphorylation by a range of NDPs k_{max} was in the range 5-30 s^{-1} whereas $K_{0.5}$ varied between 0.16 and 3.3 mM. Guanine had the lowest $K_{0.5}$ values and cytidine the highest.

Th-Pos388

NMR EVIDENCE FOR A STRONG HYDROGEN BOND IN THE MECHANISM OF TRIOSEPHOSPHATE ISOMERASE (TIM). ((**T.K. Harris**, C. Abeygunawardana, and A.S. Mildvan)) Dept. Biol. Chem., Johns Hopkins Medical School, Baltimore, MD 21205.

TIM catalyzes the reversible interconversion of GAP and DHAP, with neutral His-95 donating a H-bond to the enolate intermediate (Komives et al., *Biochem. 30*, 3011; Lodi & Knowles, *Biochem. 30*, 6948). To determine whether this is a low-barrier H-bond, ^1H NMR spectra were obtained at 600 MHz and –4 °C on yeast TIM (1.0 mM sites in 10% DMSO-d_6, 20 mM Tris-d_{11}-HCl, and 100 mM NaCl) and its complex with phosphoglycolohydroxamate (PGH), an analog of the enolate intermediate (Collins, *J. B. C. 242*, 136). While free TIM showed downfield ^1H resonances at 13.12, 11.24, 11.02, 10.72, and 10.59 ppm, the TIM-PGH complex showed signals at 14.86, 13.54, 12.28, 11.87, 11.76, 11.38, 11.27, and 10.90 ppm. The broad, deshielded signal at 14.86 ppm did not change in chemical shift or width (284 Hz) over the pH range 6.5–9.0, and showed weak NOE's from ^1H resonances at 7.6 and 7.1 ppm, consistent with a neutral histidine with a low pK_a, such as His-95. The fractionation factor of this resonance is low (ϕ = 0.40 ± 0.06), and its width increased with temperature yielding an exchange rate of 900 s^{-1} at –4 °C and an activation energy of 9.5 kcal/mol. This slow, pH-independent rate indicates partial protection from bulk solvent. From a correlation of chemical shifts from solid state NMR with H-bond lengths from X-ray studies of the same crystals (McDermott & Ridenour, *Encyc. of NMR*, p. 3820), the chemical shift of 14.86 ppm yields a H-bond distance of 2.6 Å, corresponding to a H-bond strength ≥10 kcal/mol. The downfield shift, slow exchange, and low ϕ value are consistent with a strong H-bond within a network of H-bonds (Davenport et al., *Biochem. 30*, 5821).

Th-Pos389

THE ROLE OF THE TRYPTOPHAN RESIDUES WITHIN THE CATALYTIC DOMAIN OF *PSEUDOMONAS AERUGINOSA* EXOTOXIN A. ((B.K. Beattie, G.A. Prentice, and **A.R. Merrill**)) Guelph-Waterloo Centre for Grad. Work in Chem., Dept. of Chem. & Biochem., Univ. of Guelph, Guelph, ON, CAN, N1G 2W1.

The role of the Trp residues in the substrate-binding and catalytic mechanism of an enzymatically active C-terminal fragment of *Pseudomonas aeruginosa* exotoxin A was studied by individually or jointly replacing these residues with Phe. Substitution of W-466 decreased the ADP-ribosyltransferase (ADPRT) and NAD^+-glycohydrolase (GH) activities by 20- and 3-fold, respectively. In contrast, substitution of W-417 or W-558 with Phe both resulted in a 3-fold decrease in ADPRT activity with, however, only a decrease by 40 and 70% in GH activity, respectively. Simultaneous replacement of W-466 and W-558 resulted in a 200-fold decrease in ADPRT and an 6-fold decrease in GH activities suggesting that W-466 may play a minor role in the transfer of ADP-ribose to the eEF-2 protein. Chemical modification of the Trp residues in the wild-type toxin fragment by NBS revealed the presence of a single residue important for enzymatic activity, W-466, with a minor contribution from W-558. Additionally, Trp residues, W-305 and W-417, were refractory to oxidation by NBS which likely indicated the buried nature of these residues within the protein structure. Titration of the various single and a double Trp replacement mutant protein(s) indicated that W-558 and W-466 are responsible for the substrate-induced fluorescence quenching with the former being responsible for the largest fraction of the observed quenching in the wild-type toxin. Consequently, a molecular mechanism is proposed for the substrate-induced fluorescence quenching of both W-466 and W-558. Furthermore, molecular modeling of the recent crystal structures for both exotoxin A and diphtheria toxin, combined with a variety of previous results, has led to the proposal for a catalytic mechanism for the ADPRT reaction. This mechanism features a S_N1 attack by the diphthamide residue of eEF-2 on the C-1 of the nicotinamide ribose of NAD^+, which results in an inversion of configuration likely due to steric constraints within the NAD^+-toxin-eEF-2 complex [supported by MRC, ARM].

Th-Pos390

THE INTERACTION OF THE CATALYTIC DOMAIN OF *PSEUDOMONAS AERUGINOSA* EXOTOXIN A WITH EUKARYOTIC ELONGATION FACTOR-2. ((G.A. Prentice, **F.-L. Yeh**, and A.R. Merrill)) Guelph-Waterloo Centre for Grad. Work in Chem., Dept. of Chem. & Biochem., Univ. of Guelph, Guelph, ON, CAN, N1G 2W1.

The x-ray structure of the catalytic domain of *Pseudomonas aeruginosa* exotoxin A (PE24) has recently been solved to high resolution facilitating studies on the interaction of PE24 with its target substrate, eukaryotic elongation factor-2 (eEF-2). PE24 exhibits mono-ADP-ribosyl transferase (ADPRT) activity in a mechanism that has been proposed to feature a S_N1 attack by the diphthamide residue (nucleophile) of eEF-2 on the C-1 of the nicotinamide ribose of NAD^+. The interaction of wheat germ eEF-2 with the active site of PE24 was studied by employing a competitive ELISA. The proteins associate with each other only in the presence of the enzyme's nucleotide substrate, NAD^+ and exhibit a dose-dependent association that is saturable. The apparent dissociation constant (K_d) for this protein-protein interaction is 30 nM and is salt-dependent. The association is maximal at low ionic strength and is progressively weaker at higher salt concentrations, which corroborates previous findings on the salt-dependence of ADPRT activity for this toxin. We are also investigating the pH- and temperature-dependence of the PE24-eEF-2 interaction. Furthermore, studies have been initiated to use site-directed mutagenesis to map the critical regions within the enzyme domain that dictate the association with eEF-2 [supported by MRC, ARM].

Th-Pos391

ELECTROSTATIC CHANNELING OF SUBSTRATES BETWEEN ENZYME ACTIVE SITES ((**Adrian H. Elcock** & J. Andrew McCammon)) Dept. of Chemistry and Biochemistry, Dept. of Pharmacology, University of California San Diego, La Jolla, CA 92093-0365

Enzymes catalysing sequential steps in a metabolic pathway are commonly associated into multi-enzyme complexes. In principle, one major advantage of such associations is the prospect for channeling substrates directly from enzyme to enzyme without leaving the complex, thus protecting the substrate from being hijacked for use in other metabolic pathways. We describe here Brownian dynamics simulations performed to investigate a potential role for electrostatics in promoting the channeling of charged substrates between enzyme active sites in a variety of systems. For the bifunctional enzyme dihydrofolate reductase-thymidylate synthase (DHFR-TS), the simulations suggest a substrate channeling efficiency approaching 100% at zero ionic strength: this despite the active sites being separated by around 40Å. Without electrostatic forces, the efficiency is only around 5%. As a second example, the diffusion of oxaloacetate between the active sites of malate dehydrogenase (MDH) and citrate synthase (CS) was simulated using a modeled structure for a MDH-CS fusion protein. Again, the inclusion of electrostatic forces results in an increase in channeling efficiency of between one and two orders of magnitude. The simulations therefore provide evidence that electrostatic interactions can be crucial for promoting channeling of charged substrate between enzyme active sites.

Th-Pos392

MECHANISM OF INTERACTION OF α-CALMODULIN DEPENDENT PROTEIN KINASE II (αCAMKII) AND TA-CALMODULIN. ((**K.Török**)) Department of Physiological Sciences, Univ. Newcastle NE2 4HH, UK.

The kinetic mechanism of αCAMKII interactions with calmodulin are investigated in order to understand the mechanism of activation by calcium.calmodulin. Equilibrium and stopped-flow fluorescence measurements of the interaction of mouse-αCAMKII overexpressed and purified to homogeneity from baculovirus transfected insect cells[1] with the fluorescent derivative TA-calmodulin[2] (TA-cal) were made in 100 μM $CaCl_2$ at ionic strength 150 mM, pH 7.0 and pH 6.3 at 21°C. Data obtained at pH 7.0 were consistent with a two-step mechanism in which bimolecular association of TA-cal and αCAMKII (k_{+1} = 1.4 x 10^7 $M^{-1}s^{-1}$, k_{-1} = 2.9 s^{-1}) is followed by isomerization of the TA-cal.αCAMKII complex (k_{+2} = 0.2 s^{-1}, k_{-2} = 0.3 s^{-1}), giving K_d = 82 nM. In this reaction both the initially formed and the isomerized TA-cal.αCAMKII complexes have higher fluorescence than TA-cal. In contrast, data at pH 6.3 fit either the above two-step mechanism leading to a dark isomerized TA-cal.αCAMKII complex or an alternative mechanism according to which TA-cal isoforms selectively interact with αCAMKII. The significance of the slow isomerization in the activation process and the possible contribution to the functional tuning by protonation are being investigated. 1. Brickey et al., BBRC (1990) 173, 578. 2. Török & Trentham, Biochemistry (1994) 33, 12807. *Supported by the Wellcome Trust.*

Th-Pos393

ELECTROSTATIC INTERACTIONS BETWEEN PROTEIN KINASE C AND PEPTIDE SUBSTRATES ((**Claudine N. Prowse**, Adrian H. Elcock, Tami J. Marrone, James M. Briggs, & Alexandra C. Newton)) Dept. of Pharmacology, University of California at San Diego, La Jolla, CA 92093

Protein kinase C specifically phosphorylates substrates containing Ser/Thr residues surrounded by basic amino acids. A modeled structure of the catalytic domain of protein kinase C βII, based on the crystal structure of protein kinase A, reveals a cluster of acidic groups located near the putative catalytic site which is conserved within the protein kinase C family, but not throughout the protein kinase superfamily. These residues have a profound effect on the surface electrostatic potential in this region, suggesting that electrostatic interactions between protein kinase C and substrate play a key role in targetting substrates to the kinase. This contribution investigates the relative importance of basic residues on either side of the phosphorylation site of a peptide substrate derived from the MARCKS protein (FKKSFKL): the affinity of analogs in which the Lys at the P+2 or P-2 position were changed to Ala were compared to that of the native peptide. Assuming Km values approximate binding constants, Lys to Ala substitutions resulted in ΔΔGs of 2.7 and 1.1 kcal mol^{-1}, respectively, for the two analogs. Thus the Lys at P+2 contributes approximately 1.6 kcal mol^{-1} more to the binding free energy compared to the Lys at P-2. Calculated ΔΔGs obtained using a continuum electrostatics model qualitatively reproduce the finding that removal of either Lys is unfavorable. In summary, biochemical and theoretical approaches reveal that positive charge on either side of the phospho-acceptor site contributes several kcal mol^{-1} in binding energy, with biochemical data revealing that positive charge at the P+2 position (C-terminal side) contributes considerably more to the interaction than positive charge at the P-2 position.

Th-Pos394

TIME-RESOLVED STATIC LIGHT SCATTERING (TRSLS) FOR DETERMINATION OF ENZYME KINETICS AND BIOPOLYMER SOLUTION STRUCTURE. ((David Norwood and Wayne F. Reed)) Department of Physics, Tulane University, New Orleans, LA 70118

We have found TRSLS to be a useful technique to make absolute determinations of enzymatic and other hydrolyses of biopolymers, as well as for deducing the degradation mechanism and solution structure of the biopolymers. In fact, we have developed a growing catalog of time-dependent signatures for different architectures of polymers (single and multiply stranded, branched, etc.) undergoing various types of degradation (completely random and endosydic for now), and found and analyzed several experimentally. A summary of the theory for predicting TRSLS signatures is given, followed by experimental data, absolute rates and structural deductions for several biopolymers. These include hyaluronate, proteoglycans and schizophyllan degradation by enzymatic and other agents.

PROTEIN STABILITY

Th-Pos395

SPECTRIN DOMAIN STABILITY AS MEASURED BY UREA DENATURATION: SINGLE VERSUS TANDEM SEQUENCE MOTIFS.((**T. Mitchell**, N. Menhart and L. W.-M. Fung)) Department of Chemistry, Loyola University of Chicago, Chicago, IL, 60626

Human erythrocytes have a dense, two dimensional network of spectrin and other proteins underlying the lipid bilayer on the cytoplasmic side of the membrane. As a major component of this network, spectrin is largely responsible for the typical biconcave shape of the red blood cell. Spectrin's primary structure consists mostly of repetitive, homologous units of approximately 106 amino acids. These individual sequence motifs have been proposed to form stable, independent structural domains, consisting of a triple helical bundle structure. We expressed several recombinant spectrin fragments of the α-subunit spanning the first three homologous sequence motifs. Spα 52-156, Spα 157-262, and Spα 263-368 each consisted of a single sequence motif, and Spα 52-262, Spα 157-368, and Spα 52-368 consisted of tandem sequence motifs. Our studies in buffers at physiological ionic strength and at room temperature revealed the single homologous sequence motifs as non-independent but compact and proteolytically resistant units. Tandem sequence motif peptides were more stable than peptides composed a single sequence motif, as measured by proteolysis, fluorescence or circular dichroism studies of urea or thermal denaturation and were more similar to intact spectrin than the peptides with a single sequence motif.

We also studied the unfolding of these peptides under low ionic strength and at elevated temperatures to further understand factors that stabilize the native structure of spectrin molecules. While the Spα 52-262 and Spα 52-368 peptides were unaffected by ionic strength during urea mediated denaturation, the Spα 52-156 and Spα 263-368 peptides were stabilized by the high ionic strength buffer (150 mM NaCl). Although salt can be a protein denaturant by "masking" electrostatic interactions in peptides, it can also serve as a stabilizing agent by strengthening hydrophobic effects.

Th-Pos396

THE EFFECT OF OSMOTIC PRESSURE AND HOFMEISTER SALTS ON THE HEAT AGGREGATION OF HYDROXYPROPYLCELLULOSE AND POLY-L-PROLINE

((**J. K. Chik**, S.L. Chi*, D. Rau#, S. Leikin and V.A. Parsegian)) DCRT/LSB and #ODIR/NIDDK NIH Bethesda MD 20892, Bethesda MD 20892; and *Princeton University, Princeton NJ 08544;

There are numerous instances of reversible heat aggregation of biological polyelectrolytes for instance collagen and DNA. Recently, we have studied the effect of different salts and osmolytes on the heat aggregation of hydroxypropylcellulose, a neutral polymer. As followed by optical turbidity, increasing the osmotic pressure reduces the transition temperature. A similar reduction is also observed with the addition of cosmotropic salts. Chaotropes, on the other hand, raise the transition temperature. Poly-l-proline is also known to undergo heat aggregation. Preliminary data shows similar effects of Hofmeister salts on poly-l-proline aggregation. We have also observed unexpected history dependence of the transition and of the aggregation kinetics, behavior different from hydroxypropylcellulose. The effect of salts and osmotic pressure on the heat induced aggregation will be compared and contrasted between these two polymers.

Th-Pos397

EFFECT OF ALCOHOLS, POLYOLS AND SUGARS ON PROTEIN SELF-ASSEMBLY. ((**N. Kuznetsova**[†]*, S.L.Chi[‡] and S. Leikin*)) [†]Engelhardt Inst. Mol. Biol., Russ. Acad. of Sci., Moscow, Russia; [‡]Princeton Univ., Princeton, NJ 08544; and *LSB/DCRT and ODIR/NIDDK, NIH, Bethesda, MD 20892.

Small, hydroxylic solutes such as mono- and polyhydric alcohols and sugars are often used to affect protein folding and self-assembly. Temperature-favored self-assembly of collagen triple helices is a particularly apt process for clarifying possible mechanisms of solute action since traditional self-assembly assays can be complemented by direct measurement of intermolecular forces in dense aggregates. A powerful short-range exponential repulsion and a longer-range attraction, responsible for the self-assembly, have been measured and characterized in the 0-to-10 Ångstrom separation range. Several solutes (including methanol, ethanol, ethylene glycol, and 1,2-propane diol) have only weak, apparently osmotic, effect on the self-assembly and practically no effect on the forces. In contrast, several closely related solutes (such as 1,3-propane diol, glycerol, sorbitol, methyl glucoside, and glucose) have a surprisingly strong, specific disruptive effect on attraction and self-assembly, but not on repulsion. Apparently these solutes incorporate into and disrupt specific water clusters interconnecting the collagen helices. The results obtained in this study provide additional evidence that the attractive forces responsible for collagen self-assembly are due to formation of water bridges connecting mostly polar recognition sites on the apposing molecules.

Th-Pos398

CALORIMETRIC STUDIES OF DIPHTHERIA TOXIN REPRESSOR FROM *CORYNEBACTERIUM DIPHTHERIAE* ((**Kenneth J. Mann**[1], Pamela D. Twigg[2], Donald L.D. Caspar[1])) [1] Department of Biology, Florida State University; Tallahassee, Florida 32306-3015 [2] Program in Molecular Biophysics, Florida State University; Tallahassee, Florida 32306-3015

Transcription of the diphtheria toxin structural gene is regulated by the diphtheria toxin repressor (DtxR). The DtxR, a 226 residue protein, dimerizes upon its binding of Fe^{2+} (physiologically), or various other transition metals. It is proposed, in this dimerized state, that the DtxR binds to the *tox* operator (two interrupted, palindromic 9 base-pair inverted repeat sequences), whereupon it represses transcription of the diphtheria toxin gene.

Calorimetric studies were performed on the DtxR C102→D. The 102 position is located in the metal-binding region of the protein and is extremely important for protein function. Only the wild-type and aspartate mutants retain any biological activity. High sensitivity differential scanning calorimetry was employed to determine the stability of the mutant repressor to compare it to that of the wild-type. Studies were performed with and without metal (Ni^{2+}) present. It was found that the aspartate mutant melted at ~54 degrees C with no metal present. The binding of Ni^{2+} by the protein enhances its thermal stability by at least 5 degrees. Further calorimetric studies on the wild-type will be done, with and without Ni^{2+}, in the presence of DTT.

A binding constant has been determined for Ni^{2+}, at room temperature, using a fluorescence quenching assay. This binding constant will be reevaluated using isothermal titration calorimetry (ITC).

Th-Pos399

THE KINETIC BASIS FOR THE STABILIZATION OF STAPHYLOCOCCAL NUCLEASE

((**Kelly J. Frye** and Catherine A. Royer))

University of Wisconsin at Madison, School of Pharmacy, Madison, WI 53706

The effect of xylose on the rates of folding and unfolding of staphylococcal nuclease (nuclease) have been investigated using fluorescence detected pressure-jump relaxation kinetics in order to establish the kinetic basis for the observed stabilization of nuclease by this sugar (Frye et al., *Biochemistry* 35, 1996). The activation volumes for both folding and unfolding and the equilibrium volume change for folding were all positive. Their values were within experimental error of those previously reported (Vidugiris et al., *Biochemistry* 34, 1996) and were independent of xylose concentration. The major effect of xylose concentration was to increase significantly the rate of folding. The large positive activation volume for folding was previously interpreted as indicating that the rate limiting step in nuclease folding involves dehydration of a significant amount of surface area. A large effect of xylose on the rate constant for folding provides strong support for this interpretation, since xylose, an osmolyte, stabilizes the folded state of proteins through surface tension effects. These studies further characterize the transition state in nuclease folding as lying closer to the folded, rather than the unfolded state along the folding coordinate in terms of the degree of burial of surface area. The image of the transition state that emerges is consistent with a dry molten globule.

Th-Pos400

SOLVATION THERMODYNAMICS OF HYDROPHILIC AND HYDROPHOBIC GROUPS STUDIED BY MOLECULAR DYNAMICS SIMULATION. ((**S.R. Durell and A. Wallqvist**)) NCI, NIH, Bethesda, MD 20892.

Computer molecular dynamics simulations are used to study the solvation thermodynamics of both hydrophilic and hydrophobic solutes from the gas phase to aqueous solution. The purpose is to determine the atomic-scale mechanisms responsible for the observed thermodynamic quantities, as well as calculate the energetic values for relevant solutes which can not be determined experimentally. The results will also aid the understanding of the determinative forces of biomolecular structure and function. Specific projects include calculating the energetics of the partial or full desolvation of the different amino acid sidechains as would occur in the process of protein folding. Emphasis is placed on the conditional effects due to the presence of the protein backbone and the nearby location of other sidechains.

Th-Pos401

QUANTUM YIELD OF TRANSDUCIN TRYPTOPHAN 207 GOES FROM 0.13 TO 1.0 UPON GTP ACTIVATION. ((**B. Zelent**, Y. Jia* and P.A. Liebman)) Dept. of Biochemistry and Biophysics and Dept. of Chemistry*, Univ. of Pa. Medical Center and Univ. of Pa.*, Philadelphia, PA. 19104

Steady state (ss) tryptophan fluorescence emission intensity of G proteins increases 1.5-2.5-fold upon activation by GTP (Higashijima et al., JBC 262:752, 1987). We have used the two tryptophan G protein, transducin (G_{to}), to analyse the origin of this effect. Absolute quantum yields (Φ) for W127 and W207 were determined by combining precise measurement of integral (ss) emission intensity calibrated against NATA (Φ=0.14) with the products of lifetime amplitude (α_i) and exponential decay time (τ_i) for 295nm λ_{ex} and 345nm λ_{em}. Four different ligand states of the protein with GDP, GTPγS, AlF_4 and Mg^{++} were examined in pH 7.0, 10mM PO_4 buffer at 22°C. Two lifetimes dominated each state; one nearly constant at 3.2±0.1 ns and the other varying from 6.4ns for G_α•GDP to 7.6ns for G_α•GTPγS•Mg. Though shorter lifetimes were present, $\alpha_i \times \tau_i$ for these was negligible (< 0.3% of total). Φ of the 3.2ns state proved to be constant at 0.27 in all states while Φ of the longer lived component ranged from 0.13 (G_α•GDP) to 1.0±0.05 (G_α•GTPγS•Mg). Crystal structures show location and orientation of W207 to change with ligand state while that of W127 does not. We therefore identify W127 as the Φ=0.27, τ=3.2ns component. Failure of net ss $_{em}\lambda_{max}$ to change despite the 8-fold increase in Φ_{W207} with its apparent folding into a more apolar environment (crystal structure) implies a fast, powerful, non-radiative, excited state energy conduit out of W207 in G_α•GDP. Possible structural explanations for this effect might include orientation of W207 in its parent α helix of G_α•GDP with highly constrained and well oriented H-bond formation from the indole εN. On the other hand, the stationary value of Φ=0.27, $_{em}\lambda_{max}$=336nm for W127 seems more compatible with its static apolar environment. Supported by grants EY00012, EY01583 and DRR01348 to the RLBL Laser facility of the Univ. of Pa.

Th-Pos402

ASSEMBLING THIOREDOXIN FRAGMENTS (1-73 AND 74-108): A MODEL SYSTEM TO STUDY ASSOCIATION/FOLDING PROCESSES. ((**R. Georgescu**, J-H Li and M.L. Tasayco)), Chemistry Department, City College of the City University of New York, New York, N.Y. 10031.

Experiments carried out with each isolated fragment (1-73 and 74-108) of oxidized E.coli-Thioredoxin (Trx) using COMBINED intrinsic fluorescence(Fl) of Trp28 and Trp31, the circular dichroism (CD) in the far and near UV region, the 1D-NMR spectrum and molecular sieve chromatography, indicate that these fragments behave essentially as random coil states and show different tendencies to self-associate. Remarkably, these isolated fragments associate with an apparent high affinity equilibrium constant (1×10^{-7}) to give a native-like heterodimeric structure (Tasayco & Chao, Proteins: Structure, Functions and Genetics 22:41-44, 1995) as shown using a range of spectroscopies. Denaturation and renaturation studies using fluorescence, far-UV CD and 1D-NMR spectroscopy under variable temperatures and guanidine concentration conditions indicate: (I) the heterodimer undergoes a reversible and cooperative process of denaturation and renaturation, (ii) the changes in the thermodynamic parameters ΔG, ΔH, ΔS are indicative of an association/folding process. Our results indicate that the non-covalent complex between these complementary fragments behaves as a native heterodimer protein.

Th-Pos403

SOME QUESTIONS PERTINENT TO TESTING THE VALIDITY OF THE TWO-STATE MODEL FOR PROTEIN UNFOLDING. (**M. R. Eftink**, R. M. Ionescu)) Dept. of Chemistry, University of Mississippi, University, MS 38677.

Simulations will be presented to illustrate problems in testing the validity of and extracting thermodynamic parameters for the two-state model, vis-a-vis a more complicated model, for protein unfolding. We will present the idea that the unfolded state can be described as a single macrostate composed of a distribution of microstates having different degrees of solvent accessible surface area, SASA. Using established relationships between changes in SASA and the ΔC_p, ΔH, and solvation ΔS for unfolding, we simulate how such a distribution can shift along the SASA axis upon addition of denaturant. We will also discuss the possibilities and thermodynamic consequences of having more than one unfolded macrostate and of having a denaturant that both stabilizes and destabilizes the protein's native state. Interesting observations are that, for denaturant induced unfolding, the apparent m ($=\delta\Delta G/\delta[d]$) value is usually lower (i.e., m^- pattern) than the actual m (or the sum of m_i for a multi-state transition); however, in some cases the apparent m can be larger (i.e., m^+ pattern) than the inputted values. The basis for having a m^+ pattern is either a) an intrinsic nonlinear dependence of ΔG on [d], b) the existence of a multi-state transition with the signal for the intermediate being much lower than that for the native and unfolded states, and c) a multi-state process for which the m for the first step is larger than the m for the subsequent steps. (This research was supported by NSF grant MCB 94 07167.)

Th-Pos404

GLOBAL ANALYSIS OF THE ACID- AND UREA-INDUCED UNFOLDING OF *Staphylococcal* NUCLEASE AND SOME OF ITS MUTANTS. ((**R. M. Ionescu**, M. R. Eftink)) Dept. of Chemistry, University of Mississippi, 38677.

We have studied the equilibrium unfolding of nuclease and some of its mutants, including the charge-change mutants, D77G, D83G, E75A, and H121A, over two perturbation axes (i.e., acid-induced as a function of urea concentration and urea-induced as a function of pH). The transitions were monitored by simultaneous measurements of circular dichroism, which monitors changes in secondary structure, and fluorescence, which senses changes in the local environment of Trp-140. With this multi-dimensional array of data we present a strategy of performing global analysis to determine with greater confidence the pertinent thermodynamic parameters and to reveal unfolding intermediates. For example, WT nuclease is fit reasonably well by a cooperative two-state transition with either urea or pH as denaturant; the fit is significantly improved, however, when we include the existence of an abnormal pK_a for His-121, which is normalized upon unfolding. Some of the mutants (i.e., D83G and E75A) appear to show two-state behavior, with the involvement of His-121, but are significantly destabilized. D77G appears to be partially unfolded at neutral pH and requires a three-state unfolding model. H121A nuclease shows an interesting intermediate behavior, appearing to be essentially two-state when denatured by either acid or urea (at neutral pH), but requiring a three-state model when the denaturing conditions are combined. (This research was supported by NSF grant MCB 94 07167.)

Th-Pos405

SHEAR FORCE INACTIVATION OF A MULTI-SUBUNIT ENZYME AT SUB-TURBULENT FLOW RATES. ((**Steven E. Seifried** and Jie He)) Department of Biochemistry and Biophysics, University of Hawaii, Honolulu, HI 96822.

The NTPase activity of Transcription Termination Factor rho from *E. coli* is lost when the protein is subjected to stopped flow kinetic measurements. The lost activity is recovered when the protein is aged for several hours following inactivation. While NTPase activity was lost, the effectors bound to rho did not dissociate. Two different forces may be responsible for the inactivation, pressure and shear. Pressure was determined not to be responsible for the loss of activity. Reversible shear-induced inactivation of the protein is the remaining possibility.
Using a well-controlled flow system, we observe activity to decrease as a linear function of the Reynold's number until the critical Reynold's number is reached and turbulent flow occurs. We observe significant inactivation under sub-turbulent flow conditions. Turbulent flow in a pipe generates limited inactivation, relative to the turbulent flow mixers utilized by stopped flow instrumentation, because of streaming which occurs axially down the center of the pipe. Inactivation under high Reynold's number conditions is therefore a function of the wall effect. We are now utilizing fluorescence homotransfer to observe, in the flow system, the association state of the hexameric rho protein as it is inactivated and reactivated. Rates of reactivation are slow (one the order of hours) and are observed to be approximately equal to the rate of subunit exchange. Our intent is to better understand the thermodynamic basis of shear force action upon multi-subunit proteins.

Th-Pos406

USE OF A SYNTHETIC FOUR-α-HELIX BUNDLE SCAFFOLD TO CHARACTERIZE THE STRUCTURAL FEATURES OF A VOLATILE ANESTHETIC BINDING SITE. ((**JS Johansson**, BR Gibney, F Rabanal, PL Dutton)) Johnson Foundation, University of Pennsylvania, Philadelphia, PA 19104.

The structural features of volatile anesthetic binding sites on proteins are being explored using a model system consisting of a water-soluble four-α-helix bundle scaffold with a hydrophobic core. Four-α-helix bundles were formed from the dimerization of synthetic 62-amino acid di-α-helical (helix-loop-helix) peptides. A cavity was introduced into the hydrophobic core, by replacing six leucine residues with alanines, as a first step toward designing an anesthetic binding site. The cavity is lined by leucine, alanine, tryptophan, and cysteine residues. This modification destabilizes the folded form of the bundle by 2.7 kcal/mol per alanine residue, as compared to the leucine containing core. Halothane binds to the hydrophobic core with a dissociation constant of 0.71 ± 0.04 mM as monitored by quenching of intrinsic tryptophan fluorescence. This is a four-fold higher affinity as compared to a leucine-containing core. The binding of halothane (molecular volume 123 $Å^3$) stabilizes the folded form of the bundle by 1.8 kcal/mol, indicating that additional favorable van der Waals and electrostatic interactions are being formed in the core in the presence of the anesthetic. Spin labeling with the sulfhydryl-specific methanethiosulfonate label MSTTL showed that the cavity accommodates one MSTTL molecule (molecular volume 410 $Å^3$), which also stabilizes the folded form of the bundle. The rotational correlation time of the confined spin label is 8 ns, corresponding to the motion of the bundle as a whole. These data suggest that the presence of a suitable hydrophobic cavity in a protein favors volatile anesthetic binding.

Th-Pos407

PROTEIN STABILIZATION BY AN INHALATIONAL ANESTHETIC AGENT

((**Jonathan W. Tanner***, Roderic G. Eckenhoff*, and Paul A. Liebman*))
*Department of Anesthesia and *Department of Biochemistry and Biophysics, University of Pennsylvania Medical Center, Philadelphia, PA 19104.

Inhalational anesthetics such as halothane ($CF_3CHClBr$) may alter the function of proteins by modulating stability, altering the equilibrium between native and unfolded states. For example, it has been suggested (Ueda et al., *Anesthesiology* 81:A465, 1994) that inhalational anesthetics inhibit firefly luciferase by ***destabilizing*** it through nonspecific binding to hydrophobic areas exposed in the unfolded state. Alternatively, anesthetic binding at discrete sites could enhance protein stability and alter the conformational dynamics involved in activity. We studied the effect of halothane on the stability of bovine serum albumin (BSA), a carrier protein known to bind some organic ligands. Heat capacity (C_p) of BSA (2 mg/ml), with various amounts of liquid halothane added, vs. buffer (150 mM NaCl, 10 mM $KHPO_4$, pH 7) was monitored with a differential scanning calorimeter (MicroCal Inc. MCS) from 35 to 95 °C at 90 °C/hr. Halothane increased the transition midpoint temperature (T_m) for BSA unfolding in a concentration-dependent manner (see sample thermograms in figure). These data show that halothane ***stabilizes*** the folded structure of BSA, probably through favorable interactions at discrete binding cavities or pockets (cf. Johansson et al., *Anesthesiology* 83:316, 1995, and Eckenhoff, *J.B.C.* 271:15521, 1996) that disappear upon unfolding. To our knowledge this is the first demonstration of an inhalational anesthetic favoring the native conformation of a protein. Thus, inhalational anesthetics may interact with the native conformation of some proteins and the unfolded state of others. Supported by NIH grants 5-T32-GM07612-19, GM51595, and EY00012.

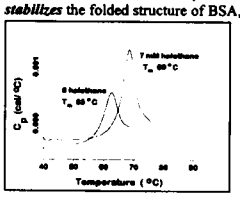

Th-Pos408

G PROTEIN ACTIVITY LOSS DUE TO GTP BINDING PRE-EQUILIBRIUM COMPETING WITH FAST IRREVERSIBLE EMPTY STATE MISFOLDING SEEN BY TRYPTOPHAN FLUORESCENCE ((**P.A. Liebman**, J.H. Parkes, and B. Zelent)) Dept. of Biochemistry and Biophysics, Univ. of Pa. Medical Center, Philadelphia, Pa., 19104. (Sponsored by David Wilson)

Transducin G_α binds Mg•GTP with $K_a=10^{10}$-10^{11} M^{-1} (Malinski et al., JBC 271:12919, 1996) suggesting that 1-10μM GTP should quantitatively replace GDP in G protein nucleotide exchange experiments. Nevertheless, substoichiometric yields of G_α•GTP from G_α•GDP in such experiments are not uncommon. In GTPγS titrations, using the known increase in tryptophan fluorescence with GTP binding (Higashijima et al., JBC 262:752, 1987), we needed 20-50μM GTPγS to reach stoichiometric completion. However, every concentration of GTPγS gave the same (exponential) relaxation time to (partial) completion at 35°C in pH7.0, 10mM PO_4 buffer with 2mM $MgCl_2$. This time course is consistent with first order release of GDP from G_α•GDP as the rate limiting step but shows that the pseudo first order rate of GTPγS binding to free G_α must be competing with the rate of irreversible G_α decay in the 1-10μM GTPγS range. This might be consistent with a reversible, non-rate limiting, GTPγS binding pre equilibrium. We find this reaction to be independent of Mg. Thus, we conclude that GTP/GDP exchange requires the momentary existence of a G_α nucleotide empty state, requiring 20-50μM GTPγS for stoichiometric saturation or kinetic competition with empty state decay. The lack of Mg dependence shows that Mg only acts at a later reaction stage to insure tight GTPγS binding and that the required G_α empty state decays rapidly. Supported by EY00012 and EY01583.

Th-Pos409

NEW TECHNIQUES FOR THE ANALYSIS OF FLUORESCENCE AND CIRCULAR DICHROIC (CD) DATA ON THE DENATURATION OF PROTEINS. (**A.G. Hirsh**, L. I. Tsonev, P.M. Mehl and S.V. Litvinovich) Transfusion and Cryopreservation Research Program, Naval Medical Research Institute, 8901 Wisconsin Avenue, Bldg. 29, Bethesda, MD 20889, USA.

Three new methods for spectral analysis of protein unfolding are described. In FRTA a ratio of signals is taken at two wavelengths, and then scaled between two ratio curves derived from control samples in known molecular configuration. The free energy of transition can then be calculated. In a generalization of this method (FRIBSTA) sample spectra are normalized to a standard space and the sum of differences at each wavelength is calculated between each of these spectra and normalized spectra of control samples in a known configuration. This allows for free energy estimation utilizing all of the spectral data available. The third, MIBS, relies on an initial best fit of a test spectrum by a linear combination of short UV CD spectra each of which is taken when the molecules are in a known configuration. The resulting spectrum is then perturbed by a linear combination of basis state spectra representing known protein configurational forms such as α-helix. This achieves extremely high quality fits to the experimental data and generates simultaneously an estimate of the free energy of transition between forms and the percentage change in the content of basic configurations as temperature varies. Supported by Naval Medical Research and Development Command, Work Unit # 1465. The opinions and assertions contained herein are the privates ones of the writers and are not to be construed as official at large.

PHOTOSYNTHESIS

Th-Pos410

CHARACTERIZATION OF THE STRONGLY COUPLED, LOW-FREQUENCY VIBRATIONAL MODES OF THE SPECIAL PAIR OF PHOTOSYNTHETIC REACTION CENTERS VIA ISOTOPIC LABELING OF THE COFACTORS. ((**K. Czarnecki**[1], J. R. Diers[1], V. Chynwat[2], J. P. Ericson[2], H. A. Frank[2], and D. F. Bocian[1]))
[1]Department of Chemistry, University of California, Riverside, CA 92521,
[2]Department of Chemistry, University of Connecticut, Storrs, CT 06269.

Low-frequency (50-425 cm^{-1}), near-infrared-excitation resonance Raman (RR) spectra are reported for bacterial photosynthetic reaction centers (RCs) from *Rb. sphaeroides* in which the bacteriochlorophyll (BChl) and bacteriopheophytin (BPh) cofactors are labeled with ^{15}N or ^{26}Mg. In order to gain a complete picture of the vibrational characteristics of the primary electron donor (P), the low-frequency RR spectra of the accessory BChls and the BPhs were examined in addition to those of P. The RR spectra of the isotopically labeled cofactors in the RCs were compared with one another and with the spectra of isolated, isotopically labeled BChl and BPh. Together, these comparisons with the predictions of semiempirical normal coordinate calculations provide a consistent set of assignments for all the RR active modes of the different BChl and BPh cofactors in the RC. The assignment indicate that the strongly coupled, low-frequency (50-250 cm^{-1}) modes of P all involved either deformations localized on pyrrole ring I or the macrocycle core. The unique interplay between structural, electronic, and vibronic characteristics of P suggests that the strong coupling of certain vibrations is an intrinsic consequence of the geometrical arrangement of the cofactors in RCs.

Th-Pos411

FTIR STUDY OF PHOTOREDUCTION OF Q_B IN A SERIES OF ASP-L213→ASN COMPENSATORY MUTATIONS OF *Rb. sphaeroides*
((**E. Nabedryk** & J. Breton)) SBE/DBCM, CEA-Saclay, Gif-sur-Yvette, France; ((M. L. Paddock & M. Y. Okamura)) Phys. Dept., UCSD, La Jolla, CA 92093

Protonation/deprotonation of carboxylic groups upon photochemistry can be revealed by FTIR difference spectroscopy and hence can provide a useful tool to probe local electrostatic environments. In reaction centers (RCs) at pH 7, a band at 1728 cm^{-1} appears in the FTIR Q_B^-/Q_B difference spectrum due to a change in protonation of a carboxylic acid. This band has been assigned to proton uptake by Glu-L212 upon Q_B^- formation and is larger in the RCs with an Asp-L213→Asn replacement (DN L213) than in native RCs[1]. The increased proton uptake implies that Glu-L212 has a lower pK_a in the DN L213 mutant RCs than in native RCs, consistent with the replacement of a negative Asp present in native RCs with a neutral Asn. The influence of second site compensatory mutations to the detrimental DN L213 replacement on FTIR spectra was studied in three double mutants carrying a Asn-M44→Asp, Arg-M233→Cys, or Arg-H177→His suppressor mutation in which forward electron and proton transfer rates were increased compared to the DN L213 mutant RCs[2]. However, only the Arg-M233→Cys suppressor mutation affected the 1728-cm^{-1} band, reducing its value to native levels. Thus, there is no clear correlation between the apparent extent of proton uptake by Glu L212 and RC function. Therefore it is likely that some effects other than electrostatic changes are a consequense of the suppressor mutations. In support of this, each of the double mutant RCs shows changes in the amide regions compared to native or DN L213 mutant RCs, suggesting backbone rearrangements which, together with side chain movements, may be necessary to compensate for the detrimental DN L213 mutation.
[1]Nabedryk et al., (1995) *Biochemistry* 34, 14722. [2]Okamura et al., (1992) *Research in Photosynth.* (Murata ed.) Vol.I, 349; Senft et al., (1995) *Photosynth.* (Mathis ed.) Vol.I, 639.

Th-Pos412

A STUDY OF THE LOW-FREQUENCY VIBRATIONAL MODES OF SELECTED CHLOROPHYLL MODEL COMPOUNDS. ((**James R. Diers** and David F. Bocian)) Department of Chemistry, University of California, Riverside, CA 92521-0403 (Spon. By Eugene Nothnagel)

We recently reported Q_y-excitation resonance Raman (RR) spectra for a number of chlorophyll and bacteriochlorophyll compounds which show a rich spectrum in the low-frequency region (< 600 cm^{-1}).[1,2] In an effort to further our understanding of these low-frequency vibrational modes, we have performed a vibrational analysis on a series of porphyrin, chlorophyll and bacteriochlorophyll derivatives. This series of derivatives affords the systematic exploration of the vibrational consequences of addition of the isocyclic ring and keto substituent to the basic porphyrin skeleton. Where available, calculated results are compared to experimental data.

[1] Diers, J. R., Zhu, Y., Blankenship, R. E. and Bocian, D. F., *J. Phys. Chem.*, **1996**, *100*, 8573.
[2] Diers, J. R. and Bocian, D. F., *J. Am. Chem. Soc.*, **1995**, *117*, 6629.

Th-Pos413

ELECTRON TRANSFER AND STRUCTURAL RELAXATIONS IN REACTION CENTER ((Ben McMahon[#], Joachim D. Müller[*], Colin Wraight[*], & G. Ulrich Nienhaus[#%])) [#]Dept. of Physics & [*]Center for Biophysics and Computational Biology, University of Illinois, Urbana, IL 61801, [%]Dept. of Biophysics, University of Ulm, 89069 Ulm.

We present a detailed model of the $P^+Q_A^- \rightarrow PQ_A$ electron transfer kinetics in photosynthetic reaction center proteins which are cooled in the PQ state and the $P^+Q_A^-$ state. Heterogeneity, relaxation, and fluctuational averaging of the protein structure are accounted for by distributions of the $P^+Q_A^- - PQ_A$ free energy difference. All other parameters of the electron transfer model are kept independent of conformation and temperature. We observe the time and temperature dependence of the dissipation of energy as the protein adjusts to charge separation and recombination at temperatures from 5 K to 300 K, at time scales ranging from 60 ms to 3000 s. Below the solvent glass transition temperature, changes in protein conformation have Arrhenius activation energies distributed about 50 kJ/mol, with a preexponential of 10^{16} s^{-1}. At higher temperatures, we find values of 130 kJ/mol and 10^{29} s^{-1}, implying cooperative rearrangements are occurring. Preliminary measurements of the influence of solvent viscosity, pH, and salt concentration on the protein relaxations are also presented.

Th-Pos414

THE MODIFICATION OF PHOTOSYSTEM I (PSI) SYNTHESIS, ACTIVITY AND LOCALIZATION CONTRIBUTES TO ENERGY TRANSDUCTION DURING N_2 FIXATION IN THE UNICELLULAR CYANOBACTERIUM *CYANOTHECE* SP. ATCC 51142. ((P. Meunier, M. Colon-Lopez, D. Tucker, D. M. Sherman* and **L. A. Sherman**)) Dept. of Biological Sciences; *Dept. of Botany and Plant Pathology, Lilly Hall Purdue University, West Lafayette, IN 47907.

Under 12h dark/12 h light (L/D) regimes, N_2 fixation in *Cyanothece* sp. ATCC 51142 peaked close to D4 (4 hours into the dark period). We observed N_2-fixation rates that were up to 100% higher when assayed in the light compared to darkness. This remained true even after the addition of DCMU blocked 90% of Photosystem II (PSII) activity. The stimulation by light was increased as carbohydrate granules were depleted. During the early portion of the dark period under L/D growth, and early in the evening when grown under continuous light, we found that PSI mRNA and protein levels increased and PSI activity in isolated thylakoid membranes was higher. Fluorescence experiments at 77K showed a greatly increased fluorescence yield of PSI during N_2 fixation. In addition, we have performed EM immunocytochemistry and have determined that some of the PSI protein is localized in unique inclusion bodies which we have termed Dark Bodies. These Dark Bodies become particularly significant during the dark period and also include cyanophycin which functions as a nitrogen-storage material in cyanobacteria. We conclude that PSI is enhanced in order to provide additional energy for N_2 fixation and that PSI may also be involved with the storage of combined nitrogen in this cyanobacterium. Supported by a grant from USDA.

Th-Pos415

BROWNIAN DYNAMICS STUDY OF THE INTERACTION BETWEEN PLASTOCYANIN AND CYTOCHROME *f*: DEVELOPMENT OF A PLAUSIBLE COMPUTER MODEL. ((**Douglas C. Pearson Jr.** and Elizabeth L. Gross.)) Department of Biochemistry and Biophysics Program, The Ohio State University, Columbus, OH 43210.

Previous work from our laboratory (Pearson et. al., Biophys. J., 71:64-76; 1996) has emphasized the search for a plausible electron-transfer-active complex between the electron transfer proteins plastocyanin (PC) and cytochrome *f* (cyt f) through manual docking methods; that is, the assembly of the two molecules based on available biochemical data, consideration of electrostatic interactions and minimization of steric hinderance, but merely considering the complexes that look good to the assembler's eye. The current study, driven by the need to "take the experimenter out of the experiment," analyzes the attraction of PC and cyt f and the resulting complex formation utilizing Brownian dynamics (BD) algorithms. A BD study simulates the motion of a mobile ligand (in this case, PC) due to electrostatic attraction to a fixed receptor (cyt f) with a small random factor simulating diffusional effects included. The two molecules are considered as rigid bodies in the BD algorithm. We discuss here the development of the BD experiments using the specific study of the interaction between poplar PC and turnip cyt f as an example, and we compare the results of these experiments to the results from the manual docking studies. This method has, in fact, allowed us to observe complexes not predicted by manual docking methods.

Th-Pos416

BROWNIAN DYNAMICS STUDY OF THE INTERACTION BETWEEN PLASTOCYANIN AND CYTOCHROME *f*: COMPARISON OF PLASTOCYANINS FROM DIFFERENT SPECIES. ((**Elizabeth L. Gross**, Douglas C. Pearson Jr., Erico S. David and Marcus Goodman.)) Department of Biochemistry and Biophysics Program, The Ohio State University, Columbus, OH 43210.

Manual docking experiments studying the interaction between plastocyanin (PC) and cytochrome *f* (cyt f) (Pearson et. al., Biophys. J., 71:64-76; 1996) resulted in the proposal of two types of complexes between the two proteins. Complex 1 involves predominately electrostatic interactions between D44 on PC and K187 on cyt f and between E59 and E60 on PC and K65 and K66 on cyt f. Complex 2 preserves the D44-K187 interaction but allows the H87 ligand to the copper on PC to interact with Y1 on cyt f. We believed that this dock had unfavorable electrostatic interactions between the positive charges over the copper and H87 on PC and the iron and Y1 on cyt f, and therefore was stabilized by hydrophobic interactions. However, Brownian dynamics (BD) studies on the interaction between the two proteins suggest otherwise. We have determined the total number of "successes" (BD trajectories taking the copper atom on PC within 35 A of the iron on cyt f) and the number of potentially electron-transfer-active complexes for plastocyanins from different species. Results from all plastocyanins interacting with turnip cyt f demonstrate the direct formation of complex 2 (a potentially electron-transfer-active complex) through only electrostatic interactions; in fact, most of the complexes involving residues involved in the predicted complex 1 show a decided tendency towards a H87/Y1 link. The strength of the electrostatic interactions also depends on the type of PC used for the studies. The 99 amino acid-containing higher plant PCs such as poplar and french bean show a greater number of total docks than does parsley PC (higher plant PC, containing 97 amino acids) or *Chlamydomonas* PC (green algal PC). We can conclude that Complex 2 can be formed using electrostatic interactions alone and that electrostatic interactions are less important for algal PCs than for higher plant PCs.

Th-Pos417

CONTROLLING ENERGY TRANSFER WITHIN LIGHT-HARVESTING COMPLEXES

((**Gregory J.S. Fowler** and C. Neil Hunter)) Department of Molecular Biology and Biotechnology, University of Sheffield, Sheffield S10 2TN, UK

The light-harvesting complexes of photosynthetic bacteria absorb light and channel the excitation energy to reaction centres, the site of photochemical charge separation. Previous work has identified some of the amino-acid residues that are involved in the binding sites for the bacteriochlorophylls in the LH2 complex of *Rhodobacter sphaeroides* (Crielaard *et al.* 1994, Fowler *et al.* 1994), observations consistent with X-ray crystallographic data that have been subsequently obtained for the related LH2 complex from *Rhodopseudomonas acidophila* (McDermott *et al.* 1995). We have shown that the absorption properties of both the B800 and B850 pigments can be independently "tuned" by alterations in the surrounding protein. Thus we are able to alter the rate at which pigments acting as "collectors" in LH2 can pass their light energy to the LH2 "reservoir" pigments. It is also possible to alter the storage characteristics of the "reservoir" pigments, and to alter the excess light energy "overflow" pathways associated with the carotenoid pigments. The ability to alter the function of LH2 (rather than to demonstrate its structure) is unique to the present work.

(1) Crielaard, W., Visschers, R. W., Fowler, G. J. S., van Grondelle, R., Hellingwerf, J. J. and Hunter, C. N. (1994) *Biochim. Biophys. Acta* **1183**, 473-482. (2) Fowler, G. J. S., Sockalingum, G. D., Robert, B. and Hunter, C. N. (1994) **299**, 695-700. (3) McDermott, G., Prince, S.M, Freer, A.A., Hawthornthwaite-Lawless, A.M., Papiz, M.Z., Cogdell, R.J. and Isaacs, N.W. (1995) *Nature* **374**, 517-521.

Th-Pos418

COMPUTER SIMULATION OF TITRATION BEHAVIOR IN BACTERIAL PHOTOSYNTHETIC REACTION CENTERS. **Cynthia Gibas**, Colin Wraight, and Shankar Subramaniam, University of Illinois at Urbana- Champaign, Urbana IL, USA.

The pH–dependent behavior and protonation states of individual residues in proteins, which are very important for protein function, are often difficult to determine experimentally. Continuum electrostatic methods have been used successfully to model the titrations of individual amino acid residues in their protein environments. We examine the photosynthetic reaction center of Rb. sphaeroides and several modeled reaction center mutants. Two amino acid residues which have been determined experimentally to be critical for proton uptake are calculated to gain 1.4 protons in the course of the reaction center's quinone reduction cycle. The pH dependence of proton uptake is successfully reproduced.

Th-Pos419

HETERONUCLEAR STRUCTURAL NMR OF *RHODOBACTER SPHAEROIDES* LH1 COMPONENTS IN DETERGENT MICELLES. ((M. E. Girvin[1], R. D. Krueger-Koplin[3], C. Anklin[2], C.C. Schenck[2])) [1]Dept. of Biochem., Albert Einstein College of Medicine, Bronx, NY 10461, [2]Bruker Instruments, Billerica, MA 01821, [3]Dept. of Biochem. and Molec. Biol., Colorado State University, Fort Collins, CO 80523-1870.

The proximal light-harvesting antenna complex (LH1) of *R. sphaeroides* consists of small transmembrane polypeptides (α, 6,837 daltons and β, 5,457 daltons) and noncovalently-bound bacteriochlorophyll *a* (BChl*a*) arranged into annular membrane-protein complexes. We have performed heteronuclear NMR experiments on purified LH1 components in detergent micelles. 2D $^1H^{15}N$ HSQC spectra of a 1mM sample of ^{15}N-labeled β-peptide in β-octylglucoside (βOG) display all of the expected 46 (48 a.a. less the two Pro) backbone and 9 side chain cross peaks. Despite the relatively low protein concentration, 3D NOESY-HSQC data yield H^N-H^N NOEs in 30 hours. 2D nitrogen-defined strips (figure, ^{15}N ppm at the top) show a sequence of 4 amides connected by H^N-H^N NOEs. Higher concentrations and longer experimental times will be used to complete the assignments and solve the structures of the α and β peptides.

β-peptide and BChl*a* associate in βOG detergent micelles to form a spectrally-defined species, B777. Upon detergent dilution, B777 dimerizes to form a β_2BChl_2 complex (β/β-B824) with maximal absorbance at 824 nm. Initial 2D $^1H^{15}N$ HSQC data for the β/β-B824 complex shows single $^1H^{15}N$ cross peaks for backbone and side chain HN pairs; we interpret this as preliminary evidence that the dimer is symmetric.

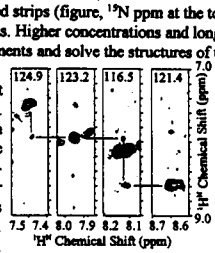

Support by NIH GM48254, AECOM, CIRB and Bruker.

Th-Pos420

INVESTIGATING THE PHOTOSYNTHETIC APPARATUS OF *RHODOBACTER SPHAEROIDES* BY PROXIMAL PROBE MICROSCOPY

((**J.J. Stewart**[1], D.L. Sampson[2], B.A. Parkinson[2], C.C. Schenck[1])) [1]Department of Biochemistry and Molecular Biology, [2]Department of Chemistry, Colorado State University, Fort Collins, CO 80523.

Light-driven charge separation in photosynthetic bacteria is effected by specialized membrane-spanning protein-pigment complexes. Two light-harvesting complexes (LH1 and LH2) serve to capture and transfer light energy to the reaction center protein, where the light-induced redox reactions of photosynthesis are initiated. The LH antenna complexes consist of small trans-membrane polypeptides (α and β) plus associated bacteriochlorophyll arranged into annular structures in the membrane.

Two-dimensional crystals of purified LH1 from *Rhodobacter sphaeroides* have been analyzed by atomic-force microscopy (AFM) and scanning-tunneling microscopy (STM) on solid/air interfaces. At low transverse magnification, AFM reveals single-thickness 2-D crystallites with transverse linear dimensions of several µm and edge depth profile 2.5 to 5 nm. At higher transverse magnification, AFM reveals no discernable topographical features on the 600-nm scale, whereas STM reveals a semi-regular lattice of 25-50 nm holes in a membrane (see figure). The mechanism of contrast in the STM image is under consideration; one possible interpretation of these results is that the high-regions in the STM image designate regions of strong electronic coupling between the metal tip and the conductive support due to the bacteriochlorin rings in the LH1 annulus. Support by NIH GM48254 and DOE-OER #DE-FG02-92ER1430 8.

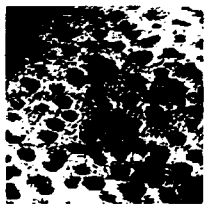

0nm 600nm

Th-Pos421

SITE-DIRECTED MUTAGENESIS OF L212-GLU IN THE PHOTOSYNTHETIC REACTION CENTER OF *RHODOBACTER SPHAEROIDES*

((**E. Takahashi** and C. A. Wraight)) University of Illinois, Urbana, IL 61801

The residue L212-Glu of the photosynthetic reaction center (RC) from *Rb. sphaeroides* plays an important role in the proper turnover of the RC complex. L212-Glu and neighboring L213-Asp, located in the vicinity of the secondary quinone (Q_B) binding site, have been implicated in the proton transfer to Q_B (1, 2). The electrostatic influences exerted by the two ionizable residues on RC function are revealed in the pH dependences of electron and proton transfer reactions of the wild type, L212-Glu → Gln and L213-Asp → Asn mutant RCs (1, 2). In the current study, the effects of substituting a positively charged residue for the native carboxylic acid were investigated by altering L212-Glu to lysine. The nearby residues L213-Asp and M44-Asn were also mutated, in combination, to give three mutants: (A) L212-Glu → Lys (L212EK), (B) L212EK + L213Asp → Asn (Double mutant), and (C) Double mutant + M44 Asn → Asp (Triple mutant). The Triple mutant was constructed for comparison with the herbicide resistant L212EK mutant found in *Rps. viridis* (3), where wild type residue L213 is Asn and M43 (homologous to M44 in *Rb. sphaeroides*) is Asp. All three mutants displayed inhibited Q_B binding characteristics, as expected from the structural nature of the substitution and the *Rps. viridis* study. The $P^+Q_B^-$ back reaction rates for the three mutants differed considerably, with values of 4.9 s^{-1}, 0.11 s^{-1} and 0.98 s^{-1} (pH 8.0) for L212EK, Double and Triple mutants, respectively (wild type = 0.75 s^{-1}). Unlike the wild type, the $P^+Q_B^-$ back reaction rates for all three mutants were roughly pH independent from pH 7.0 to 11.0. The first electron transfer rates (pH 8) did not vary as widely as the $P^+Q_B^-$ back reaction rates: 2400 s^{-1}, 1800 s^{-1}, and 1300 s^{-1} for L212EK, Double and Triple mutants, respectively (wild type = 5500 s^{-1}). The second electron transfer rates (pH 8) were 460 s^{-1}, 1.1 s^{-1}, and 30 s^{-1} for L212EK, Double and Triple mutants, respectively (wild type = 1000 s^{-1}). Further analysis of Q_B binding behavior will also be presented.

(1) Paddock et al. (1989) Proc. Natl. Acad. Sci., 86: 6602-6606
(2) Takahashi and Wraight (1992) Biochemistry, 31: 855-866
(3) Albert et al. (1994) Biochemistry, 33: 11355-11363

Th-Pos422

95 GHz (W-band) pulsed ENDOR of Ubiquinone Anion Radicals in Frozen Solution and in the Mutant HIS(M266) of *Rhodobacter sphaeroides* R26.*

((**M.Rohrer#**, T.F.Prisner, B.Vrieze, K.Möbius)) Freie Univ. Berlin, 14195 Berlin, Germany. ((A.Gardener, F.Lendzian, W.Lubitz)) Techn. Univ. Berlin, 10623 Berlin, Germany. # present adress: National High Magnetic Field Lab., FSU, Tallahassee 32310 Fl, USA.

Taking advantage of the high electron - Zeeman interaction at an external magnetic field of 3.4 T, (corresponding to a microwave frequeny of 95 GHz (W - band) in the EPR experiment for systems with $g \approx 2$), the g - anisotropy of randomly oriented semiquinone anion radicals is well resolved. Besides the determination of the principal values of such systems, the separation of the corresponding field positions allows for highly orientation - selective ENDOR studies of these systems. W - band ENDOR studies of UQ-10 semiquinone anion radicals in different solvents (deuterated and protonated) and in the protic surrounding of $Fe^{2+} \rightarrow Zn^{2+}$ substituted mutants His M266 → Cys of bacterial photosynthetic reaction centers *Rhodobacter sphaeroides* R26, are presented. The hyperfine data are extracted with the help of computer simulation of the high-field powder ENDOR spectra (1). They are partially assigned by using results from single crystal ENDOR studies performed at X - band (2).

(1) Rohrer, Plato, MacMillan, Grishin, Lubitz, Möbius, (1995) J.Magn. Reson. **A116** 59. (2) Isaacson, Abresh, Feher, Lubitz, (1995) Biophys. Journ. **68** A246. *Work supported by DFG

Th-Pos423

CHEMILUMINESCENCE AS A PROCESS OF FREE-OXYGEN RADICALS DE-EXCITATION IN THYLAKOID MEMBRANES

((Lubomir Dvorak, Jiri Skotnica, Jiri Fiala)) Department of Experimental Physics, Faculty of Science, Palacky University, Tr. Svobody 26, 771 46 Olomouc, Czech Republic.

The chemiluminescence peaks were observed at about 50 °C and 70 °C (see E. Hideg, I. Vass Photochem. Photobiol. (1993), 58:280-283, whose identified the high temperature peak only) on the intact leaves of barley heated by a constant heating rate. The appearance of these peaks depends on the atmospheric composition (increased in the presence of molecular oxygen and diminished in the presence of carbon dioxide or nitrogen without oxygen). The chemiluminescence needs chlorophyll *a* as well as the previous freezing of the thylakoid. These peaks are observable in samples without previous light excitation. The shapes of the peaks depend on the rate of sample heating, possibly due to some type of phase transition and the membrane lipid peroxidation when a slow heating rate is used (less than 10 °C.min^{-1}). The origin of this chemiluminescence may be explained by an energy transfer between free-oxygen radicals and the chlorophyll molecules. (Supported by GACR 202/96/1666)

NUCLEIC ACID CONFORMATION AND STRUCTURE

Th-Pos424

THERMODYNAMICS OF A DNA NICK.

((**T.M. Paner**[1], I. Kashin[1], B.Li[1], F.J.Gallo[2], B.D. Faldasz[1], A.S. Benight[2] and M.J. Lane[3])) [1]Tm Technologies, Inc. 82 Cummings Park, Woburn, MA 01801; [2]Department of Chemistry, University of Illinois, Chicago IL 60607; [3]Departments of Medicine and Microbiology/Immunology, SUNY-Health Science Center at Syracuse, Syracuse, NY 13027.

High resolution optical melting curves were collected in 115 mM Na^+ for DNA duplex complexes formed between 5'-dangling-ended hairpins and single strand oligomers with sequences complementary to the hairpin dangling-end. Sequences and lengths of the hairpin dangling-ends and complementary single strand oligomers were chosen such that the complexes formed contained a nick or a gap in the middle of the resultant 29 base pair duplex regions. Because of the much higher stability and concentration independence of the melting of the dangling-ended hairpins alone compared to melting of the oligomer-dangling-end complexes, melting transitions of the two structures were clearly resolved. For the nicked and gapped complexes analysis of these transitions in terms of a three-state equilibrium model enabled evaluation of the thermodynamics of both nicked and gapped duplexes. Results of the analysis revealed that a nick is favored over a gap by as much as 2.4 kcal/mol in this molecular context and suggest thermodynamic origins of the observed stabilization are primarily entropic. Results of similar analysis of single base mismatches will also be reported.

Th-Pos425

PREDICTING MELTING TEMPERATURES OF SHORT DUPLEX DNA OLIGOMERS.

((**P.M. Vallone**, R. Owczarzy, F.J. Gallo and A.S. Benight)) Department of Chemistry, University of Illinois, Chicago, IL 60607.

We have tested how well three published sets of nearest-neighbor sequence dependent thermodynamic parameters are able to predict experimentally measured t_m's (melting temperatures) of short duplex DNA oligomers of arbitrary sequence and G-C composition. The three sets were: (1) From our laboratory evaluated from melting analysis of DNA dumbbells in 115 mM Na^+; (2) Breslauer's laboratory obtained from melting analysis of a mixture of DNA oligomers and polymers in 1.0 M NaCl and; (3) A new "improved" set from SantaLucia's laboratory determined from melting curves of DNA oligomers measured in 1.0 M NaCl. Experimental melting curves of over 35 short self-complementary and non-self complementary linear duplex DNA oligomers ranging in length from 10 to 22 base pairs were measured as a function of DNA concentration in solvents containing 1.0 M and 115 mM Na^+. Using the three parameter sets t_m's were predicted from the sequences of these DNAs as a function of strand concentration. When employed as reported, none of the nearest neighbor sets could accurately predict all the experimental t_m's. Fits of all three nearest neighbor sets were greatly improved when a simple correction factor dependent on DNA length and G-C content was employed. Potential thermodynamic origins of this correction will be presented.

Th-Pos426

MELTING BEHAVIOR OF DNA HAIRPINS CONTAINING THE UNIVERSAL BASE 5-NITROINDOLE.

((**Peter M. Vallone** and Albert S. Benight)) Department of Chemistry, University of Illinois, Chicago, IL 60607.

Seven variants of a 16 base self-complementary DNA sequence were synthetically prepared and studied by melting analysis. Five of these contained a 5-nitroindole base analog substituted at one or more positions along the sequence. Sequences of the oligomers were designed such that they could form intramolecular hairpin structures. Optical melting curves of the oligomers measured as a function of strand concentration in solvent containing 115 mM Na^+ revealed the melting transition parameters of the oligomers were concentration independent over the 50 fold range from 0.8 to 40 μM. Sequences were designed to investigate the influence of the 5-nitroindole analog base (X) when it replaced either a T on the 5'-3' strand or an A on the complementary strand or both bases at the position of the fourth base pair of the stem sequence. The sequences in which the T_4 loop was replaced by a T-X_2-T or X_4 loop were also prepared. Comparisons were made to the control sequence with a T_4 end-loop. The stability of these molecules were studied by optical (absorbance and circular dichroism) and calorimetric melting experiments conducted in 115 mM Na^+. Results revealed the X-A and T-X mismatches were the most destabilizing compared to the natural control sequence (Δt_m = -17.2°C). In contrast, the hairpins with X_4 and T-X_2-T loops were more stable than the control sequence (Δt_m = +6.8 and +1.4°C, respectively).

Th-Pos427

EFFECTS OF IONIC STRENGTH AND CATION VALENCE ON THE ELASTIC RESPONSE OF SINGLE DNA MOLECULES.

((C.G. Baumann, S.B. Smith*, C. Bustamante* and V.A. Bloomfield)) Department of Biochemistry, University of Minnesota, St. Paul, MN 55108 and *Institute of Molecular Biology and Department of Chemistry, University of Oregon, Eugene, OR 97403

DNA properties are influenced by solution ionic strength (I) and cation valence. The persistence length (P) of DNA at low I is lengthened due to electrostatic "stiffening". Experimental determinations of P typically require corrections for excluded volume present in large molecules, or are conducted using very short DNA fragments near P. We utilized a dual-beam laser trap to record the elastic response of single lambda-phage DNA molecules as a function of I. A worm-like chain model fit the data yielding low and high salt P values of ~960 and ~450 Å, respectively. P decreased sharply with increasing I for I < 10 mM, reaching the high salt P value at I ≈ 20 mM. DNA in aqueous solution undergoes ordered collapse, or condensation, induced by trivalent cations (*i.e.* spermidine and hexaammine cobalt) yielding toroidal particles similar to those released from lysed phage heads. The impetus for DNA condensation is thought to arise either from attractive side-by-side interactions or from a "buckling" elastic force exerted by nearly neutralized DNA as postulated by Manning (1985). We tested these ideas by conducting isometric manipulations of single molecules in the presence of Mg^{2+}, putrescine, spermidine and hexaammine cobalt at molecular extensions which prevented intramolecular contacts. All cations generated a retractive elastic force caused by a decrease in P. Our results show both di- and trivalent cations generate a retractive elastic force in DNA; however, trivalent cations alone are able to neutralize the critical amount of DNA phosphate charge required for ordered collapse in aqueous solution.

Th-Pos428

EFFECTS OF TELOMERE REPEAT SEQUENCE INSERTS ON DNA CONDENSATION BY COBALT (III) HEXAAMMINE

((**Jason R. Schnell,*** Judith Berman,# and Victor A. Bloomfield*)) Depts. of *Biochem and #Plant Biology, Univ. of Minnesota, St. Paul, MN 55108. (Spon. by W. J. Baumann)

Yeast Telomere Repeat Sequence (TRS) DNA is highly conserved: $(C_{1\text{-}3}A)_n$. We have used total intensity light scattering and electron microscopy (EM) to monitor the effects of yeast TRS on *in vitro* DNA condensation by cobalt (III) hexaammine. Insertion of 72 bp of TRS into a 3.3 kb plasmid depresses condensation as seen by light scattering and results in a 35-50% decrease in condensate size as measured by EM. The depression in total light scattering intensity is greater when the plasmid is linearized with the TRS at an end (39-49%) than when linearized with the TRS in the interior (18-22%). The condensation kinetics of TRS-containing plasmids show an unusually abrupt plateau ~5 minutes after addition of cobalt (III) hexaammine. These results, along with analysis of toroidal condensate dimensions suggest that the growth stages of condensation are inhibited by the presence of a TRS insert. A fragment ~100 bp long and containing the same 72 bp of TRS inserted into the plasmid has been isolated along with a non-repeating fragment of similar length. Condensation studies show that the non-repeating fragment forms large networked aggregates, while the TRS-containing fragment forms discrete structures 100-200 Å in diameter. Intensity of light scattering from the condensed TRS-containing fragment is 100-fold less than that of the non-repeating fragment. Circular dichroism of the TRS-containing fragment show subtle differences not attributable to differences in nucleotide composition. These results suggest that TRS DNA inhibits condensate growth, by a TRS structure which disrupts close packing. This hypothesis is being explored further through co-condensation studies of a 3.3 kb plasmid with the 100 bp fragments, in which condensed and uncondensed fractions are separated and analyzed for the presence of the fragment DNA.

Th-Pos429

GLOBAL COMPARISON OF PUBLISHED NEAREST-NEIGHBOR SEQUENCE DEPENDENT THERMODYNAMIC PARAMETERS.

((**Richard Owczarzy**, Frank J. Gallo and Albert S. Benight)) Department of Chemistry, University of Illinois, Chicago, IL 60607.

Eight experimentally derived and two theoretical sets of nearest neighbor sequence dependent interactions in DNA have been published.To clarify which set to use when calculating duplex stability we have conducted a systematic comparison to ascertain similarities and differences between sets and determine their reliability. The free-energy of duplex formation at 25°C, $\Delta G_{25°C}$, was calculated for the 524,800 possible unique 10 base pair sequences. Distribution functions of $\Delta G_{25°C}$'s were quite different revealing large differences in the $\Delta G_{25°C}$ values predicted from the different nearest neighbor sets. Then pairs of sequences for which the two nearest neighbor sets predicted the opposite order of stability were denoted as *discordant* pairs. The smallest number of *discordant* pairs were obtained in comparisons of the sets derived from melting analysis of DNA polymers and restriction fragments in solvents ranging from 20 mM to 200 mM NaCl. Significantly larger numbers of *discordant* pairs were found when these sets were compared with those determined from analysis of DNA oligomers in 1.0 M NaCl. Melting experiments were performed on several of the 10-mer duplexes representative of the most *discordant* pairs. Results indicated which nearest neighbor sets predicted the observed stability of the 10-mers.

Th-Pos430

UNCONVENTIONAL HELICAL PHASING OF REPETITIVE DNA MOTIFS REVEALS THEIR RELATIVE BENDING CONTRIBUTIONS

((**Mensur Dlakic** and Rodney E. Harrington)) Department of Biochemistry, School of Medicine, University of Nevada at Reno, Reno, NV 89557-0014. (Sponsored by R. E. Harrington)

A new implementation of DNA phasing analysis was developed in which all sequence motifs of interest are clustered together in several oligomers of identical base composition, but with different phasing relationships to each other. Synthetic DNA sequences were ligated and analyzed by gel mobility and 2D cyclization assays to determine their global curvature. At first approximation, the results show that relative bending contributions to the global curvature of studied oligomers are AAAAA > GGGCCC > GAGAG. However, these results have deeper meaning when examined by the criteria of different models for DNA bending. This is shown by modeling studies using different scaling of two trinucleotide models.

Th-Pos431

5-FLUORODEOXYCYTIDINE AND 5-FLUORODEOXYURIDINE AS PROBES OF NUCLEIC ACID STRUCTURE: HAIRPINS, DOUBLE HELICES AND UNUSUAL BASE PAIRING

((**Caryn Evilia**, Xiaolin Zhang, Jean Kanyo and Ponzy Lu)) Department of Chemistry, University of Pennsylvania, Philadelphia, PA 19104

Whenever the 3 D structure of DNA is solved both alone and with protein, it never resembles uniform B structure. The structure is always distorted and/or bent, sometimes with bases displaced from the double helix. We ask the question whether double helical nucleic acids uncomplexed with protein have a uniform structure or is it predisposed to structure that is related to it's function. ^{19}F NMR spectra of DNA with the nucleotide analogs, 5-fluorodeoxyuridine and 5-fluorodeoxycytidine, are useful in addressing this question. We have incorporated these probes into several systems and used the ^{19}F spectra to look at the structure as we change environmental conditions such as ionic composition and temperature. We have examined the T7 and *E. coli* RNA polymerase promoters, *lac* and tetracycline operators as well as hairpins, loops, and bulges as controls.

This work is supported by the US ARO.

Th-Pos432

CIRCULAR DICHROISM OF POLYNUCLEOTIDES - A COMPUTATIONAL STUDY. ((N. Sreerama and R.W. Woody)) Department of Biochemistry and Molecular Biology, Colorado State University, Fort Collins, CO 80523, USA. (Spon. by Aichun Dong)

Circular dichroism spectra of polynucleotides were calculated using the matrix method. The electronic transition parameters (wavelength, intensity and transition dipole moment direction) of individual bases were from the polarized reflection studies of single crystals of the purine and pyrimidine bases by Clark. CD spectra were computed for different sequences of polynucleotides in A, B and Z conformations and were compared with the experimental CD data. CD spectra were also computed for three oligonucleotides with known solution structure (Dr. A.N. Lane, MRC Labs, London) and were compared with the experimental CD spectra (Dr. S.R. Martin, MRC Labs, London). The computed spectra reproduced most major features in the spectra, but some of the observed bands in the 260-285 nm range were not predicted or were shifted significantly in wavelength. The $n\pi^*$ transitions and environmental effects, which were neglected in these calculations, are expected to influence the long-wavelength region of the spectrum. Calculations based upon transition parameters from semi-empirical MO theory, as modified by the electrostatic fields, have thus far given results substantially poorer than those obtained from the empirical transition parameters. Efforts are under way to improve these calculations. (Supported by NIH grant GM 22994.)

Th-Pos433

EVALUATING STABILITIES OF DUPLEX RNA WITH DIFFERENT STRUCTURAL ELEMENTS BY TGGE. ((Jian Zhu and Roger M. Wartell)), School of Biology, Georgia Institute of Technology, Atlanta, Georgia.

The thermal stabilities of RNA duplexes with single base pair differences at several locations were investigated by temperature gradient gel electrophoresis(TGGE). DNA templates for in vitro transcription were generated by several steps of PCRs. The transcribed sense and antisense RNAs were annealed to form homologous 345bp ds RNA. UV melting experiments were used to characterize selected duplex RNAs and verified their predicted three step transitions. All possible base pair substitutions, mismatches, single base bulges and some double mismatches were examined at six specific sites, and more limited changes were investigated at five other sites. Parallel TGGE was used to determine the relative stabilities of ds RNAs, and perpendicular TGGE was employed to obtain mobility transition curves and midpoint transition temperatures(T_m) of the RNA duplexes. The stabilities of RNA molecules with single base pair substitutions and mismatches were influenced by the identities of the substitutions and mismatches as well as by the site's neighboring base pairs. For each site, the difference in transition temperatures(δT_m) between pairs of RNAs with base pair or mismatch differences ranged from 0 to 5°C(use the RNA carrying CG or GC as reference). The free energy differences of the corresponding pairs were calculated from available stacking free energies ($\delta\Delta G°_{37}$) given by Serra and Turner(Methods of Enzymology 259, 242, 1995). Linear correlations between $\delta\Delta G°_{37}$ and δT_m were observed for all sites. Using this information, the free energies of all eight single base bulges at six sites were determined within a range from 0 to 2.7 kcal/mol. An unpaired base identical to one of its adjacent bases caused less destabilization than an unpaired base with an identity differing from its neighbors. On average, single base bulges closed by two AUs are about 1.4kcal/mol less stable than those closed by only one AU. The free energies of double mismatches were determined by a similar approach. They ranged from -1.3 to 1.1 kcal/mol, and on average double mismatches closed by two AUs were about 0.7kcal/mol less stable than those closed by only one AU.

Th-Pos434

KINETICS OF FOLDING OF THE *TETRAHYMENA THERMOPHILA* GROUP I INTRON. ((B. Sclavi[†], S. Woodson[§], M. Sullivan[†], M.D. Brenowitz[‡], M.R. Chance[‡†])) Depts. of Physiology and Biophysics[†] and Biochemistry[‡], Albert Einstein College of Medicine, Bronx, NY,(USA) and Dept. of Biochemistry[§], Univ. of Maryland, College Park, MD, (USA).

The *Tetrahymena thermophila* ribozyme is a 400 bases self-splicing intron. In order to be catalytically active this large RNA must fold into a specific tertiary structure (Celander and Cech, 1991). We have applied the method of stopped-flow x-ray footprinting to the study of the kinetics of folding of this large RNA.

Preliminary hand-mixing results reveal three classes of protection kinetics. The first set of rates is too fast to be measured with this experiment, the first time point being at 30s. The regions folding at these fast rates include most of the P4-P6 domain, except for part of the P5-P5a region which becomes protected at about 2 min^{-1}. The slowest folding domain is the P3-P7 domain, folding at rates from 1 to 0.5 min^{-1}, in agreement with data reported by Zarrinkar and Williamson (1994). A folding mechanism is proposed where some regions begin to fold simultaneously followed by an obligatory sequential pathway. We are currently carrying out stopped-flow experiments which will be used to better distinguish the faster steps in the folding process. This work was supported by grants from the NIH (GM39929 and GM52348) and the NFS (MCB-9410748).

Cech, T.R. (1993) in The RNA World (Gesteland, R.F., Atkins, J.F. eds) pp.239-269, Cold Spring Harbor Laboratory Press, New York.
Celander, D.C., Cech, T.R., (1991) Science 251, 401-407.
Zarrinkar, P.P. & Williamson, J.R. (1994) Science 265, 918-924

Th-Pos435

FREE ENERGY OF BASE FLIPPING IN DAMAGED DNA.
((R. Nirmala and Roman Osman)) Department of Physiology and Biophysics, Mount Sinai School of Medicine, One Gustave L. Levy Place, New York, NY 10029-6574

DNA damage by UV radiation results predominantly in the formation of pyrimidine cyclobutane dimers. Endonuclease V recognizes the damaged DNA through several mechanisms. We have shown that bending of the DNA (1), counterion redistribution (2) and solvation changes provide recognition elements to the enzyme. Crystal structure of endonuclease V complexed with damaged DNA (3) shows that an extrahelical adenine opposite to the 5' side of the thymine dimer is inserted into a pocket in the protein. The importance of the extrahelical base for damage recognition is unclear. Molecular dynamics simulation of the solvated dodecamers d(TCGCGT=TGCGCT)-d(AGCGCAACGCGA) with intrahelical and extrahelical adenine opposite to thymine dimer reveal that the structures differ mainly in ε of A18, γ and ε of A19 (the extrahelical base) and γ of C20. Free energy perturbation simulations are conducted to estimate the energetic preference of extrahelical base in damaged DNA compared to normal DNA. Potential of mean force simulations of base flipping delineate the conformational changes in the backbone occurring in this process.

(1). Miaskiewicz et al. (1996) J. Am. Chem. Soc., 118, 9156-9163
(2). Osman et al. (1994) in Radiation damage in DNA. ed. Alfred F. Fuciarelli and John D. Zimbrick, Battelle press, pp. 323-331
(3). Vassylyev et al. (1995) Cell, 83, 773-782

Supported by US PHS Grant CA63317

Th-Pos436

PORPHYRIN BINDING TO MULTI-STRANDED DNA. ((N. V. Anantha & R. D. Sheardy)) Department of Chemistry, Seton Hall University, South Orange, NJ 07079

We have recently reported the cation-induced self-assembly of DNA oligomers of general sequence $C_4T_4G_4T_{1-4}G_4$ into high molecular weight multi-stranded structures. The architecture of the proposed structure consists of a series of four leafed G-4 tetrads tethered together via one or two T_{1-4} strands and thus resembles a long four sided hollow tube with periodic "pockets" [Marotta et al, *Biochemistry* 1996, *32*, 10484]. These pockets possess electrostatic, hydrogen bonding and hydrophobic contact points and thus should be ideal candidates for the binding of small molecules. We have investigated the interaction of tetrakis(4-N-methylpyridyl)-porphine (H_2TMPyP) with DNA sequences T_4G_4, $G_4T_2G_4$, C_4T_4-$G_4T_2G_4$ and a double strand forming control sequence $(CG)_2ATAT(CG)_2$ via CD, fluorescence and UV/VIS methods under conditions favoring self-assembly. Analysis of binding isotherms indicate that H_2TMPyP binds quite differently to each type of DNA oligomer. In addition, energy transfer experiments and induced CD in the Soret region indicate that H_2TMPyP intercalates into into all DNAs studied. The data will be discussed in terms of a 2 site model for binding to the self-assembling DNA oligomers: a high affinity site, considered to be the "pocket", and a site of lower affinity, the quadraplex itself.

Th-Pos437

ENHANCED FLEXIBILITY OF B-DNA IN THE PRESENCE OF MULTIVALENT COUNTERIONS. ((I.F.Rouzina &V.A.Bloomfield)) Biochem, U of Minn, St.Paul MN 55108.

We propose a new purely electrostatic mechanism through which multivalent counterions substantially increase the flexibility of B-DNA. The decrease in the DNA persistence length P to as little as 20 - 40 nm upon addition of small amounts of multivalent cations cannot be explained simply by better electrostatic shielding of the DNA since the high ionic strength value of P in sodium buffer is 50nm.

The simplest model of this effect consists of a uniformly charged cylinder, characterized by a single bending force constant A. The screening counterions form a thin 2D layer on its surface. This layer is uniform along the surface in the case of monovalent counterions, but develops structure due to strong mutual repulsion between screening multivalent counterions. As a result, the screened cylinder looks almost neutral a few angstroms away from the surface if screened by monovalent ions, but has a + / - pattern on it when screened by multivalent ions. The charge inhomogenity on any particular face of the cylinder makes bending towards this face easier, and away from it harder. The local bending constant thus aquires a component dependent on the radial angle ϕ: $A_i = A(1 - \alpha\Gamma_2 a/P_0 \cdot \cos\phi)$. Here Γ_2 is the 2D coupling of the counterions within the surface layer, a is the size of the charge inhomogenity, P_0 is the unperturbed persistence length of the DNA, and α is a constant near unity. Each screening counterion induces a transient, directed thermal fluctuation resulting in an overall larger bending angle and a persistence length shorter than that of a neutral cylinder.

Th-Pos438

DIFFERENTIAL BEHAVIOUR OF TELOMERIC SEQUENCES AND OLIGONUCLEOTIDES WITH SEVERAL CONTIGUOUS GUANINES.
((K Poon & RB Macgregor)) Faculty of Pharmacy, University of Toronto, Toronto, Ontario M5S 2S2

$d(T_{15}G_{15})$, TG, self-associates to form extremely stable aggregates that bind $d(A_{15})$. Similar behaviour is observed with $d(A_{15}G_{15})$. The polymerization of TG is presumably driven by the fifteen consecutive guanine residues. The ability to form high molecular weight complexes is also influenced by the relative length of the non-guanine portion in the oligomer. Alternating thymines and guanines within the telomeric sequence, $d(T_{15}G_4T_2G_4)$ (TGTG), stabilizes high-molecular weight species with a longer non-guanosine portion. The complexes formed by TG are composed of consecutive integer numbers of strands, rather than multiples of four strands observed for complexes of TGTG. Mg^{2+} favours complex formation by TG whereas K^+ potentiates the self-association of TGTG. All guanines in TG complexes are methylated by dimethylsulfate, none are methylated in TGTG complexes. However, methylated TG retains its ability to polymerize, but methylated TGTG does not. Thus, the guanine N7's of TG are not critical for complex formation. These results suggest different interactions stabilize TG and TGTG complexes, *e.g.*, standard G-tetrads for TGTG complexes and the continuous helical hydrogen-bonding proposed by Sasisekharan *et al.* (*J. Mol. Biol. 92*, 171-179) for TG complexes.

Th-Pos439

PROBING HIGH AFFINITY CARCINOGEN BINDING DNA SEQUENCES WITH PORPHYRIN. ((**Q. Liang**, R. D. Sheardy & S. A. Winkle)) Department of Chemistry, Seton Hall University, South Orange, NJ 07079 and Department of Chemistry, Florida International University, Miami, FL 33199. (Spon. by R. D. Sheardy).

The use of porphyrins to probe DNA structures is well established. Ideal candidates for these probes are DNA oligomers which possess high affinity binding sites for carcinogens such as AAAF and NQO. We have investigated the interaction of tetrakis(4-N-methylpyridyl)-porphine (H_2TMPyP) with a variety of such DNA sequences via CD and UV/VIS methods. Analysis of binding isotherms indicate that H_2TMPyP binds quite differently to each type of DNA oligomer. In addition, induced CD in the Soret region indicate that H_2TMPyP intercalates into all DNAs studied. The binding of the porphyrin, with a +4 charge, should be quite sensitive to ionic strenghth. The results of these studies confirm that sensitivity.

Th-Pos440

SEQUENCE SPECIFICITY IN THE BINDING OF Co(III) TO DNA. ((**M. Hicks**, R. D. Sheardy, G. Wharton, III, T. Pantano, W. R. Murphy, Jr. & D. H. Huchital)) Department of Chemistry, Seton Hall University, South Orange, NJ 07079 (Spon. by M. Petersheim).

The interaction specificities of Co(III) with DNA were investigated via consideration of thermodynamic characteristics of the duplex to single strand transition for DNA oligomers incubated in the presence of $[Co(NH_3)_5(OH_2)](ClO_4)_3$. It has previously been demonstrated that incubation of $[(5medC\text{-}dG)_4]_2$ with this cobalt complex leads to coordination of the cobalt center to the DNA, presumably at N7 of guanine bases [Calderone, D. C.; Mantilla, E. J.; Hicks, M.; Huchital, D. H.; Murphy, W. R., Jr.; Sheardy, R. D. *Biochemistry* **1995**, *34*, 13841]. DNA oligomers of different sequence were incubated with $[Co(NH_3)_5(OH_2)](ClO_4)_3$ and the treated oligomers were subjected to thermal denaturation for comparison to the untreated oligomers. The values of T_m, ΔH^o and Δn (the differential ion binding term) were determined in order to assess the sequence specificity of the interaction. Although there was no significant reaction between the cobalt complex and oligomers possessing an isolated -GA- or -CG- sites, the results indicate a remarkable preference for Co(III) binding to the DNA oligomer possessing an isolated -GG- site. In addition, a DNA oligomer possessing an isolated -GC- site was also modified by the treatment with the cobalt complex. The specificity noted above has also been confirmed via restriction enzyme nuclease digestion studies. Supported by NIH grant GM51069-01.

Th-Pos441

STRUCTURE OF DNA-CATIONIC LIPID COMPLEXES: HIGHER ORDER SELF-ASSEMBLY AND APPLICATIONS TO GENE THERAPY.
((**I. Koltover**, T. Salditt, J. Raedler, A. Lin, N. Slack, C. Safinya)) Materials, Physics Departments and Biochemistry and Molecular Biology Program, UCSB, Santa Barbara, CA93106.

DNA-cationic lipid complexes are among the most promising synthetically-based non-viral carriers of DNA vectors used in gene therapy. Using high-resolution synchrotron x-ray diffraction and optical microscopy we have established the structure of DNA-cationic lipid complexes [1]. The complexes are liquid-crystalline globules comprised of alternating lipid bilayers and monolayers of DNA. The linear λ–DNA strands are found to form a one-dimensional periodic lattice, resulting in a novel two-dimensional polymer smectic intercalated between the lipid bilayers. Diluting the positively charged lipids with neutral lipids in the isoelectric regime (overall neutral complexes) we are able to expand the DNA lattice from 24.5Å to 80 Å. Salt-dependence studies unambiguously show the existence of an electrostatically induced long range repulsive interaction between the DNA strands. Analysis of the x-ray line-shape of DNA peak along the dilution line allows us to measure the elastic constants of DNA lattice and elucidate the possibility of DNA-DNA correlations from layer to layer. The parameters controlling precise structural packing of lipid-DNA complexes appear to correlate with transfection efficiency results, relevant for gene therapy.
Work supported by NSF grant DMR-9624091, the Petroleum Research Fund (No.31352-AC7) and a Los Alamos CULAR grant No.STB/UC:95-146.
1. J. Raedler, I. Koltover, T. Salditt, C. Safinya, *Science* in print.

Th-Pos442

EFFECTS OF LOW DIVALENT CATIONS CONCENTRATIONS ON DNA PROTONATION: A RAMAN MICROSPECTROSCOPIC STUDY.
((C. M. Muntean[1], G. J. Puppels[2], J. Greve[3])) Institute of Isotopic and Molecular Technology, Cluj-Napoca, Romania; [2]General Surgery Rotterdam University Hospital "Dijkzigt", the Netherlands; [3]Department of Applied Physics, University of Twente, the Netherlands.

Binding of H^+ to DNA, may lead reversibly to unusual, alternative DNA structures. Studies are required to elucidate how can be influenced the equilibrium between protonated and nonprotonated DNA structures. In our Raman microspectroscopic study, measurements were carried out on calf-thymus DNA at neutral pH and pH 3 in the presence of low concentrations of Mg^{2+} and Ca^{2+} cations. Main results are: a) low concentrations of Mg^{2+} cations protect more effective DNA against protonation of cytosine, than low concentrations of Ca^{2+} cations (characteristic line at 1262 cm^{-1}); b) low salt concentrations do not protect adenine and G(N7) against binding of H^+ (characteristic lines at 1304 cm^{-1} and 1488 cm^{-1}, respectively). It therefore appears that low concentrations of divalent cations act as a mechanism of selectivity for the protonation of cytosine and adenine in DNA.
This work was supported by CEC grant, under contract nr. ERB-CIPA-CT-92-2223.

Th-Pos443

SUPRAMOLECULAR SELF-ASSEMBLY OF $d(TGG)_4$. ((**Fu-Ming Chen**)) Department of Chemistry, Tennessee State University, Nashville, TN 37209-1561

Absorbance spectral evidence reveals that molar concentrations of K^+ can induce aggregate formation in $d(TGG)_4$. The kinetic profile via 320-nm absorbance monitoring indicates that, in the presence of 2 M KCl, it requires nearly 2 hrs for the onset of aggregation to occurs at 20 °C. The kinetic profile is reminiscent of the autocatalytic reactions, consisting of an induction period followed by accelerative and leveling phases. The presence of Mg^{++} greatly facilitates the aggregate formation and results in the prominent appearance of an intense ψ-type CD. For example, the presence of 20 mM Mg^{++} in 2M KCl solution reduces the induction time for aggregation by an order of magnitude. Furthermore, the presence of 20 mM Mg^{++} reduces the requirement of the $[K^+]$ for aggregation by two orders of magnitude. The effects of K^+ and Mg^{++} ions are synergistic, since the presence of 20 mM Mg^{++} alone does not induce aggregate formation in this oligomer. In addition, thermal stabilities of the aggregates are strongly dependent on the concentrations of these two ions. Although the aggregates formed by 2M K^+ alone melt around 55 °C, the presence of 20 mM Mg^{++} increases the melting temperature to approximately 90 °C with some aggregates remianing unmelt even at 95 °C. The interplay of these two ions appears to be unique, since the replacement of K^+ by Na^+ or the replacement of Mg^{++} by other divalent cations does not lead to the observed self-assembly phenomenon. A mechanism for the formation of self-assembled structures is speculated.

Th-Pos444

HYDRATION DEPENDENT POLYMORPHISM OF A HETEROGENEOUS DNA--DNA DUPLEX. ((K.K. Reeves, J.W. Powell, V. Mohan[1], R.H. Griffey[1], H. Sasmor[1]))
Reed College, Portland, OR, 97202, [1]Isis Pharmaceuticals Carlsbad, CA, 92008. (Spon. J.W. Powell)

A 21-mer DNA duplex consisting of one strand linked by phosphodiester and the other by phosphorothioate linkage have been examined by FTIR spectroscopy in the frequency range of 500-1800 cm^{-1}. The intensity of the antisymmetric and symmetric PO_2^- stretches at 1250 and 1090 cm^{-1} are found to be greatly reduced, compared to wild-type DNA duplexes. The structure of the hetero duplex has been found to be a polymorphic one, with characteristics of both A- and Z-form DNA at low relative humidity. Hydration dependent conformational changes have been inferred through the shifts in the frequencies of the gycosidic and backbone regions. The duplex adopts a structure similar to the standard B-form conformation at high relative humidities.

Th-Pos445

HYDRATION ANALYSIS OF DNA BASES BASED ON THE PROXIMITY CRITERIA: A MOLECULAR DYNAMICS STUDY OF THE DNA DUPLEX d(CGCAAATTTGCG)$_2$ AND d(CGCTTTAAAGCG)$_2$ IN AQUEOUS SOLUTION USING AMBER 4.1

((K. J. McConnell, D. Sprous, D. L. Beveridge)) Wesleyan University, Molecular Biophysics Program, Department of Chemistry Middletown, CT 06459

In our current study we present a detailed study of the water structure around nucleic acid bases as observed in the molecular dynamic simulations of d(CGCAAATTTGCG)$_2$ and d(CGCTTTAAAGCG)$_2$ duplexes. Of interest in the current study is the difference of the fine structural properties of the A-track and T-track regions. It has be observed in gel migration studies that a poly A sequence behaves differently than a poly T sequence. Where the poly A track sequence bends far more than a poly T-track sequence. We examine the difference in the fine structural properties and hydration patterns as observed in the molecular dynamic trajectories. Both simulations were carried out using AMBER4.1 and the Cornell 1994 force field, with explicit TIP-3P water and Na^+ counter ions with run lengths grater than 1ns. The resulting trajectories are analyzed for the water structure around each of the four nucleic acid bases as well as for the DNA structure. The geometries of the water position are calculated for the first shell of hydration. A detailed description of the ion atmosphere and hydration and for each of the base atoms with respect to hydrogen bond angle and distance is presented and compared to crystallographic studies. Also the change in hydration as a function of groove width is discussed.

Th-Pos446

STRUCTURES OF DNA OLIGONUCLEOTIDES CONTAINING SEQUENCES OF ADENINES IN PHASE WITH THE HELICAL REPEAT ((**M.A. Young** and D.L. Beveridge)) Molecular Biophysics Program, Wesleyan University, Middletown, CT 06459 USA.

Sequences of DNA containing stretches of Adenines (A-tracts) positioned in phase with the 10.5 base pair helical repeat of B-form DNA have been known for some time to exhibit a variety of unique structural features. One consequence of their unique properties is that properly positioned phased A-tract sequences have been shown to be capable of enhancing transcriptional activation of certain genes which are regulated by DNA-binding proteins which bend DNA[1,2]. Thus, determining the structural features of phased A-tract DNA may help to understand a mechanism for structurally attenuated gene regulation, most possibly involving DNA bending. Despite continuing study, there is still not a unique atomic level structure or model which can account for the entire range of experimental data on the structure of A-tracts. In the current series of studies, computer modeling has been used to generate time-resolved atomic resolution structures of representative phased A-tract sequences. The all-atom systems modeled include over two helical turns of DNA, explicit solvent, and various ionic salts. The structures generated qualitatively reproduce many of the macroscopic features which have been experimentally observed for this class of sequences, including pronounced concerted DNA bending and progressive narrowing of the A-tract minor grooves in the 5' to 3' direction.

1. Gartenberg, M. R., and D. M. Crothers. 1991. Synthetic DNA bending sequences increase the rate of in vitro transcription initiation at the Escherichia coli lac promoter. *J Mol Biol.* 219:217-30.
2. Bracco, L., D. Kotlarz, A. Kolb, S. Diekmann, and H. Buc. 1989. Synthetic Curved DNA Sequences Can Act As Transcriptional Activators in *E. coli*. *EMBO J.*:4289-4296.

Th-Pos447

THE EFFECT OF pH ON THE THERMALLY INDUCED MELTING OF TWO INTRA-MOLECULAR OLIGONUCLEOTIDE TRIPLEXES: CALORIMETRIC STUDIES.

(([1]I.Haq, [1]B.Z. Chowdhry, [2]T. Brown and [3]A.N. Lane)) [1]University of Greenwich, School of Chemical and Life Sciences, London, SE18 6PF, UK, [2]University of Southampton, Department of Chemistry, Southampton, SO17 1BJ, UK, [3]MRC National Institute for Medical Research, London, NW7 1AA, UK.

Two C^+-G•C containing hexameric DNA triplexes have been formed from the constituent single strands which have been covalently linked with either hexaethylene glycol or octanal-8-diol phosphodiester. The requirement of the third strand cytosines to be protonated gives rise to a pH dependence of triplex formation and unfolding. We have investigated the thermodynamic properties of this pH dependent melting behaviour using high sensitivity differential scanning calorimetry. These data show that between pH 4 and 5.5 melting is bi-phasic with a low temperature, pH dependent, transition and a high temperature, pH independent transition. In this study we report a full thermodynamic characterisation of the pH dependent melting of these intra-molecular triplexes. Such data is a pre-requisite for a rational approach to the design of novel treatments in the antigene approach to cancer therapy.

HEME PROTEINS II

Th-Pos448

THE INFLUENCE OF pH AND SALTS ON THE A-STATES OF MYOGLOBIN ((Joachim D. Müller*, Ben McMahon# & G. Ulrich Nienhaus%#)) #Department of Physics & *Center for Biophysics and Computational Biology, University of Illinois at Urbana-Champaign, IL 61801, % Department of Biophysics, University of Ulm, 89069 Ulm.

The IR-active stretch frequency ν_{CO} of carbonmonoxymyoglobin is sensitive to the protonation state of the distal histidine (H64), a proximal histidine (H97) and acid induced unfolding. We model the unfolding and protonation process using global analysis methods and determine the pK's of H64, H97 and the unfolding transition together with the physical spectra of the protonation and unfolding states. We study the influence of a variety of Hofmeister salts on the A-states. The pK's, but not the spectra, depend on the strength and type of buffer or salt added. All salts raise the pK of the distal histidine and the unfolding transition, but chaotropic salts are especially potent. The pK of H97, on the contrary, is nearly unaffected by salts. We will discuss and compare our results to the model of preferential binding to and exclusion of cosolvents from the protein.

In addition we present preliminary measurements of the influence of salts on the rebinding kinetics of CO to myoglobin. (Supported by NIH PHS 2 R01 GM18051).

Th-Pos449

VISCOSITY DEPENDENCE OF NO REBINDING TO MYOGLOBIN ON THE PICOSECOND TIME SCALE.

((A.P. Shreve, S. Franzen, M.C. Simpson, W.H. Woodruff and R.B. Dyer)) Biosciences and Biotechnology Group (CST-4); Los Alamos National Laboratory; Los Alamos, NM

The kinetics of NO rebinding to native horse-heart myoglobin have been examined as a function of enviromental viscosity. Following photolysis, the rebinding of NO occurs predominantly on the picosecond time scale with a time course that is markedly non-exponential. We observe a significant change in the kinetics as the solution viscosity is increased by the addition of glycerol (see Figure). If the non-exponential rebinding process is modeled using a multi-exponential function, the most significant change seen upon increasing viscosity is an increase in amplitude of the fastest component of the rebinding. Detailed modeling will be reported and potential implications of this result for myoglobin function will be discucssed.

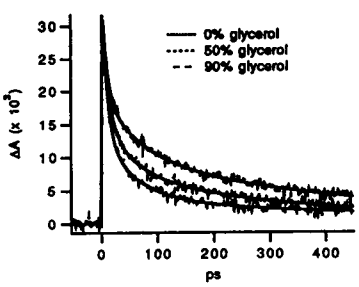

Th-Pos450

RESONANCE RAMAN STUDY OF THE BAND III AND Q-BAND ELECTRONIC TRANSITIONS IN DEOXY MYOGLOBIN

((Stefan Franzen, Andrew P. Shreve,
Stacie E. Wallace-Williams, R. Brian Dyer, William H. Woodruff))
Biosciences and Biotechnology Group, CST-4 Mail Stop J586,
Los Alamos Natl. Lab., Los Alamos, NM 87545

The band III electronic transition has been studied extensively as a probe of heme protein dynamics in deoxy myoglobin. The weak electronic transition ($\varepsilon \approx 250$) with a band maximum at 762 nm exhibits a frequency shift in the MbCO photoproduct and also show kinetic hole burning at low temperature [1,2]. Based on single crystal absorption spectra and extended Huckel calculations this band has been assigned as a $a_{2u} \rightarrow d_{xy}$ charge transfer transition [3]. We have recently obtained resonance Raman spectra for the entire spectrum (100 cm^{-1} - 1700 cm^{-1}) with excitation wavelengths from 700 nm to 850 nm (see Figure below). Comparison of the excitation profile of enhanced non-totally symmetric modes with the excitation spectra obtained in the Q-band region of the spectrum (500 nm - 630 nm) demonstrates that band III obtains its oscillator strength by vibronic coupling to the Soret band. The similarity of the spectra in the Q-band and band III indicates that there is little or no A-term scattering in resonance with band III. These findings mean that there is little or no coupling to iron-histidine out-of-plane modes or heme doming modes as has been suspected based on the charge transfer character of band III.

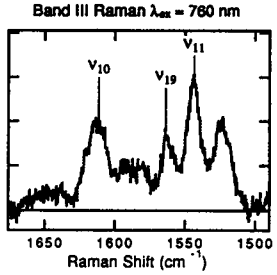

1. Steinbach et al. Biochemistry, 1991, 30, 3988
2.Ahmed et al. Chem. Phys. 1991, 158, 329
3. Eaton et al. JACS 1978, 100, 4491

Th-Pos451

IDENTIFICATION OF CONFORMATIONAL SUBSTATES INVOLVED IN NITRIC OXIDE BINDING TO FERRIC AND FERROUS MYOGLOBIN THROUGH DIFFERENCE FOURIER TRANSFORM INFRARED SPECTROSCOPY.

((**Lisa M. Miller**, Ana J. Pedraza, and Mark R. Chance)) *Department of Physiology and Biophysics, Albert Einstein College of Medicine of Yeshiva University, Bronx, NY 10461.*

The important physiological role of nitric oxide, and its interaction with numerous hemeproteins, has only recently been appreciated. Unlike carbon monoxide and oxygen, which have been studied extensively, the reactions of NO with hemeproteins are not well characterized. In this study, NO binding to myoglobin is studied using Fourier transform infrared spectroscopy. By using photolyzed / unphotolyzed FTIR difference spectroscopy of isotopically labeled MbNO, the NO stretching frequencies in both the ligand-bound states (A states) and photoproduct states (B states) are determined as a function of pH and iron oxidation state. Two A states are observed for ferrous MbNO; they fall at 1607 and 1613 cm^{-1}. For ferric MbNO, a single A state is observed (1927 cm^{-1}). The pH-dependence of the A states reveals a destabilization of the ferrous iron to the ferric state in low pH MbNO. The B states for both $Mb^{II}NO$ and $Mb^{III}NO$ are identical and fall at 1852 and 1857 cm^{-1}. This finding suggests a constant docking site environment for the NO ligand in the heme pocket regardless of its ligand-bound orientation. Overall, our results show that the NO ligand can be completely photodissociated from both ferric and ferrous MbNO at cryogenic temperatures, opening the field to a method for characterizing intermediate states involved in the process of NO-binding. In addition, the large difference in the frequency between the ferric and ferrous A states demonstrates the diverse nature by which NO can bind to hemeproteins and provides an excellent marker for the characterization of other heme-NO systems. This work is supported by the NIH Grant HL-45892.

Th-Pos452

PRESSURE DEPENDENCE OF LIGAND BINDING KINETICS TO MYOGLOBIN AND CONFORMATIONAL CHANGES NEAR THE HEME IRON.

((A. Schulte, O. Galkin, J. Kaesberg)) Department of Physics and Center for Research and Education in Optics and Lasers, University of Central Florida, Orlando, FL 32817.

The sensitivity of the iron-proximal histidine bond to variations in protein structure may be utilized by heme proteins to regulate the activity of the heme iron. Pressure allows one to change the molecular interactions in a controlled way and to separate thermal and volume effects on both the reaction rate and protein conformational states. We employ Raman and transient absorption spectroscopy to study structural and kinetic changes in CO and O_2 ligand binding to (horse) myoglobin at variable pressure (0.1 - 185 MPa) and temperature (80 - 295 K). Flash photolysis experiments in the time range $5 \cdot 10^{-8}$ to 10^{2} s monitoring the Soret absorption band show that the multistep kinetics at intermediate temperatures speeds up with pressure. We discuss a model which connects the rebinding kinetics with the relaxation of a conformational coordinate involving the heme iron and the linkage to the protein.
(Supported by NSF, Grant No. MCB-9305711).

Th-Pos453

THE STRUCTURAL RELAXATION OF MYOGLOBIN UPON REDUCTION

((**D.C. Lamb**[1], A. Ostermann[1], V.E. Prusakov[2], and F.G. Parak[1]))
[1]Physics Dept. E17, TU-Munich, Munich, Germany,
[2]Inst. of Chemical Physics, Russian Acad. of Science, Moscow, Russia

Met myoglobin has been reduced at low temperature (20 K). Upon reduction, an intermediate state is formed where the water molecule is bound to the heme iron in a 2+ low spin configuration, but the structure of the protein is frozen in the met conformation. Above 150 K, the protein begins to relax to the deoxy conformation. This protein relaxation has been monitored optically as a function of time and temperature from seconds to hours and from 150 K to 200 K. Between 150 K and 180 K, the kinetics are non-exponential in time and can be described by a static distribution of barrier heights. It is possible to enhance the relaxation by irradiating the protein with visible light.

The relaxation has been measured in both sperm whale and horse myoglobin. The relaxation in horse myoglobin begins at slightly lower temperatures than sperm whale myoglobin. The photo-enhanced relaxation occurs at 100 K and above in sperm whale myoglobin, but can be observed even at 20 K in horse myoglobin.

The structure of the intermediate state has been measured at 115 K using x ray diffraction. A met myoglobin crystal was irradiated with x rays at 90 K for 90 hours to create the intermediate state and the x ray diffraction data collected. The crystal structure verifies that the structure of the intermediate state is similar to that of met myoglobin and the water molecule is still bound to the heme iron.

Th-Pos454

A DIFFERENCE INFRARED SPECTROSCOPIC STUDY OF HEME-COPPER OXIDASES.

((James A. Bailey,‡ Sandra L. Mecklenburg,‡ Gina M. MacDonald,‡ Andromachi Katsonouri,† Stacie E. Wallace-Williams,‡ Robert B. Gennis,† R. Brian Dyer,‡ and William H. Woodruff‡))
‡ Biosciences and Biotechnology Group, CST - 4, MS J586, Los Alamos National Laboratory, Los Alamos NM 87545; † School of Chemical Sciences, University of Illinois, Champaigne-Urbana IL.

Difference FTIR spectroscopy was used to study protein changes associated with carbon monoxide (CO) photodissociation in two heme-copper oxidases, Cytochrome c Oxidase (CcO) isolated from bovine heart muscle and Cytochrome bo (Cbo) isolated from Escherichia coli. Low temperature infrared data were obtained before and after photodissociation of CO from the heme iron in CcO. The resulting light-minus-dark difference spectra contain changes associated with the transfer of the CO ligand from iron to copper, and any accompanying protein and cofactor changes associated with this exogenous ligand transfer. These difference spectra were obtained using samples in water and deuterium oxide in order to investigate the origin of the vibrational modes observed. Time-resolved (TR) difference data were obtained at room temperature after photolysis of CO from the heme iron. This data reveals protein and heme changes occurring on the timescales of 5 us to 20 ms. TR difference FTIR data obtained on the two species of heme-copper oxidases is discussed.

Th-Pos455

TIME-RESOLVED MAGNETIC CIRCULAR DICHROISM SPECTROSCOPY OF PHOTOLYZED FULLY-REDUCED AND MIXED-VALENCE CARBONMONOXY CYTOCHROME C OXIDASE.

((**YiRen Gu**, Artur Sucheta, Robert A. Goldbeck, Ólöf Einarsdóttir and David S. Kliger)) Dept. of Chemistry and Biochemistry, University of California, Santa Cruz, CA 95064.

As the terminal enzyme in the respiratory chain, cytochrome *c* oxidase (CcO) transfers electrons from cytoplasmic cytochrome *c* to molecular oxygen, conserving the released redox energy by means of a proton pumping mechanism that is not understood. Various spectroscopic techniques have been applied to investigate the pathways of electron transfer between the metal centers in this multi-subunit protein, which contains two hemes (*a* and a_3) and three Cu's. Time-resolved magnetic circular dichroism (TRMCD) in particular is sensitive to changes in spin state, and thus to ligation changes in heme Fe complexes, and to changes in oxidation state. Ns TRMCD measurements (100 ns to 100 ms) of the photolysis products of fully-reduced and mixed-valence CO complex of CcO are presented. The TRMCD results for fully reduced enzyme provide the most direct spectroscopic evidence for a ligand-shuttle mechanism in CcO (Woodruff, et al., 1991, *Proc. Natl. Acad. Sci. USA 88*, 2588). The results for the mixed valence complex are discussed in terms of current models for electron transfer between hemes *a* and a_3 after photolysis.

Th-Pos456

RESONANCE RAMAN INVESTIGATION OF SITE-DIRECTED MUTANTS OF CYTOCHROME bc_1.

(F.Gao[a], H.Qin[b], D.B. Knaff[b], A.Sami Saribas[c], K.Gray[c], F.Daldal[c], and M.R. Ondrias[a*]) a: Dept. of Chem., Univ. of N.M., Albuquerque, NM 87131, b: Dept. of Chem. and Biochem., Texas Tech Univ., Lubbock, Tx 79409-1061, c: Dept. of Biology, Univ. of Penn., Philadelphia, Pennsylvania 19104.

Here we report the latest results in our on-going efforts to characterize the local environments of the three heme active sites in the *Rb.capsulatus* cytochrome bc_1 complexes using resonance Raman spectroscopy. The effects of hemepocket mutagenesis, electron transfer inhibitor binding and quinone binding were monitored using Q-band excitation resonance Raman spectroscopy. Mutagenesis produces only small changes in heme geometry, but the binding of Q_o inhibitors produced some reproducible spectral shifts for several of the mutants, suggesting that the inhibitors perturb the b_L heme of the mutant. These results will be discussed in the context of other recent theories of bc_1 function.

(supported by the NIH (GM33330 to MRO and GM38237 to FD), the USDA (to DBK), the Robert A. Welch Foundation (to DBK), and NSF (to DBK))

Th-Pos457

EXPRESSION, PURIFICATION, AND CHARACTERIZATION OF MEMBRANE BOUND CYTOCHROME C FROM BACILLUS SUBTILIS.

((**Pamela S. David,** Megan R. Morrison, Sui-Lam Wong and Bruce C. Hill.)) Department of Biochemistry, Queen's University, Kingston, Ontario, Canada, K7L 3N6.

Bacillus subtilis posseses a membrane bound cytochrome c-550nm as part of its energy transducing electron transport chain. The cytochrome c gene has been cloned and sequenced, (von Wachenfelt and Hederstedt, 1990, JBC 265, 13939-13948) and designated cccA. Wildtype B. subtilis transformants containing a plasmid encoded copy of cccA in addition to the genomic copy produce a level of cytochrome c about 3 times that of a wildtype culture. We have engineered a B. subtilis cytochrome c to contain a six histidine carboxy terminal tail. Transformants containing a plasmid encoded copy of histidine tagged cccA produce cytochrome c at a level about twice that of a wildtype culture. Purification of the histidine-tagged cytochrome c is then possible in a single step via Ni^{2+} affinity chromatography. The presence of the histidine tag on cytochrome c allows a higher level of purification to be obtained using fewer steps compared to native B. subtilis cytochrome c. Properties of the histidine tagged cytochrome c will be reported and compared to those of native cytochrome c. [Research supported by a grant from MRC Canada.]

Th-Pos458

LIGAND PHOTOLYSIS AND RECOMBINATION OF CYTOCHROME C IN 4.5 M GUANIDINE HYDROCHLORIDE

((**Shui-Lin Niu** and Randy W. Larsen)) Department of Chemistry, University of Hawaii at Manoa, 2545 The Mall, Honolulu, HI 96822

The initial ligand rebinding process subsequent to laser-photolysis of CO-bound cytochrome c (II) in 4.5 M guanidine hydrochloride has been characterized using single wavelength transient absorption spectroscopy. In the presence of 4.5 M guanidine hydrochloride in 100 mM phosphate buffer, pH 7.0, photolysis of CO-cytochrome c (II) results in a biphasic transient kinetics with rate constants of $(1.99 \pm 0.06) \times 10^5\ s^{-1}$ and $(4.00 \pm 0.17) \times 10^3\ s^{-1}$. Lowering the CO concentration reduces the rate of the slower phase, whereas no change is observed for the faster phase. This indicates that the faster phase is due to the binding of an intrinsic ligand, while the slower phase arises from CO replacement of the bound ligand. The pH dependence study indicates the rebinding ligand is most likely a non-native histidine. No protein folding event is observed under our experimental conditions due to competing CO-binding. A model has been constructed describing ligand binding in the unfolded protein based upon our kinetic data.

Th-Pos459

IDENTIFICATION OF A FUNCTIONAL WATER CHANNEL IN CYTOCHROME P450 ENZYMES

((T.I. Oprea[1,2], G. Hummer[1] and A. E. García[1])) [1]Theoretical Biology and Biophysics Group, T10 MS K710, Los Alamos National Laboratory, Los Alamos, NM 87545. [2]Astra-Hässle AB, S-431 Mölndal, Sweden. (Spon. by T. Terwilliger)

We postulate a two-state model in which a conserved arginine, stabilizing the heme propionate in all known cytochrome P450 crystal structures, changes from the initial, stable side-chain conformation, to another rotamer (meta-stable). In this new state, a functional water channel (aqueduct) is formed from the active site to a water cluster located on the thiolate side of the heme, close to the protein surface. This water cluster communicates with the surface in the closed state, and is partly replaced by the flipping arginine side-chain in the open state, forcing water molecules to exit to the surface, or to re-access the active site. This two-state model can explain the exit pathway for water from the active site to the surface, as it is displaced by the incoming substrate, and the access of water from the surface to the active site as the catalytic product leaves the binding site.

Th-Pos460

HIERARCHICAL ORGANIZATION OF CONFORMATIONAL SUBSTATES IN (CO)-$P450_{LM2}$ AND (CO)-$P450_{SCC}$.

((**D. Lavalette,**[a] C. Tetreau,[a] & R. Lange[b]))
a) INSERM U350 , INSTITUT CURIE, 91405-Orsay France. b) INSERM U128, 34033-Montpellier France.

The kinetics of CO geminate rebinding with cytochromes $P450_{LM2}$ and $P450_{SCC}$ at temperatures down to 77K have been previously shown to be non-exponential. Our findings were similar to those reported for Hb chains, Mb, Hr and Az, and similarly interpreted as due to the presence of protein conformational substates reacting at different rates.

The enthalpy distributions reconstructed using the Maximum Entropy Method are complex, exhibiting new features which are in contrast to those reported for other hemoproteins. The new features are: 1-measurements of CO rebinding in the Soret show that p(H) is the sum of two well separated subdistributions with distinct peak enthalpy. 2- the protein populations at the origin of the enthalpy subdistributions are in a Boltzmann equilibrium well below the freezing point of the solvent. These results imply that the hierarchical organization of substates for the carboxy-complexes of cytochromes P450 may differ from that currently proposed for oxygen carriers.

Th-Pos461

INVESTIGATION OF THE ORIENTATION OF THE AXIAL IMIDAZOLE IN DEOXY Co-SUBSTITUTED HEMOPROTEINS AND PORPHYRIN MODELS BY ELECTRON SPIN ECHO ENVELOPE MODULATION SPECTROSCOPY: COMPARISON WITH CRYSTAL STRUCTURES.

((H. Caroline Lee and Jack Peisach)) Dept. of Physiology and Biophysics, Albert Einstein College of Medicine, Bronx, NY 10461.

ESEEM spectroscopy of deoxyCo-substituted globins, functional and EPR-active analogues of O_2-carrying hemoproteins, and of penta-coordinate imidazole complexes of deoxyCo tetraphenylporphyrin (TPP) reveal electron-nuclear coupling to the remote nitrogen of the axial imidazole and to the equatorial porphyrin nitrogens. Tau-suppression effects make it possible to isolate the spectral features arising from the axial nitrogen. Simulation of these features provides an estimate of the relative orientation of the g tensor and the nuclear quadrupole tensor for that nitrogen. On the basis of magnetic tensor assignments from single crystal EPR studies of deoxyCo-substituted myoglobin (deoxyCoMb) and from single crystal ESEEM studies of Cu(II) imidazole complexes, the orientation of the axial imidazole in deoxyCo-substituted hemoproteins and models can be obtained from the ESEEM-derived tensor orientations. This study demonstrates that for deoxyCoMb, the deoxyCo-substituted subunits of a partially-ligated iron-cobalt hemoglobin, and two deoxyCoTPP models, the orientation of the axial imidazole obtained by ESEEM spectroscopy compares well with those revealed by X-ray crystal structures. (Supported by N.I.H. grants GM40168 and RR02538.)

Th-Pos462

ESEEM AND EXAFS STUDIES OF MODELS OF OXYCo-SUBSTITUTED HEMOPROTEINS: CORRELATING ELECTRON-NUCLEAR INTERACTIONS AND METAL-LIGAND BOND LENGTHS. ((H. Caroline Lee, Eva Scheuring, Jack Peisach and Mark R. Chance)) Dept. of Physiology and Biophysics, Albert Einstein College of Medicine, Bronx, NY 10461.

Electron spin echo envelope modulation (ESEEM) spectroscopy demonstrates that the magnitude of the electron-nuclear hyperfine and nuclear quadrupole couplings to the cobalt-bound ^{14}N of 1-methylimidazole (1-MeIm) in oxyCo [tetraphenylporphyrin(TPP)][1-MeIm] decrease with an increase in the solvent polarity. For oxyCo[(σ-R)$_1$TPP][1-MeIm] (where R=—H, —NHCOC$(CH_3)_3$, —NHCOCH$_3$ or —NHCONHC$_6$H$_5$, an ortho substitutent on one of the four meso phenyls of TPP), couplings to the axial nitrogen decrease with increased electron-withdrawing strength of R, i.e., with increased acidity of the amide proton of R that may interact with the bound O_2. These results confirm a previously established relationship that reduction in couplings to the axial nitrogen results from an increase in the ionicity of the Co-O_2 bond. Earlier ESEEM studies also predict that reduction in couplings is accompanied by the shortening of both axial metal-ligand bonds. Extended X-ray Absorption Fine Structure (EXAFS) measurements demonstrate that the cobalt-imidazole and the cobalt-porphyrin nitrogen bonds are shortened in complexes exhibiting smaller axial ^{14}N couplings. The cobalt-dioxygen bond, however, remains essentially unchanged.
(Supported by N.I.H. grants GM40168, RR02538, HL45892, and RR01633.)

Th-Pos463

Ligand Photolysis and Recombination of (Dimethylsulphoxide)$_2$ Fe(II)Porphyrin Complexes. ((E. W. Findsen[1], and R. W. Larsen[2])).[1] Department of Chemistry, University of Toledo, Toledo, OH-43606 [2] Department of Chemistry, University of Hawaii at Manoa, Honolulu, HI-96822.

Steady-state optical absorption and nanosecond transient absorption spectroscopy have been employed to examine ligand photolysis and recombination of (dimethylsulphoxide)$_2$ Fe(II) protoporphyrin IX ((DMSO)$_2$ Fe(II)PPIX), (DMSO)$_2$tetrakis-4-(sulphonatophenyl) Fe(II)porphyrin, ((DMSO)$_2$Fe(II)4SP), and (DMSO)$_2$Fe(II) Uroporphyrin ((DMSO)$_2$Fe(II)URO) complexes in neat DMSO. The steady-state optical absorption data indicate that all three complexes are six-coordinate and low-spin. The corresponding nanosecond transient absorption data demonstrate that photo excitation of the (DMSO)$_2$Fe(II)PPIX and (DMSO)$_2$Fe(II)URO complexes results in formation of a transient species with an absorption maximum and minimum at ~434 nm and ~424 nm, respectively. These species decay exponentialy with rate constants of ~2x10^6 s^{-1}. Excitation of the ((DMSO)$_2$Fe(II)4SP, on the other hand, produces a transient species with a broad absorption maximum centered at ~438 nm with a minum at ~424 nm in the kinetic difference spectrum. The initialy formed transient decays exponentialy with rate constants of ~1.5x10^5 s^{-1}. Examination of the temperature dependence of the rate constants for ligand recombination reveals that the activation enthalpy is higher for ligand recombination to (DMSO)Fe(II)4SP complex than either the (DMSO)Fe(II)PPIX or (DMSO) Fe(II)URO complexes (8.8 kcal/mole, 6.1 kcal/mole, and 6.8 kcal/mole for Fe(II)4SP, Fe(II)PPIX, and Fe(II)URO, respectively). These results demonstrate significant steric control of ligand recombination in the (DMSO)$_2$Fe(II) porphyrin systems.

Th-Pos464

Conformational Dynamics of CO-Binding to Fe(II)Protoporphyrin IX In Detergent Micelles. ((R. W. Larsen)). Department of Chemistry, University of Hawaii at Manoa, Honolulu, HI-96822.

The focus of this study is to explore the role of conformational and thermodynamics of ligand binding to heme proteins using a model system consisting of CO-Fe(II)Protoporphyrin IX (COFe(II)PPIX) encapsulated in cetyltrimethylammonium bromide (CTAB) micelles. Temperature dependent photoacoustic calorimetry was employed to probe the thermodynamics and time-resolved volume changes associated with CO-photolysis. The results of the acoustic analysis reveal an enthalpy associated with this process of (15.8±3) kcal/mole. In addition, the analysis demonstrates that ligand photolysis results in a volume increase of 11.5±0.9 ml/mole that occurs on a time scale less than 100 ns. The corresponding ligand recombination occurs with a pseudo first-order rate constant of (4.1±0.2)x10^3 s^{-1} (at 23°C). The corresponding enthalpy of activation (ΔH^+) for CO recombination is found to be 18±2 kcal/mole. The data are consistent with a model in which significant heme distortion occurs upon formation of the five-coordinate transient species which distorts the micelle structure resulting in micelle expansion. Comparison of the present results with previous photoacoustic data of the heme protein myoglobin reveal very similar thermodynamics and volume changes.

Th-Pos465

DIFFERENT CONFORMATIONS AND NON-PLANAR DISTORTIONS OF NI(II) *MESO*- TETRAPHENYPORPHYRIN IN CS_2. ((E. Unger, W. Dreybrodt and **R. Schweitzer- Stenner**)) Institut für Experimentelle Physik, Universität Bremen, 28359 Bremen, Germany (Spon. by Sanford A. Asher).

In order to study the influence of *meso*-substitution on the structure of porphyrins we have measured the Raman spectra of Ni(II)-*meso*-tetraphenylporphyrin (NiTPP) in CS_2 solution with various excitation wavelengths covering the region of the Q_0-, Q_V-, B_0- and B_V -band. The band shapes of the macrocycle modes ν_1, ν_2, ν_8, ν_{10}, ν_{11}, ν_{19} and the phenyl mode ϕ_8 were found to be asymmetric and composed of two subbands, the intensity ratios of which depend on the excitation wavelength. The low frequency (LF) subbands of the core size marker bands ν_{11}, ν_{19}, ν_2 and ν_{10} exhibt Raman excitation profiles (REPs) that are red shifted by 150±30 cm^{-1} with respect to the REPs of the corresponding high frequency (HF) subbands. For ν_8, however, a red shift is observed for the REP of the HF subband. All subbands with red shifted REPs can be attributed to a conformer exhibiting a non-planar macrocycle, whereas the remaining ones result from planar molecules. Contrary, the REPs of the ν_1- and ϕ_8- subbands can be scaled onto each other, respectively. Their heterogeneity most likely results from another pair of NiTPP conformers which differ in the orientation of the phenyl groups. The depolarization ratios (DPRs) of the B_{1g}- and B_{2g}-modes show no dispersion. Contrary, some A_{1g}-modes show a weak and the A_{2g}-modes a strong DPR-dispersion. This indicates that the non-planar conformer is simultaneously ruffled and saddled, owing to the combined effect of B_{1u}- and B_{2u}-distortions. This is in accordance with the recently obtained structure of crystallized NiTPP.

Th-Pos466

STRUCTURAL DYNAMICS OF METAL-OCTAETHYLPORPHYRINS IN SOLUTION STUDIED WITH LOW-TEMPERATURE OPTICAL ABSORPTION AND RESONANCE RAMAN SPECTROSCOPIES: ROLE OF THE CENTRAL METAL ((A. Cupane[1], M. Leone[1], L. Cordone[1], R. Schweitzer-Stenner[2], E. Unger[2], M. Beck and W. Dreybrodt[2])). [1] Istituto di Fisica, University of Palermo, 90123 Palermo, Italy; [2] Institut für Experimentelle Physik, Universität Bremen, 28359 Bremen, Germany.

We have measured the Soret band of various metal-octaethylporphyrins (Me-OEP; Me=Ni(II), Cu(II) and Pd(II)) in the glass forming solvent IPEE (50%v/v mixture of isopentane and ethyl ether) as a function of temperature between 40 and 300 K. In parallel we have measured the Raman spectra with Soret excitation to obtain the vibronic coupling parameters of all relevant A_{1g} modes Franck-Condon coupled to the Soret transition. The band positions of spectrally distinguishable conformers (e. g. for NiOEP) were obtained from the resonance excitation profiles of subbands underlying the conformation sensitive ν_{10} band. Excellent agreement between optical absorption and resonance Raman data was obtained in all cases. Besides the natural Lorentzian width, the Soret band linewidth exhibits a temperature dependent Gaussian contribution that results from low frequency modes (both out of plane modes of the porphyrin involving the central metal atom and molecular motions within the liquid environment) to which the electronic transition is coupled. At temperatures above the solvent glass transition the amplitudes of these motions increase well above the values predicted by a purely harmonic model; the deviations from harmonicity are quite pronounced for NiOEP and PdOEP, but comparatively small for CuOEP. Moreover, for PdOEP, a large Gaussian spectral heterogeneity is observed even at 40 K. The results can be rationalized in terms of the different size and electronic structure of the central metal ion and point out its role in determining the conformational and dynamic properties of porphyrins.

Th-Pos467

^{13}C NMR SPECTROSCOPY OF PARAMAGNETIC HEMES: A POWERFUL TOOL FOR THE STUDY OF INTERPROTEIN INTERACTIONS ((M. Rivera†, M. Rodriguez†, F. Qiu† and R. Stark‡)) †Department of Chemistry, Oklahoma State University, Stillwater, OK 74078. ‡Department of Chemistry, , City University of New York, College of Staten Island, NY, 10314.

1-^{13}C-5-aminolevulinic acid (ALA) and 3-^{13}C-ALA were used to selectively label the heme propionate carbons of mitochondrial cytochrome b_5. Assignment of the isotropically shifted resonances arising from the heme propionate carbons in cyt. b_5 was carried out by a combination of one-and two-dimensional experiments. Selectively labeled cyt. b_5 was titrated with horse heart cytochrome c while monitoring the ^{13}C resonances arising from the cyt. b_5 heme propionate carbons. Resonances arising from the propionate located on the solvent exposed heme edge of cytochrome b_5 were shifted as a function of cytochrome c concentration. These experiments provide conclusive experimental evidence corroborating the selective participation of the solvent exposed heme propionate in binding to cytochrome c, and also indicate that acidic residues Glu44, Glu48, Glu56 and Asp60, which surround the exposed heme edge, participate in the electrostatic binding to cytochrome c, as previously postulated on the basis of molecular dynamics calculations (Northrup *et al.*, *Biochemistry*, **32**, 6613, 1993). A conditional binding constant, K = 3.8 x 10^4 at μ = 0.02 M was obtained for the complex by fitting the experimental binding curves to a model based on this stoichiometry.